1 Contract Number: C46-45-01

2. **Timing of volcanism and intrusive activity in and around the Faroe Islands**

3. Dr Alison M Halton, Dr Sarah C Sherlock

4. Department of Environment, Earth and Ecosystems, The Open University, Walton Hall, Milton Keynes, UK

5. September 2012

6. b. Regional geology and the evolution of the entire Faroese area.

7. Budget total: 2,110,726.00 DKK

8. Start date of Contract: 01/06/10 End date of Contract: 30/05/12

9. Abstract

This study is focused on the timing and duration of volcanic activity on the Faroe Islands – focussing on the Beinisvørð, Malinstindur and Enni Formations, and major intrusive units. The study attempted to cover as much of the stratigraphy as possible. The ages are complex and are strongly indicative of a range of different processes that have affected the Ar/Ar system – uptake of excess argon, argon-loss through recoil (reactor induced process that affects ultra-fine grained minerals), K-redistribution during hydrothermal alteration and fluid flux. We also believe that the volcanological style of the lavas is influencing the Ar/Ar system (those more rapidly cooled 'locking in' the Ar/Ar age, though with the potential for more excess argon if it is derived from the magma chamber, for example). In spite of these it has been possible to date the Beinisvørð Formation in the Lopra 1/1A borehole (56.30±0.99 Ma), the Malinstindur Formation (top Malinstindur 56.53±1.1 Ma), the Enni Formation (top and base Enni 53.6±3.2 Ma). The intrusives yielded the following ages: Eysturoy Sill 52±1 Ma; Streymoy Sill 51±1 Ma; Prestfjall: no discernible age. The new ages imply that the FIBG was erupted in < 2 Myr. Disturbances to the Ar/Ar system are the overwhelming aspect of the dataset but it is clear that the FIBG is almost unique in the widespread nature of these disturbances. This renders it an important area for developing new knowledge and theories of the processes, their implications for the Ar/Ar system and their implications for the migration of matter through basaltic provinces.

10. Introduction

10.1 Background Geology of Faroes

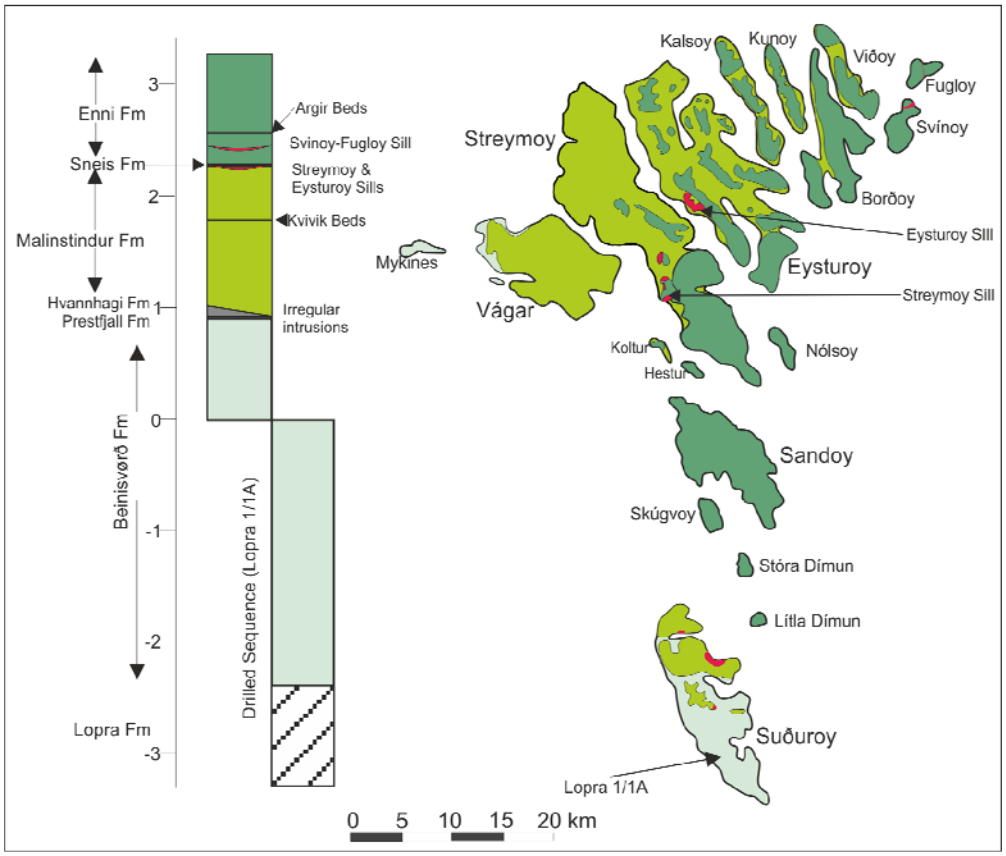

Figure 1. Geological map and stratigraphic column of the Faroe Islands Basalt Group after Passey & Bell (2007) (scale on the column is in Km)

The Faroe Islands stratigraphy (shown in figure 1) consists of the 7 formations of the Faroe Islands Basalt Group (FIBG) (Passey & Jolley 2009). The oldest formation in the FIBG is the Lopra Fm and is only known from the base of the Lopra 1/1A borehole, with a known thickness of ~1075m, it may extend beyond the base of the borehole (Ellis et al. 2002; Passey & Jolley 2009) and is composed of volcaniclastic units intruded by basaltic sills and/or invasive lava flows (Ellis et al. 2002). The borehole was drilled to a depth of 2184m (in 1981), and was deepened to 3158m in 1996, a sidetrack (Lopra 1A) drilled from 3091m in 1996, reaching a total depth of 3565m.

The oldest formation exposed on the Faroe Islands, is the Beinisvørð Fm, with a total stratigraphical thickness of ~3250m, of which ~890m is exposed on the Faroe Islands, the rest, drilled in the Lopra 1/1A borehole (Rasmussen & Noe-Nygaard 1970; Hald & Waagstein 1984; Ellis et al. 2002). The Beinisvørð Fm is comprised of laterally extensive, subaerial sheet flows, with average flow thicknesses of ~20m (Passey & Bell 2007; Passey & Jolley 2009; Waagstein et al 1984; Waagstein 1988; Ellis et al 2002). The majority of the basalts are aphyric, finely crystalline (<1mm) tholeiites (Noe-Nygaard & Rasmussen 1968; Rasmussen & Noe-Nygaard 1970; Hald & Waagstein 1984), with columnar jointing common in the uppermost ~200m (Passey & Bell 2007).

The Beinisvørð Fm was followed by a hiatus in eruption and the deposition of the sedimentary, Prestfjall Fm, with an average thickness of ~9m on Suðuroy (Rasmussen & Noe-Nygaard 1970). After the Prestfjall Fm, the Hvannhagi Fm represents a syn-eruption facies, with pyroclastic and sedimentary lithologies, with deposition restricted to topographic depressions in the paloelandscape (Passey & Jolley 2009). The Hvannhagi Fm is intruded by numerous irregular dolerite sills, with similar chemistry to the overlying Malinstindur Lavas (high TiO_2, olivine phyric lavas) (Waagstein 1988; Hald & Waagstein 1991)

Volcanism resumed with the deposition of the Malinstindur Fm, (max 1350m stratigraphic thickness), predominantly of compound lava flows (Passey & Bell 2007), which are generally poorly exposed on gentle grass slopes. The pahoehoe flow lobes are generally 10's cm up to >4m which average thickness of ~2m, forming compound flows averaging 20m thickness (Rasmussen & Noe-Nygaard 1970; Waagstein 1988; Passey & Bell 2007). Interbed sediment horizons become much more frequent and thicker within the upper 1/3 of the Malinstindur Fm, above a prominent interbed horizon, the Kvivik Beds. The Sneis Fm, above the Malinstindur Fm represents a significant break in volcanism and the deposition of a sedimentary package which can be mapped across the Faroe Islands.

The Enni Fm is the youngest formation on the Faroe Islands, with a minimum stratigraphical thickness of ~900m and is formed of both compound and simple lava flows; with interbed sedimentary horizons more abundant than in the Malinstindur Fm and regionally correlated horizons such as the Argir Beds which are useful in locating position within the stratigraphy. The lavas of the Malinstindur and Enni Fms include both high and low TiO_2 lavas, with aphyric lavas and both plagioclase and olivine phyric basalts occurring. In the Enni formation both the simple and compound lavas can be composed of aphyric, plagioclase phyric and olivine phyric basalts

Intruding into the FIBG are various intrusive rocks, including large saucer shaped sills which intrude the upper part of the stratigraphy, with the Eysturoy and Streymoy Sills intruding at about the level of the Sneis Fm and the smaller Svínoy-Fugloy sill intruding within the Enni Fm (close to the level of the Argir Beds). As well as the large saucer

shaped sills, numerous smaller, irregular intrusives are found within the Prestfjall and Hvannhagi Fms and within the Sneis Fm, where they occur as aphyric to olivine-phyric stratiform basaltic sills (Passey & Jolley 2009). The Eysturoy and Svínoy-Fugloy sills have high TiO_2 compositions, while the Streymoy Sill has a low TiO_2, MORB like composition (Hald & Waagstein 1991). There are also many dykes intruding the FIBG in various orientations, with a total of 845 dyke exposures mapped by Rasmussen & Noe-Nygaard (1969) and despite all the exposures, they are not seen anywhere to be feeding the lava flows leading to the suggestion that they post-date the lavas (Rasmussen & Noe-Nygaard 1969, 1970; Hald & Waagstein 1991).

10.2. Previous dating

10.2.1. Previous dating of the Lopra and Beinisvørð formations

The timing of commencement of volcanism on the Faroe Islands, in the absence of knowledge of the pre-volcanic substrate (as the borehole did not penetrate the base of the lavas), has relied on dating of the oldest/lowest recovered horizons from within the borehole. This has previously been attempted using various methods, including biostratigraphy and magnetostratigraphy as well as radiometric dating of the basaltic lava horizons.

Radiometric investigation has focused on the lowest lavas of the Beinisvørð Fm, with $^{40}Ar/^{39}Ar$ dating of samples from the Lopra 1/1A borehole previously carried out by Storey et al. (2007) and Waagstein et al. (2002). Waagstein et al. (2002) studied samples from the Lopra 1/1A borehole using both $^{40}Ar/^{39}Ar$ and K/Ar methods and the correlations between paleomagnetic investigation and suggested that that eruption of the Beinisvørð Fm began at 58.8±0.5Ma and ended, after a slowing of eruption rate, at 55.8±0.1Ma. This age of Waagstein et al. (2002) was based on the K/Ar ages and the fit to the paleomagnetic data with older $^{40}Ar/^{39}Ar$ ages from samples from Lopra 1/1A regarded as too old, with the samples having been affected by ^{39}Ar recoil. Storey et al. (2007) dated plagioclase separates from 2 samples from the Lopra 1/1A borehole, L1-0337.5 and L1-1923.1, giving plateau ages of 59.9±0.7Ma and 60.1±0.6Ma respectively. One of the samples from the Lopra 1/1A borehole (L1-0337.5) was dated by both Storey et al. (2007) and Waagstein et al. (2002), producing ages of 59.9±0.7Ma (plagioclase separate, Storey et al. 2007) and 60.5±1.0Ma (whole rock age, Waagstein et al. 2002) and although this age was considered reliable by storey et al. (2007) the whole rock age of Waagstein et al. (2002) was regarded as too old due to probably ^{39}Ar recoil loss and/or relocation during irradiation.

Biostratigraphical investigation of sediments within the lava sequence from the Lopra borehole have suggested the pre-break up succession in the Faroe Islands (the Beinisvørð and Lopra Fms) correlates with the Flett Fm (sequence T40), implying an age no older than 57.2Ma on Gradstein et al. (2004) timescale (Passey & Jolley 2009; Jolley 2009;Jolley et al. 2002). The biostratigraphical age determination for the Prestfjall Fm, constrains the age of the top of the Beinisvorð Fm, with a correlation to the base of unit 2 of the Flett Fm (base of sequence T45) and an age of ~54.8Ma (Jolley 1997; Jolley et al. 2002).

10.2.2. Previous dating of the Malinstindur – Enni Fm

Storey et al. (2007) dated 1 sample from the Malinstindur Fm and 1 from the Enni Fm, producing ages of 54.9±0.7 Ma and 55.2±0.7 Ma respectively (ages from plagioclase separates and giving within error but out of order ages relative to

the stratigraphy). Biostratigraphical correlation of the Malinstindur and Enni Fms to sequence T45 (Jolley et al 2002; Jolley 2009) suggests an age of between 54.5 and 54.8 Ma (Gradstein et al. 2004 timescale) is in reasonable agreement with the radiometric ages for this part of the stratigraphy, and with the reversed magnetic polarity correlated to C24r (Waagstein 1988; Waagstein et al. 2002). This short time interval for the Malinstindur and Enni Fms is in agreement with the 300Ka interval for the emplacement of the correlated syn-break up volcanism in East Greenland (using the cooling history of the Skaergaard Intrusion) (Larsen & Tegner 2006; Larsen et al. 1999). Away from the main FIBG lava field, palynological evidence shows a considerable variation in age of the end of volcanic activity, with isolated volcanic centres having more restricted stratigraphical extents, making them less useful in establishing the end of activity in the exposed FIBG.

10.2.3. Previous work on the Intrusives of the Faroe Islands

The intrusive rocks of the Faroe Islands have not previously been dated, with the ages of the sill complexes and the dykes inferred from cross cutting relationships. Hald & Waagstein (1991) suggested that the dykes and sills appear broadly contemporaneous with the youngest lavas of the FIBG and are chemically similar and unlike in East Greenland, there is no evidence of late stage acid and alkalic activity (late intrusives) in the Faroe Islands. Hald & Waagstein (1991) suggested that the sills were emplaced in the final stages of volcanic activity, or immediately after, while Geoffroy et al. (1994) suggested they were emplaced in response to reverse faulting in NE-SW compression, shortly before onset of N Atlantic opening. The sills of the Faroe Islands have not been observed to be cut by the dykes and so it is thought that the sills represent the final stage of volcanic activity on the Faroe Islands (Hald & Waagstein 1991). That none of the dykes have been seen to be feeding the lavas has lead to the suggestions that dykes are formed as a result of slight crustal doming (Waagstein 1977) and Rasmussen & Noe-Nygaard (1969;1970) suggest that the majority of the dykes post date the lavas. The relationships been some of the large sill complexes and the dyke systems have been investigated by recent detailed mapping and this has shown that some dyke systems (thickness c.0.5to c.4m) intersect the area that is underlain by sills but the few exposed accessible dyke-sill contacts suggest that the sub-vertical dykes predate the sills (Hansen et al. 2011). No observations to suggest that any of the inclined dykes acted as conduits for magma transport between sills during emplacement (Hansen et al 2011).

On Suðuroy, the irregular intrusives in the Prestfjall Fm are chemically similar to the olivine-phyric and aphyric compound lava flows of the Malinstindur Fm and have therefore been interpreted as shallow feeders for these lavas (Waagstein 1988; Hald & Waagstein 1991). Irregular intrusives are also found within the sedimentary units of the Sneis Fm and were previously described as lava flows, but have been shown to be intrusive (Passey & Jolley 2009).

Within the Faroe Shetland Basin, the numerous small-scale intrusives, collectively termed the Faroe-Shetland Sill Complex (Gibb & Kanaris-Sotiriou 1988), have been sampled by boreholes in various parts of the basin (e.g. Gibb & Kanaris-Sotiriou 1988; Smallwood & Maresh 2002). A wide range of ages have been suggested but the majority suggest that much of the Faroe Shetland sill complex was emplaced in the late Paleocene – early Eocene, with most activity was concentrated between 56-52Ma, approximately synchronous with the opening of the North Atlantic and the eruption of the Malinstindur and Enni Fms on the Faroe Islands (Ritchie & Hitchen 1996). Structural investigation of the sill complex (e.g. Gibb & kanaris-Sotiriou 1988) suggests a maximum age of Eocene while geochemistry suggests

that the sills are more closely related to the Enni Fm basalt (Gibb & Kanaris-Sotiriou 1988; Gibb et al. 1986). More recently an age of 56.0 ± 1.2Ma was obtained from a dolerite sample from the sill complex in Well 6004/16-1z (Smallwood and Harding 2009).

11. Methods

Samples were prepared by first removing weathered edges to the samples on the rock saw and then the sample was crushed. The crushed material was sieved and washed and then hand picked with a binocular microscope, taking care to select the freshest pieces of basalt. Size fractions picked from depended slightly on the grain size of the sample, with the key aim being to select the freshest pieces of crystalline whole rock basalt, containing no visible alteration (in particular organic rich clays or zeolites which occur in many of the vesicles) or larger crystals. Samples were washed in acetone and deionised water and each split into 2 Al foils for irradiation at the McMaster reactor in Canada. The mineral standard GA1550 (98.79 ± 0.96 Ma Renne et al., 1998) was included either side of every 10 basalt samples to monitor the neutron flux during irradiation and the calculated J values for each sample are included in the results table, (appendix 2). Step-heating of samples was carried out using an IR laser and analysed using MAP 215-50 noble gas mass spectrometer. Data was corrected for system blanks measured either side of each step or every 2 steps, corrected for mass discrimination of 283, ^{37}Ar decay and using corrections for reactor produced reactor produced neutron induced interference reactions. The following correction factors were used: $(^{39}Ar/^{37}Ar)_{Ca}$ = 0.00065 ± 3.25E-^{06}, $(^{36}Ar/^{37}Ar)_{Ca}$ = 0.000265 ± 1.325E-^{06}, and $(^{40}Ar/^{39}Ar)_{K}$ = 0.0085 ± 4.25E-^{05}; based on analyses of Ca and K salts.

For a plateau age to be statistically valid it must contain at least 50% of the ^{39}Ar released from at least 3 successive steps (preferably 60%+ of the ^{39}Ar) All ages are stated with 2σ errors.

12. Results

12.1 Beinisvørð Fm from the Lopra 1/1A borehole

Much of the Ar data produced from the samples from the Lopra borehole was discussed in the interim report and is summarised below, including the data for sample L13 which was not available at the time of production of the interim report.

Stratigraphic position*	Sample	split	Plateau age	%^{39}Ar	Inverse isochron age	^{40}Ar/^{36}Ar intercept	Weighted mean
Lava 1	L1	A2	59.35 ± 0.65Ma	75.2	59.30 ± 0.99Ma	300 ± 100	
-1260	L2	A3					59.01±0.49Ma (75.5%)
		A4					59.62± 0.64Ma (74.3%)
	L3	A5					58.81±0.44Ma (68.2%)
		A6	59.47 ± 0.74Ma	54	58.3 ± 1.7Ma	360 ± 91	
Lava 2	L4	A7	66.0 ± 2.0Ma	54.9	44.3 ± 6.5Ma	373 ± 18	
-1770	L5	A9	56.3 ± 1. Ma	65	56.3 ± 5.5Ma	296 ± 26	
		A10	57.1 ± 1.3Ma	50.4	71 ± 12Ma	226 ± 56	
	L6	A11	60.1 ± 1.3Ma	61	62 ± 26 Ma	287 ± 110	
		A12	61.9 ± 1.6Ma	61.4	54.7 ± 5.7Ma	332 ± 31	
	L7	A13	60.7 ± 1.4Ma	74.7	58.2 ± 8.2Ma	305 ± 31	
	L8	A15					54.9±1.8Ma (68.1%)
		A16					56.2±1.6Ma (78.4)
Lava 3	L9	A17	67.2 ± 2.3Ma	66.8	59 ± 13Ma	316 ± 30	
-2140		A18					65±4.6Ma (64.4%)
	L10	A20	68.9 ± 2.3Ma	58.3	64 ± 11Ma	307 ± 25	
	L11	A21					63.3±4.3Ma (65.8%)
	L12	A23	70.1 ± 2.1Ma	64.3	61 ± 12Ma	313 ± 22	
		A24	76.6 ± 3.1Ma	50.7	65 ± 14Ma	312 ± 15	
Lava 4	L13	A63	56.60 ± 0.80Ma	62.2	52.9 ± 3.7Ma	354 ± 57	
-2850		A64	55.71 ± 0.77Ma	65.8	51.7 ± 3.3Ma	384 ± 42	
Lava 5	L14	A25	45.6 ± 1.4Ma	60.7	50 ± 10Ma	253 ± 87	
-3100		A26	50.8 ± 1.3Ma	56.6	45.7 ± 6.8Ma	334 ± 50	

Table 1: ^{40}Ar/^{39}Ar data summary for samples from the Beinisvorð Fm sampled from the Lopra 1/1A borehole *= stratigraphic positions relative to the base of the Malinstindur Fm (in meters). All samples are of basalt groundmass.

12.1.1. Lava 1 (borehole depth of 337.73 - 338.72m)

The uppermost sampled interval of the Lopra 1/1A borehole, produced plateau ages of 59.35±0.65Ma and 59.47±0.74Ma (from L1 and L3 respectively). A weighted mean of these plateau ages is 59.40±0.49Ma and although analysis of L2 and repeats of L1 and L3 failed to meet the statistical criteria for a plateau age they produce weighted mean ages of much of the release spectra and inverse isochrons which are similar to the plateau ages. If the weighted mean ages from the non-plateau samples are included in the average, the weighted mean an age is 59.09±0.24Ma.

12.1.2. Lava 2 (borehole depth of 860.19 – 862.73m)

5 samples were dated from this interval, samples (L4 to L8) (equating to ~1770m below the top of the Beinisvørð Fm) and the plateau ages show a much larger spread of ages than expected, with the spread of ages for samples from this

lava interval shows the Ar system to be disturbed and questions the validity of any of the ages. Sample L4 produced an older than expected age of 66.0±2.0Ma with a much younger inverse isochron age and a $^{40}Ar/^{36}Ar$ ratio suggesting the presence of excess argon. Sample L5 produced younger plateaus age of 56.3±1.0 and 57.1±1.3Ma (with an average of 56.60±0.79Ma). Sample L6 produced plateau ages of 60.1±1.3Ma and 61.90±1.6Ma, the inverse isochrons show large errors and produce ages different to the plateau ages, and $^{40}Ar/^{36}Ar$ intercepts suggesting some excess argon, and from Sample L7 the plateau age is error of those from L6, at 60.7±1.4Ma Sample L8 failed to produce a plateau age but the spectra are close to fulfilling the plateau criteria with a weighted mean of the final 68% of ^{39}Ar release producing an age of 54.9±1.8Ma (split a15) and the final 78% ^{39}Ar release from split a16 giving a weighted mean age of 56.2±1.6Ma. These ages are similar to those from sample L5.

12.1.3. Lava 3 (borehole depth of 1218.53 – 1219.48m)

From the Lava 3 interval (equating to ~2140m below top of Beinisvørð Fm) 4 samples were analysed (L9 to L12). Sample L9 produced a plateau age of 67.2±2.3Ma and the inverse isochron has large errors but suggests a younger age with a $^{40}Ar/^{36}Ar$ intercept within error of atmospheric. The plateau age produced from sample L10 is also older than expected at 68.9±2.3Ma. Sample L11 failed to produce a plateau age with apparent ages dropping from old apparent ages in initial steps to younger ages but failing to produce a plateau. The inverse isochron suggests an age of 53.2±5.1Ma and the $^{40}Ar/^{36}Ar$ ratio suggests the presence of excess argon {similar pattern shown by both splits of the sample}.The age produced by sample L12 is the oldest produced at 70.1±2.1Ma.

All the plateau ages produced from this interval are too old (Cretaceous) for the Beinisvørð Fm.

12.1.4. Lava 4 (borehole depth of 1922.6m)

Sample L13 is from Lava 4 (equating to ~2850m below the top of the Beinisvørð Fm), and analysis of 2 splits of sample L13 produced plateau ages of 56.60±0.80Ma and 55.71±0.77Ma (splits a63 and a64 respectively). The inverse isochrons for this sample suggest the presence of some excess argon with $^{40}Ar/^{36}Ar$ intercepts greater than the atmospheric ratio of 295.5 and this may be responsible for the older apparent ages in the initial steps of the release spectra. A weighted mean of these 2 plateau ages is 56.11±0.57Ma and is the best estimate for the age of this sample.

12.1.5. Lava 5 (borehole depth of 2177.65m)

The stratigraphically lowest sample is sample L14, from the interval named Lava 5 in this study, (equates to ~3100m below the top of the Beinisvørð Fm). The apparent ages produced from this sample are younger than those from the previous samples, with plateau ages of 45.6±1.4Ma and 50.1.3Ma (for splits a25 and a26 respectively).

The variation in ages stratigraphically is discussed in the discussion section

12.2. Malinstindur and Enni formations

The samples from the Malinstindur and Enni formations were collected with the aim of covering as much of the stratigraphy as possible. The practicalities of sampling poorly exposed grassy slopes in the lower 2/3 of the Malinstindur Fm and the presence of fresh enough material for dating means that the coverage of the stratigraphy is not ideal. Location data for the samples collected from the Malinstindur and Enni formations is in appendix 1. Tables 2 & 3 contain the step-heating and inverse isochron results for the samples from the Malinstindur and Enni formations respectively.

Stratigraphic position*	**Sample**	**split**	**Plateau age**	**%^{39}Ar**	**Inverse isochron age**	**^{40}Ar/^{36}Ar intercept**
0	AMH3	A31	49.1 ± 1.3Ma	61.4	48.9 ± 3.4Ma	319 ± 17
0	AH10-4	A37			45.8 ± 4.6Ma	428 ± 67
1	AH10-15	A43 A44	34.9 ± 1.6Ma 34.4 ± 2.0Ma	69.8 60.2	32 ± 19Ma 26 ± 13Ma	301 ± 32 308 ± 21
8	AH10-16	A41	No plateau			
796	AH10-39	A69	No plateau			
801	AH10-41	A71	No plateau			
780	AH10-56	A49 A40 (plagioclase)	35.8 ± 1.0Ma 42.4 ± 1.9Ma	41 75.1	37.5 ± 4.3Ma	336 ± 28
847	AH10-45	A67 A68	No plateau No plateau		52.1 ± 1.7Ma	356 ± 26
1167	AH10-25	A29 A32 (plagioclase)	No plateau 35.7 ± 1.5Ma	67.4	32 ± 13Ma	318 ± 20
1240	AH10-27	A79 A80	48.2 ± 1.5Ma 51.74 ± 0.86Ma	53 57.2	32 ± 9.5Ma 49.9 ± 3.8Ma	467 ± 110 361 ± 73
1260	AH10-28	A81 A82	56.86 ± 0.62Ma	53.8	56.2 ± 2.0Ma	489 ± 110

Table 2: ^{40}Ar/^{39}Ar data for samples from the Malinstindur Fm. *= stratigraphic positions relative to the base of the Malinstindur Fm (in meters). All samples are of basalt groundmass unless labelled as plagioclase.

12.2.1. From the base of the Malinstindur Fm

The samples dated from the base of the Malinstindur Fm show a range of ages and disturbed release spectra (figure 2), with all plateau ages being younger than the expected age of the base of the Malinstindur Fm. AMH3 (figure 2A) produced a plateau age of 49.1±1.3Ma; the inverse isochron age for this data is within error of the plateau age while the ^{40}Ar/^{36}Ar intercept is above atmospheric (319±17). Sample AH10-4 failed to produce a plateau age (figure 2B), with a spectrum that dropped from 70 to 46Ma and the inverse isochron shows the presence of excess argon within the sample, with a ^{40}Ar/^{36}Ar intercept of 427±14.Sample AH10-15 shows disturbance to the spectra (figure 2C) but both splits of

this sample produced plateau ages of 34.4±2.0Ma and 34.9±1.6Ma. The inverse isochrons from these analyses also show considerable disturbance, while sample AH10-16 also show a disturbed release spectrum (not shown in figure 2) with ages dropping from 60Ma to ~0Ma and fail to produce an inverse isochron.

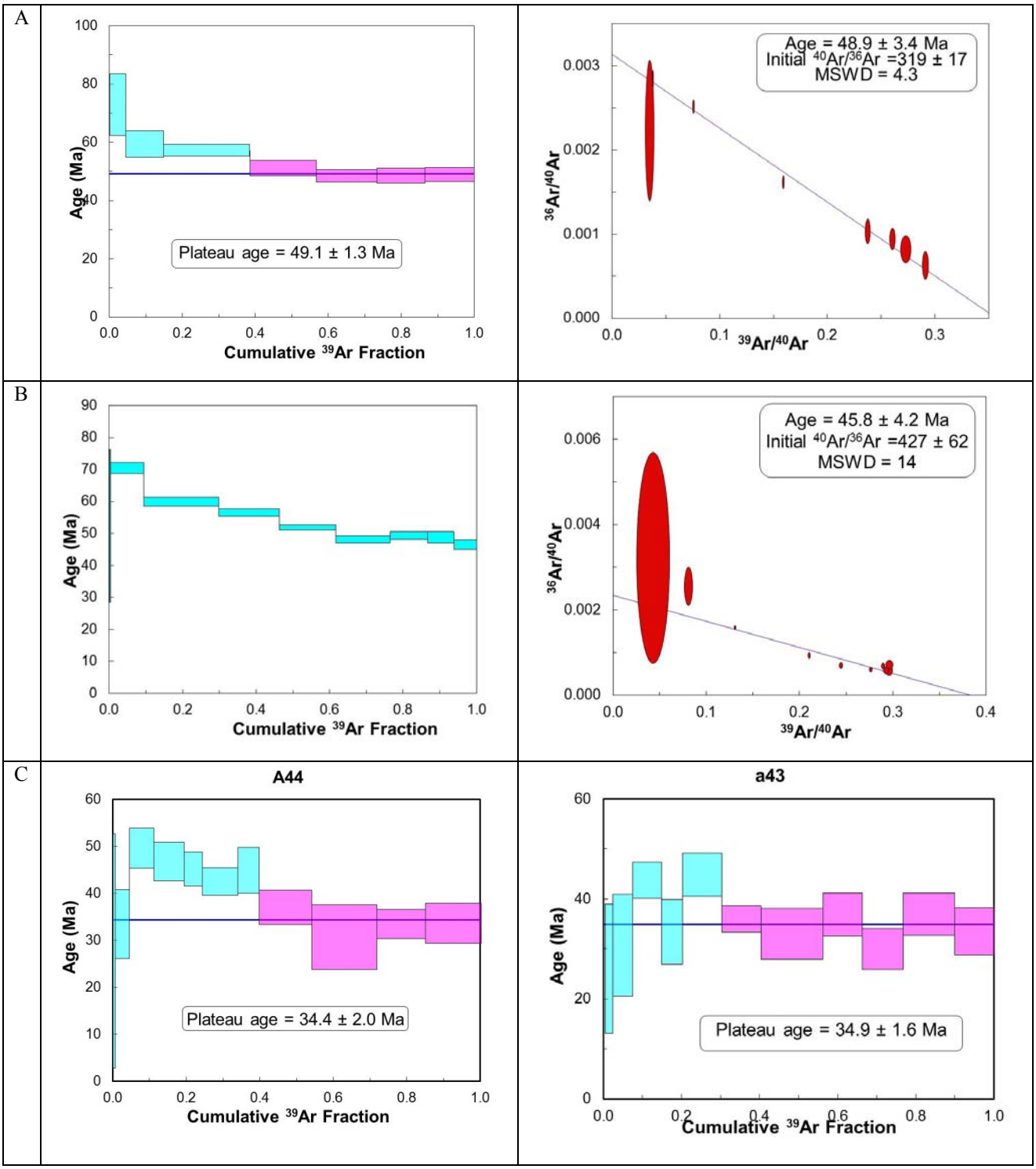

Figure 2: Step heating diagrams and inverse isochrons from the base of the Malinstindur Fm. A = AMH3, B = AH10-4, C = AH10-15 (A44) and AH10-15 (A43),

12.2.2. Samples from close to the Kvívík Beds

The release spectrum from samples AH10-39 (figure 3A) and AH10-41 both show disturbed patterns of release, with ages dropping rapidly to 0Ma (or to negative apparent ages). The large errors on the apparent ages for the steps of both these samples may be in part, related to the very low K contents and very high Ca contents, shown by the very high $^{37}Ar_{Ca}/^{39}Ar_K$ ratios from these samples.

From sample AH10-56, a groundmass separate (figure 3B) produced a descending release spectra (apparent ages dropping from ~52 to 35Ma) and failed to produce an inverse isochron. A plagioclase separate from this sample (figure 3C) produced a plateau age of 42.4±19Ma, the inverse isochron plot of this data gives a younger age of 36.5±4.3Ma and the $^{40}Ar/^{36}Ar$ intercept suggests the presence of excess argon, with a ratio of 334±33.

From sample AH10-45 (stratigraphically above AH10-39 & 41 from the same hillside), the release spectrum shows some disturbance (figure 3D), but not as much as for AH10-39 & 41 and from 1 of the analysed splits from this sample the inverse isochron suggests an age of 52.1±1.7Ma and a $^{40}Ar/^{36}Ar$ ratios above atmospheric at 356±26. This age is within error of the weighted mean age of the last 4 steps of the release spectrum (failed to produce a plateau age but these steps are similar in apparent age) [weighted mean of last 4 steps = 53.24±0.42Ma].

A	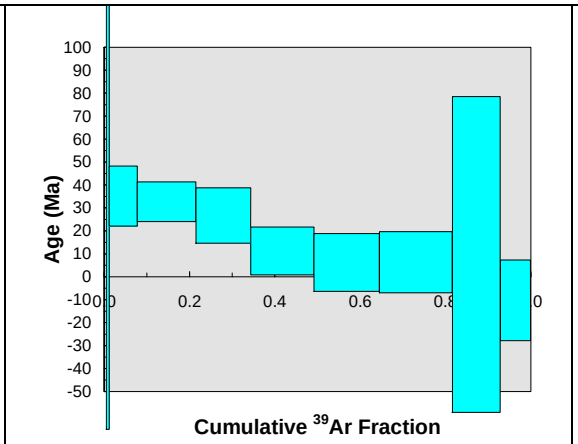	
B	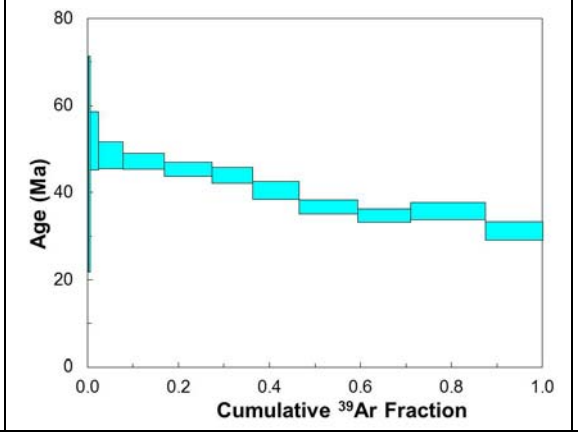	

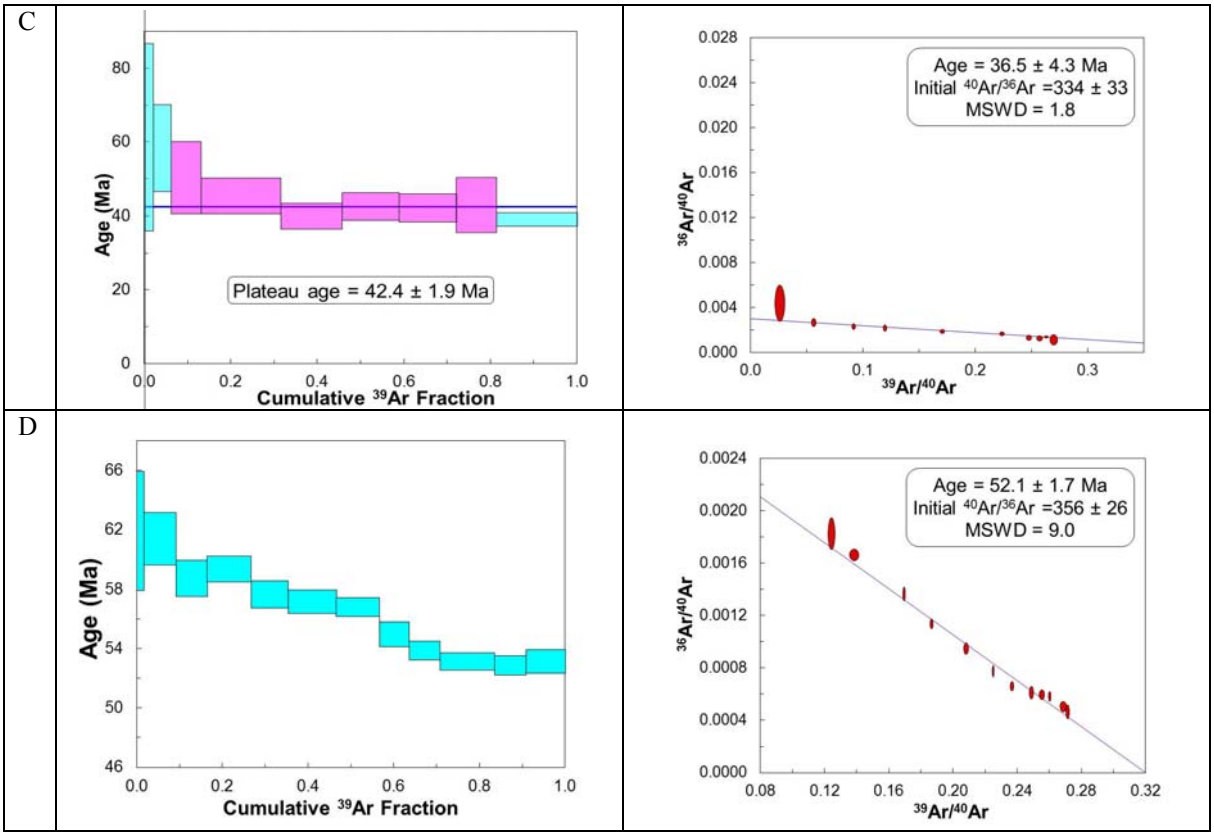

Figure 3: Step heats and inverse isochrons from the middle of Malinstindur Fm, A = AH10-39, B = AH10-56 (Whole rock), C = AH10-56 (plagioclase), D = AH10-45

12.2.3. From the top of the Malinstindur Fm

Groundmass analysed from Sample AH10-25 failed to meet the plateau criteria (figure 4A), with the most concordant portion of the release spectrum, steps 2-8, giving a weighted mean age of 54.1±1.5Ma, the inverse isochron shows large disturbance and big errors. A plagioclase separate from this sample produced a much younger plateau age of 35.7-±1.5Ma and the clustering of the data on the $^{39}Ar/^{40}Ar$ axis of the inverse isochron plot produces poor determination of the age and $^{40}Ar/^{36}Ar$ intercept. Sample AH10-27 produced 2 plateau ages from the 2 splits analysed, 48.2±1.5Ma (A79, figure 4B) and 51.74±0.86Ma (A80, figure 4C), these 2 ages are not within error of each other. Inverse isochrons from these data show ages younger than the plateau age for A79, (32.0±9.5Ma) and an age within error of the plateau age for A80 (49.9±3.8Ma), the $^{40}Ar/^{36}Ar$ intercepts from these inverse isochrons show large errors (467±110 for A79 and 361-±73 for A80). Sample AH10-28 (figure 4D) was collected from the flow above AH10-27, and produced a plateau age of 56.86±0.86Ma from split A81 while split A82 failed to meet the plateau criteria but a weighted mean of the final 55.9% of the ^{39}Ar release (last 5 steps) gives an age of 58.88±0.31Ma. The inverse isochron of this sample suggests an age within error of the plateau age for split A81, at 56.2±2.0Ma; the $^{40}Ar/^{36}Ar$ ratio has a large error on but suggests a value above atmospheric (489±110).

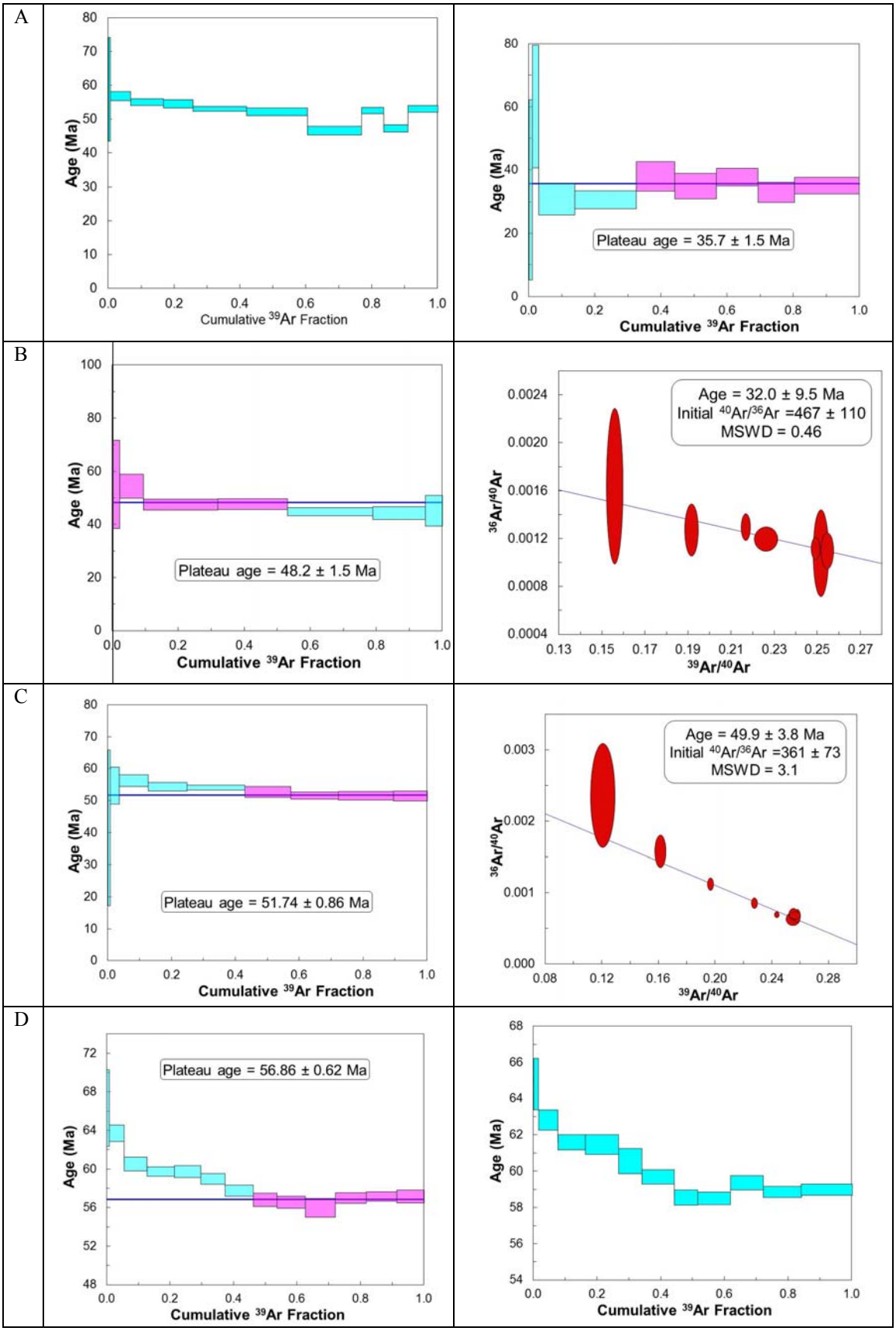

Figure 4: Step heats and inverse isochrons from the top of the Malinstindur Fm. A = AH10-25 Whole rock and plagioclase, B = AH10-27 (A79), C = AH10-27 (A80), D = AH10-28

12.2.4 .Enni Fm

Stratigraphic position*	Sample	split	Plateau age	%^{39}Ar	Inverse isochron age	^{40}Ar/^{36}Ar intercept
1577	AH10-18	A47	43.32 ± 0.7Ma	44.1		
1597	AH10-19	A52	No plateau			
1664	AH10-21	A100	51.4 ± 1.3Ma	70	49.5 ± 2.8Ma	313 ± 23
		A101	50.6 ± 1.6Ma	72.5	47.5 ± 2.9Ma	346 ± 31
1664	AH10-22	A90	50.9 ± 2.1Ma	98.1	48.7 ± 3.9Ma	308 ± 19
		A91	49.5 ± 2.1Ma	79.1	49.3 ± 5.6Ma	299 ± 24
1358	AH10-33	A73	No plateau			
		A74	44.4 ± 2.7Ma	61.2	34.1 ± 3.4Ma	305.9 ± 4.6
1643	AH10-50	A98	48.0 ± 1.6Ma	65.1		
		A99	46.8 ± 1.4Ma	87.9	49.7 ± 2.4Ma	217 ± 52
1367	AH11-1	A87	58.66 ± 0.89Ma	87.9	57.0 ± 1.3Ma	311 ± 12
1338	LCF25	A102	51.4 ± 2.0Ma	64.2	54.3 ± 4.5Ma	281 ± 13
		A103	49.4 ± 2.6Ma	100	47.3 ± 3.7Ma	302.1 ± 8.6

Table 3: ^{40}Ar/^{39}Ar data for samples from the Enni Fm. *= stratigraphic positions relative to the base of the Malinstindur Fm (in meters). All samples are of basalt groundmass.

Sample AH10-33 from within the Enni Fm shows a lot of disturbance (figure 5A), with a release spectrum that has large errors and apparent ages dropping to ~0Ma, the ^{37}Ar/^{39}Ar ratios are very high for this sample and it fails to calculate an inverse isochron age. The release pattern from a repeat of this sample (A74) produced a much more coherent release pattern, with a plateau age of 44.4±2.7Ma. The inverse isochron from this data suggests a younger age of 34.1±3.4Ma with a ^{40}Ar/^{36}Ar intercept of 305.9±4.6. The very high ^{37}Ar/^{39}Ar ratios from this sample, up to ~140, suggest that the sample had very low K content, especially in the higher temperature portion of the release, the release from Ca plagioclase and pyroxenes (minerals with essentially no K_2O).

Sample AH10-18 from the Enni Fm (figure 5B) also produced a disturbed release spectrum and the very narrow range of ^{39}Ar/^{40}Ar ratios leads to clustering on the inverse isochron and it fails to produce a meaningful age or ^{40}Ar/^{36} Ar intercept value. Sample AH10-19 from the Enni Fm failed to produce a plateau age, with a decreasing age spectrum, the weighted average of all the steps gives an age of 55.1±3.1Ma but the data fail to plot an inverse isochron. Sample AH10-21 (figure 5C) produced a plateau age of 51.4±1.3Ma from split A100 and the inverse isochron produces a slightly younger age of 47.2±2.0Ma and a ^{40}Ar/^{36}Ar intercept above atmospheric at 328±20. Split A101 from this sample produced a plateau age of 50.6±1.6Ma and again a younger inverse isochron age of 47.5±2.9Ma and higher ^{40}Ar/^{36}Ar intercept ratio of 346±31. Sample AH10-22 (figure 5D) produced a plateau age of 50.9±2.1Ma (from split A90) and 50.8±2.1Ma from split A91. The average of these 2 ages is 50.9±1.5Ma and the inverse isochrons produced ages within error of the plateau ages with ^{40}Ar/^{36}Ar ratios within error or only slightly higher than atmospheric (313±17 for A90 and 297±24 for A91).

A plateau age of 48.0±1.6Ma was produced from sample AH10-50 (split A98) and slightly younger, but within error age from repeat (split A99) of 46.8±1.4Ma (figure 5E). With this sample all the points plot with almost the same ratios on an inverse isochron correlation plot and so fail to produce meaningful isochron ages of $^{40}Ar/^{36}Ar$ ratios. Sample AH11-1(figure 5F) produces a plateau age of 58.66±0.89Ma with the inverse isochron plot producing an age within error at 57.0±1.3Ma and a $^{40}Ar/^{36}Ar$ ratio only slightly higher than atmospheric at 311±12. The 2 plateau ages produced from sample LCF25 (figure 5G) are within error although that from A102 (51.4±2.0Ma) shows greater disturbance with younger ages in the initial low temperature release portion than the release spectrum from A103 (49.4±2.5Ma) where the plateau contains 100% of the gas released.

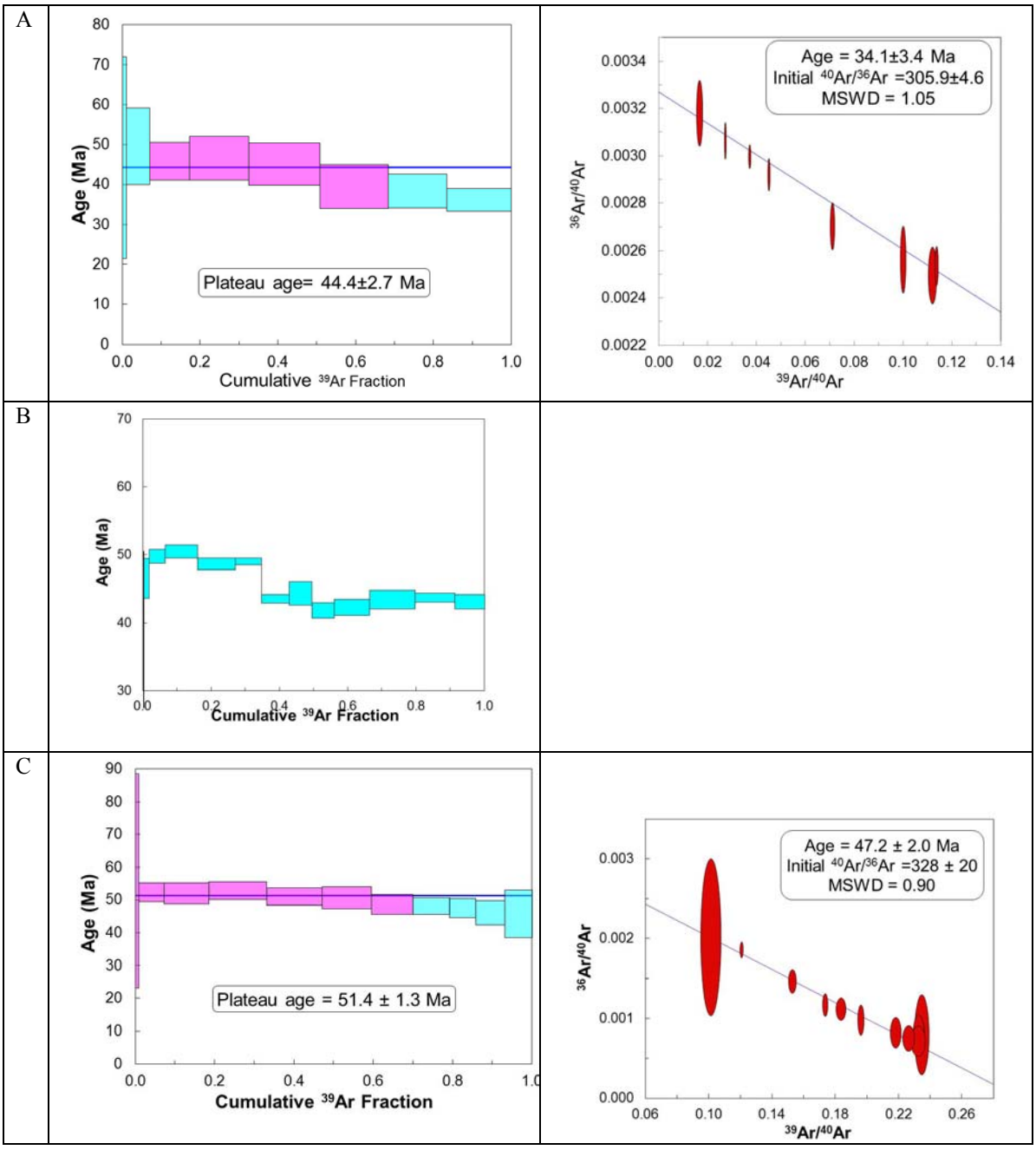

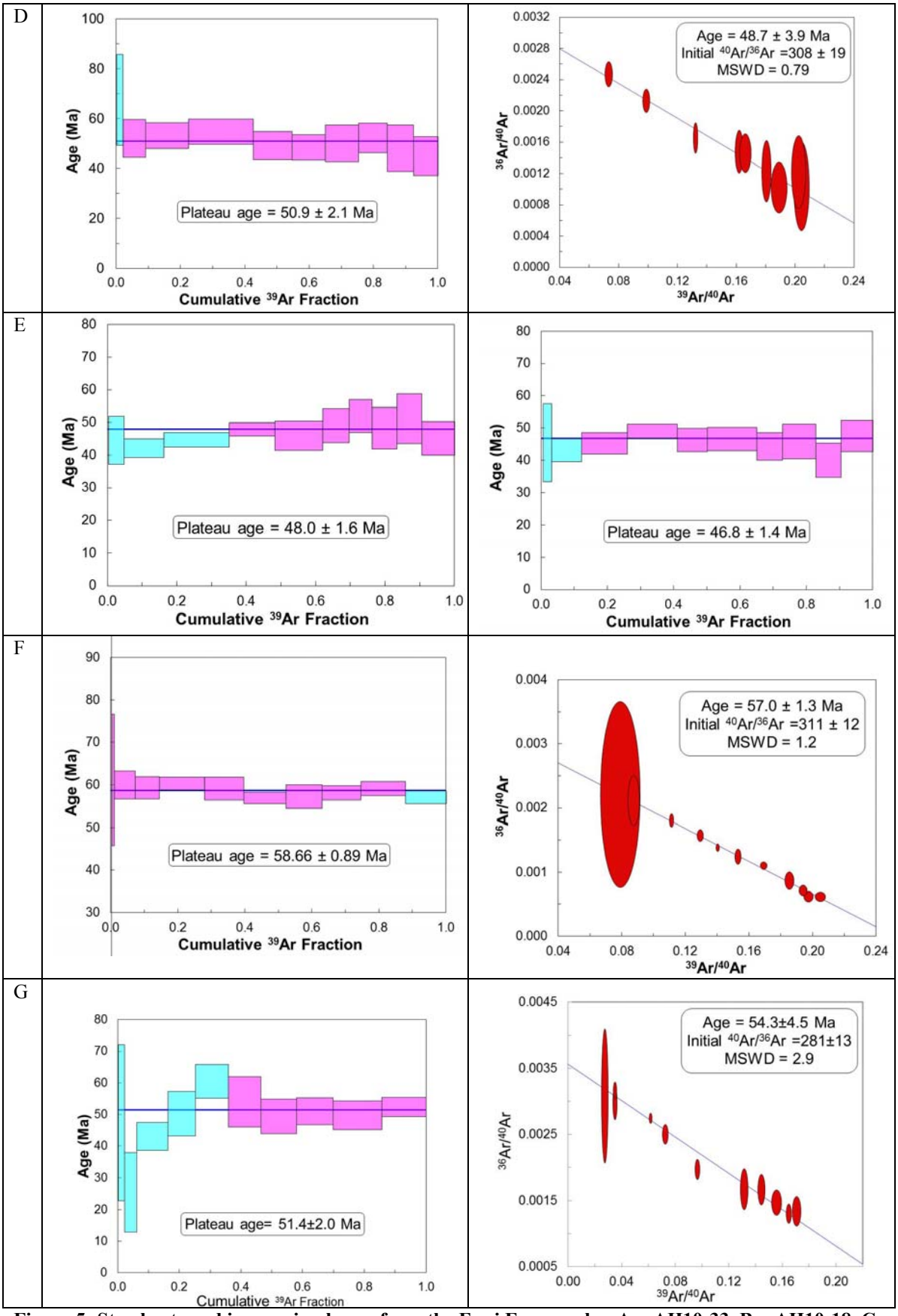

Figure 5: Step heats and inverse isochrons from the Enni Fm samples. A = AH10-33, B = AH10-18, C = AH10-21 (A100), D = AH10-22 (A90), E = AH10-50 (A98 & A99), F = AH11-1, G = LCF 25 (A102)

12.3. Intrusives

Intrusion	Sample	split	Plateau age	%^{39}Ar	Inverse isochron age	^{40}Ar/^{36}Ar intercept
Eysturoy Sill	AH10-36	A65	51.57 ± 0.57Ma	54.8	50.77 ± 0.99Ma	403 ± 47
		A66	No plateau		52.2 ± 1.1Ma	361 ± 40
Eysturoy Sill	AH10-37	A92	61.0 ± 1.4Ma	44.5		
Eysturoy Sill	AH10-38	A77	51.31 ± 0.81Ma	62.8	48.4 ± 1.5Ma	379 ± 29
		A78	No plateau			
Streymoy Sill	AH10-48	A53	No plateau		50.9 ± 6.2Ma	318 ± 15
		A54	No plateau			
Streymoy Sill	AH10-49	A75	No plateau		29 ± 16Ma	402 ± 51
		A76	No plateau		51.8 ± 2.8Ma	335 ± 12
Prestfjall	AH10-1	A57	41.84 ± 0.76Ma	73.2		
Prestfjall	AH10-12	A45	No plateau		33.0 ± 7.0Ma	472 ± 85

Table 4: ^{40}Ar/^{39}Ar data summary for intrusives from the Faroe Islands. All data are from basalt groundmass. GPS location information for the samples is in Appendix 1.

12.3.1. Eysturoy Sill

Sample AH10-36 (figure 6A) from the base of the Eysturoy Sill, produced a plateau age of 51.57±0.57Ma (split A65), and an inverse isochron age within error of this at 50.77±0.99Ma. The ^{40}Ar/^{36}Ar intercept of 403 ±47, from the inverse isochron is above the atmospheric ratio of 295.5. Another split from this sample (A66) produced a release spectrum with the final step containing 41.6% of ^{39}Ar release, an inverse isochron of all steps gives an age of 52.2 ± 1.1 Ma (with a ^{40}Ar/^{36}Ar intercept of 361±40, an intercept above atmospheric, suggesting there may be some excess argon within the sample, probably releasing in the lower temperature steps which have older apparent ages).

Sample AH10-37 (figure 6B) was taken from the coarser grained centre of the sill and failed to produce a statistically valid plateau age (Split A92), with an age of 61.0±1.4Ma from steps 4-6 of the release, containing 44.5% of the ^{39}Ar release. The final 30% of the release spectra gives a younger apparent age of 54.6±2.2Ma while the inverse isochron plot fails to calculate an age or ^{40}Ar/^{36}Ar intercept due to the small spread of ratios.

From the top of the Eysturoy sill sample AH10-38 (figure 6C), produced plateau age of 51.31 ± 0.81 Ma, (split A77) and an inverse isochron gave an age of 48.4±1.5 Ma. The initial ^{40}Ar/^{36}Ar ratio from the isochron, of 379±29, is above atmospheric ratio, suggesting the presence of excess argon within the sample. The other split of this sample (a78) produced a descending release spectrum and the inverse isochron shows the data does not fall upon 1 line and so is unable to calculate an age.
A weighted mean of the 2 plateau ages from the Eysturoy sill 51.48±0.47Ma (n=2).

A	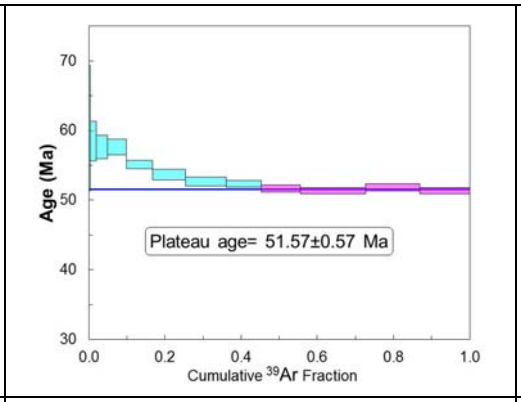 Age (Ma) Plateau age= 51.57±0.57 Ma Cumulative ^{39}Ar Fraction	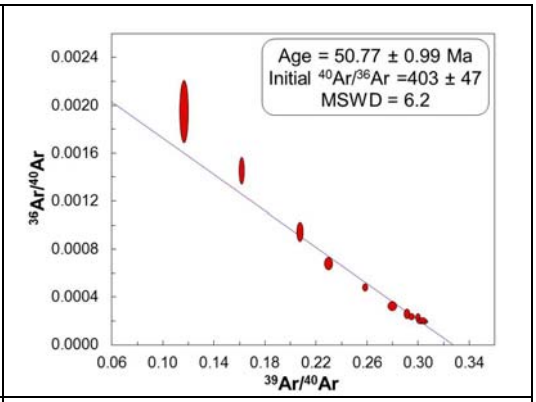 Age = 50.77 ± 0.99 Ma Initial ^{40}Ar/^{36}Ar =403 ± 47 MSWD = 6.2 ^{36}Ar/^{40}Ar ^{39}Ar/^{40}Ar
B	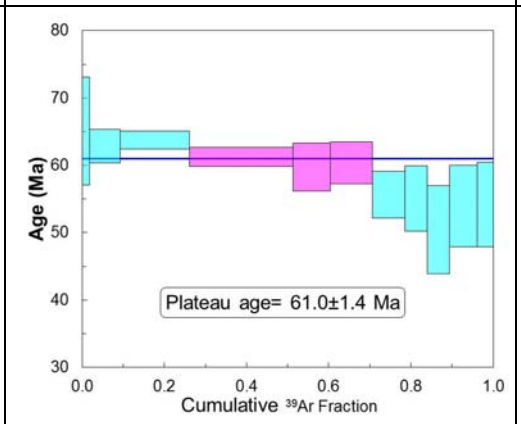 Age (Ma) Plateau age= 61.0±1.4 Ma Cumulative ^{39}Ar Fraction	
C	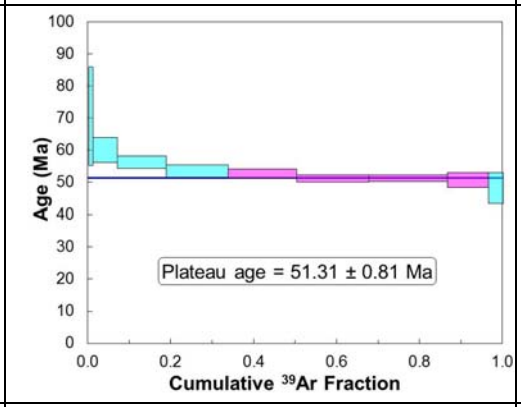 Age (Ma) Plateau age = 51.31 ± 0.81 Ma Cumulative ^{39}Ar Fraction	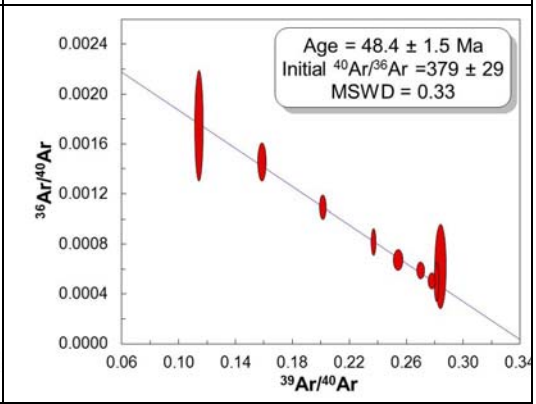 Age = 48.4 ± 1.5 Ma Initial ^{40}Ar/^{36}Ar =379 ± 29 MSWD = 0.33 ^{36}Ar/^{40}Ar ^{39}Ar/^{40}Ar
D	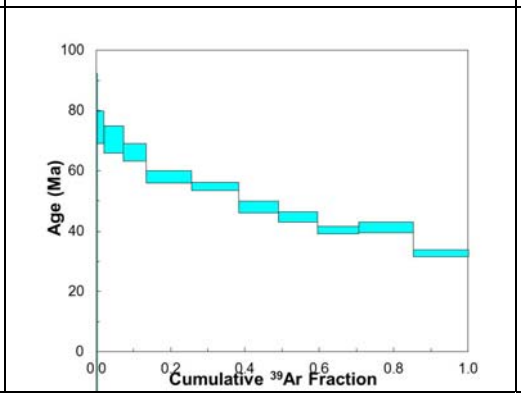 Age (Ma) Cumulative ^{39}Ar Fraction	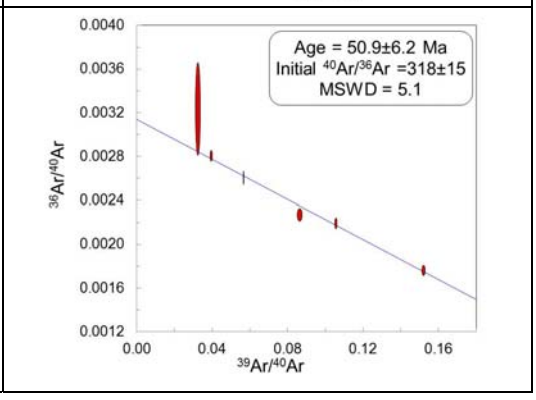 Age = 50.9±6.2 Ma Initial ^{40}Ar/^{36}Ar =318±15 MSWD = 5.1 ^{36}Ar/^{40}Ar ^{39}Ar/^{40}Ar

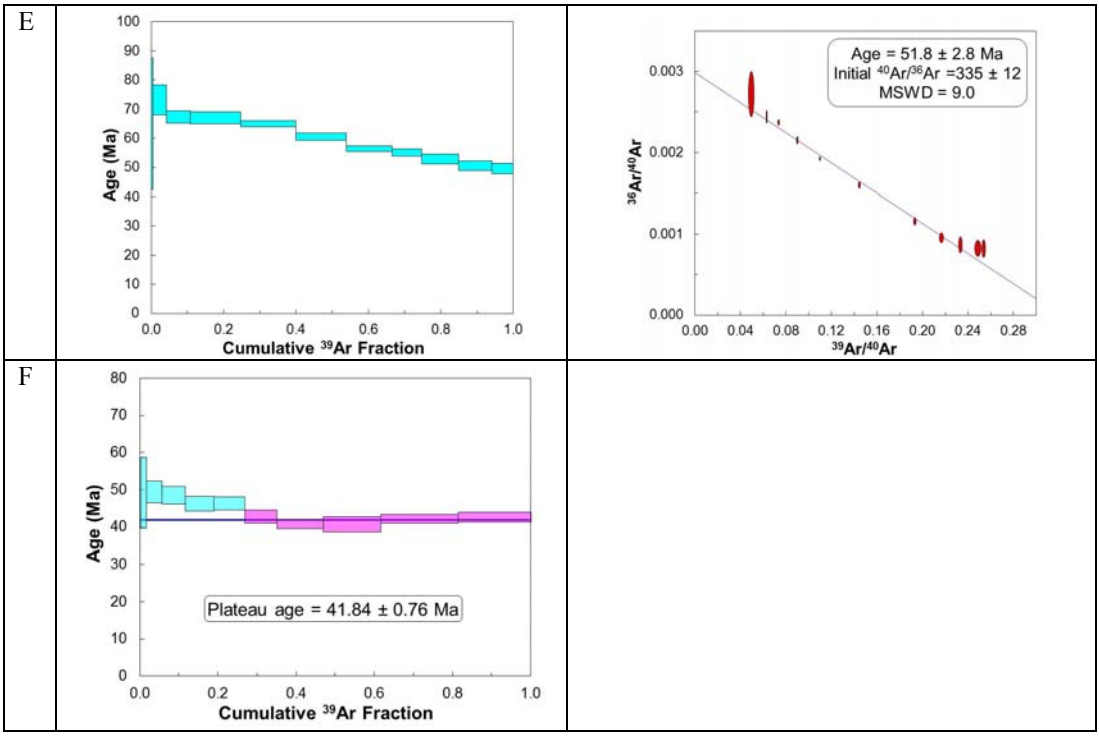

Figure 6: Step heating diagrams and inverse isochrons from samples from the Faroe Islands Intrusives. A = AH10-36 (A65), B = AH10-37, C = AH10-38, D = AH10-48, E = AH10-49, F = AH10-1,

12.3.2. Streymoy Sill

2 samples were collected from the Streymoy Sill, sample AH10-48 is from the base of the sill and is very fine grained and appears chilled in contact with the lava below, whilst AH10-49 is from ~1m above the base, where the basalt is more massive. Both splits (a53 and a54) from AH10-48 (figure 6D) have a decreasing release spectrum, matched to increasing $^{37}Ar/^{39}Ar$ spectra with increasing temperature release. The inverse isochron of this sample shows points falling within 2 groups, using the 1st 6 steps of the step heat the inverse isochron gives an age of 50.9 ± 6.2 Ma with a $^{40}Ar/^{36}Ar$ ratio of 318±15. From sample AH10-49, A75 shows a decreasing spectrum, from ~80Ma in the initial low temperature steps to ~40Ma in the final 3 steps, the inverse isochron also shows disturbance, with an age of 29±16Ma and a $^{40}Ar/^{36}Ar$ intercept greater than atmospheric composition, at 402±51. Split A76 from sample AH10-49 (figure 6E) shows a very similar spectrum to A75, although the drop in ages with increasing temperature is less dramatic, from 67Ma to 49Ma and the $^{37}A/^{39}Ar$ ratios in A75 reach a maximum of ~28, whilst the ratios in A76 reach ~58. The inverse isochron plot for this split of the sample gives an age of 51.8±2.8Ma with a $^{40}Ar/^{36}Ar$ intercept ratio of 335±12. Irradiation induced recoil loss of ^{39}Ar may be responsible for the disturbances to the release spectra of these fine grained sill samples, leading to older apparent ages in the initial low temperature steps and the best estimate for the age is the inverse isochron age of 51.8±2.8Ma, an age within error of that produced for the Eysturoy Sill.

12.3.3. Irregular Intrusions

2 samples from irregular intrusions within the Prestfjall Fm were dated. Sample AH10-1 (figure 6F) produced a plateau age of 41.84±0.76Ma and sample AH10-12 failed to produce a plateau, with a descending release spectra and an inverse isochron showing discordance (inverse isochron age of 33.0±7.4Ma and a $^{40}Ar/^{36}Ar$ intercept of 472±90). Both these

samples show high levels of alteration in the field/hand specimen and this is likely to be responsible for the disturbed Ar data and the younger than expected plateau age from sample AH10-1.

12.3.4. Dykes

Sample	split	Plateau age	%^{39}Ar	Inverse isochron age	^{40}Ar/^{36}Ar intercept
AH10-52	A55	36.0 ± 1.2Ma	63.2	31.2 ± 4.4Ma	321 ± 13
	Plagioclase	51.6 ± 2.6Ma	92.8	52.2 ± 2.9Ma	286 ± 20
AH10-53	A94	49.2 ± 1.8Ma	100	48.5 ± 2.8Ma	300 ± 13
AH10-55	A97	49.2 ± 2.0Ma	100	48.9 ± 2.6Ma	299 ± 23
AH11-2	A89	53.0 ± 2.4Ma	91.9	51.7 ± 6.0Ma	309 ± 76
	A88	52.6 ± 2.7Ma	67.6		
AH11-3	A104	55.5 ± 2.5Ma	74.3	55.5 ± 3.7Ma	295.5 ± 9.8
AH11-4	A107	58.7 ± 2.1Ma	65.3	52.4 ± 3.1Ma	336 ± 23

Table 5: ^{40}Ar/^{39}Ar data summary for Dyke samples. All samples are of basalt groundmass unless labelled as plagioclase. GPS location data for the samples is in Appendix 1.

A multiple dyke was sampled at Stykkid, near Kvívík on Streymoy that is ~5m wide with large plagioclase phenocrysts which are aligned parallel to the sides of the dyke. On either side of the dyke there is a fracture zone (1-2m wide) and the presence of slickensides on some of the surfaces suggests some movement and the dyke may have exploited this pre-existing fracture. 3 samples were dated from the exposure, AH10-52, AH10-53 and AH10-55. Sample AH10-52 (figure 7A) produced a plateau age of 36.0±1.2Ma from a groundmass separate whilst a plagioclase separate gave an age of 51.6±2.8Ma. The plateau ages produced from samples AH10-53 and AH10-55 from the multiple dyke are within error of each other, at 49.2±1.8Ma (for AH10-53) and 49.2± 2.0Ma (from AH10-55, figure 7B). The inverse isochrons from samples AH10-53 and AH10-55 produced ages within error of the plateau ages and have ^{40}Ar/^{36}Ar intercepts within error of an atmospheric ratio of 295.5. These plateau ages are within error of the plateau age from the plagioclase separate from sample AH10-52.

Samples were also collected from 3 other dykes, cutting lavas of the Malinstindur Fm on Eysturoy. Sample AH11-3, produced a plateau age of 55.5±2.5 Ma (figure 7D), which is older than (but within error of) the age of the Malinstindur Fm. An older than expected age was also produced from sample AH11-4, which gave a plateau age of 58.7±2.1Ma (figure 7E). From this sample, the inverse isochron suggests a younger age of 52.4±3.1Ma and a ^{40}Ar/^{36}Ar intercept of 336±23, suggesting the presence of excess argon within the sample and this may be causing the older plateau age, which is older than the lavas it intrudes. The plateau age from sample AH11-2 (figure 7C) was younger than that from AH11-3 and AH11-4 at 52.6±2.7Ma (split A88) and 53.0±2.4Ma (split A89). There is less discordance in the release spectra for split A89 and the inverse isochron calculates an age of 51.7±6.0 with a ^{40}Ar/^{36}Ar intercept ratio of 309±76 (within error of atmospheric). The average of the 2 plateau ages from sample AH11-2, at 52.8±1.8Ma is the best estimate for the age of this dyke.

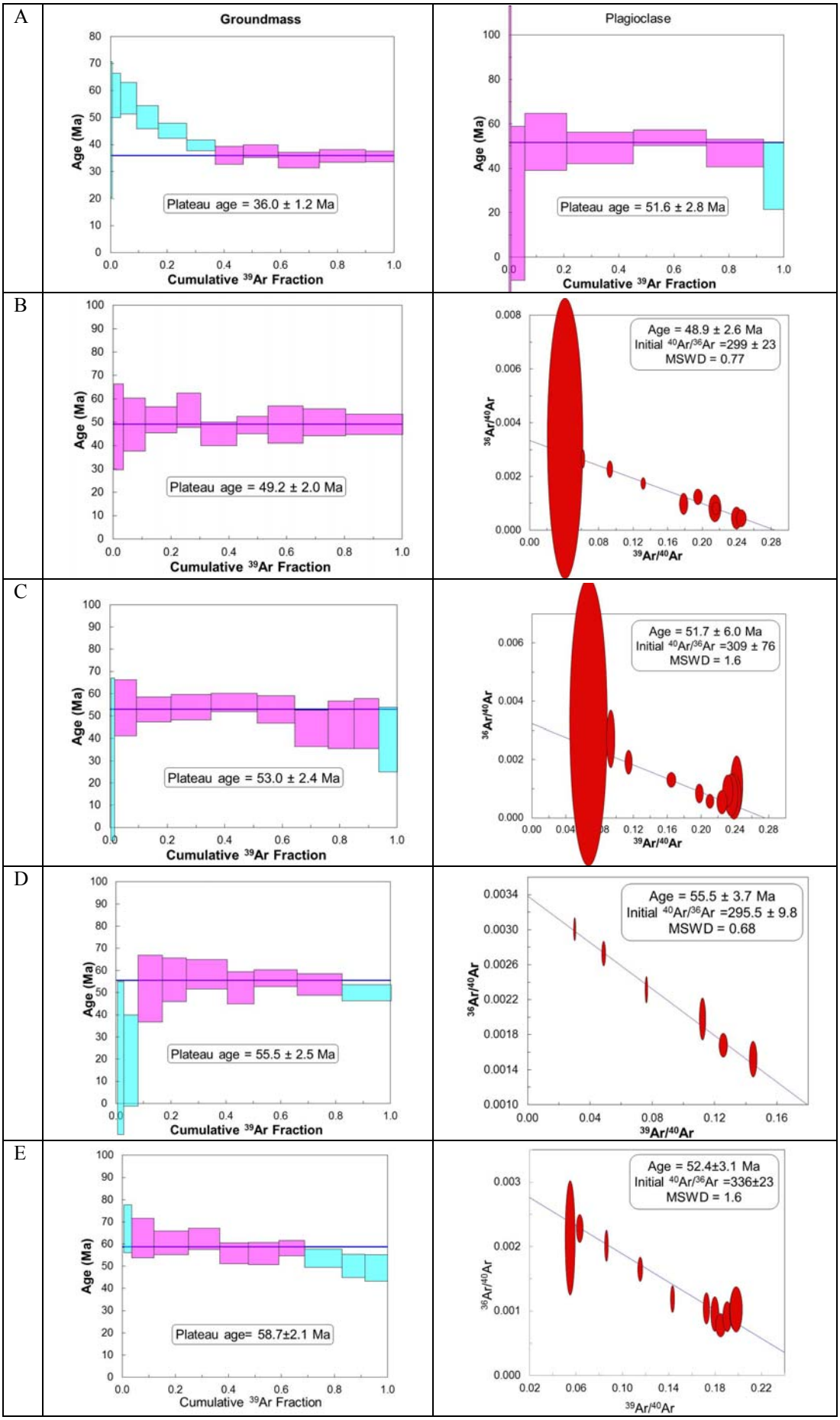
A
Groundmass
Age (Ma)
Plateau age = 36.0 ± 1.2 Ma
Cumulative ^{39}Ar Fraction
Plagioclase
Plateau age = 51.6 ± 2.8 Ma
B
Plateau age = 49.2 ± 2.0 Ma
Age = 48.9 ± 2.6 Ma
Initial ^{40}Ar/^{36}Ar =299 ± 23
MSWD = 0.77
^{36}Ar/^{40}Ar
^{39}Ar/^{40}Ar
C
Plateau age = 53.0 ± 2.4 Ma
Age = 51.7 ± 6.0 Ma
Initial ^{40}Ar/^{36}Ar =309 ± 76
MSWD = 1.6
D
Plateau age = 55.5 ± 2.5 Ma
Age = 55.5 ± 3.7 Ma
Initial ^{40}Ar/^{36}Ar =295.5 ± 9.8
MSWD = 0.68
E
Plateau age= 58.7±2.1 Ma
Age = 52.4±3.1 Ma
Initial ^{40}Ar/^{36}Ar =336±23
MSWD = 1.6

Figure 7: Step heating diagrams and inverse isochrons for Faroe Island Dykes. A = AH10-52, B = AH10-55, C = AH11-2, D = AH11-3, E = AH11-4,

13. Discussion

13.1. Ages for the Beinisvørð Fm

The analysis samples from the 5 intervals of the Beinisvørð Fm from the Lopra 1/1A borehole show a range of plateau age and show that the Ar system in these basalts has been disturbed. The lack of consistency (both within samples from the same interval and between intervals) makes the interpretation of the data more difficult. The age of 59.40±0.49Ma from the uppermost dated sample from the Lopra 1/1A borehole (Lava 1, 1260m below top of Beinisvørð Fm) is within error of the age of 59.9±0.7Ma from this interval published by Storey et al. (2007). The lava 2 interval produced a range of ages (between 56.3 and 66Ma) with inverse isochrons suggesting excess argon affecting the Ar system in this interval. The ages from Lava 3 are Cretaceous and can be disregarded as too old and due to excess argon. The plateau ages from lava 4 interval (-2850m) give an average of 56.11±0.57Ma, this age is much younger than the age produced for the top of the Lopra 1/1A borehole and the published age for this interval of 60.1±0.6Ma (Storey et al. 2007). The plateau ages from the stratigraphically lowest sample dated (3100m below top Beinisvørð, Lava 5) are also younger than those above at 45.6±1.4 and 50.8±1.3Ma and together the data show that there is no apparent increase in age with depth as would be expected but the data appear to show increasing disturbance to the Ar system with depth, this could be due to increase temperatures due to burial depth (see section 13.4.2) and/or variations in chemistry (section 13.4.4).

13.2. Age of the Malinstindur and Enni Fm Volcanism

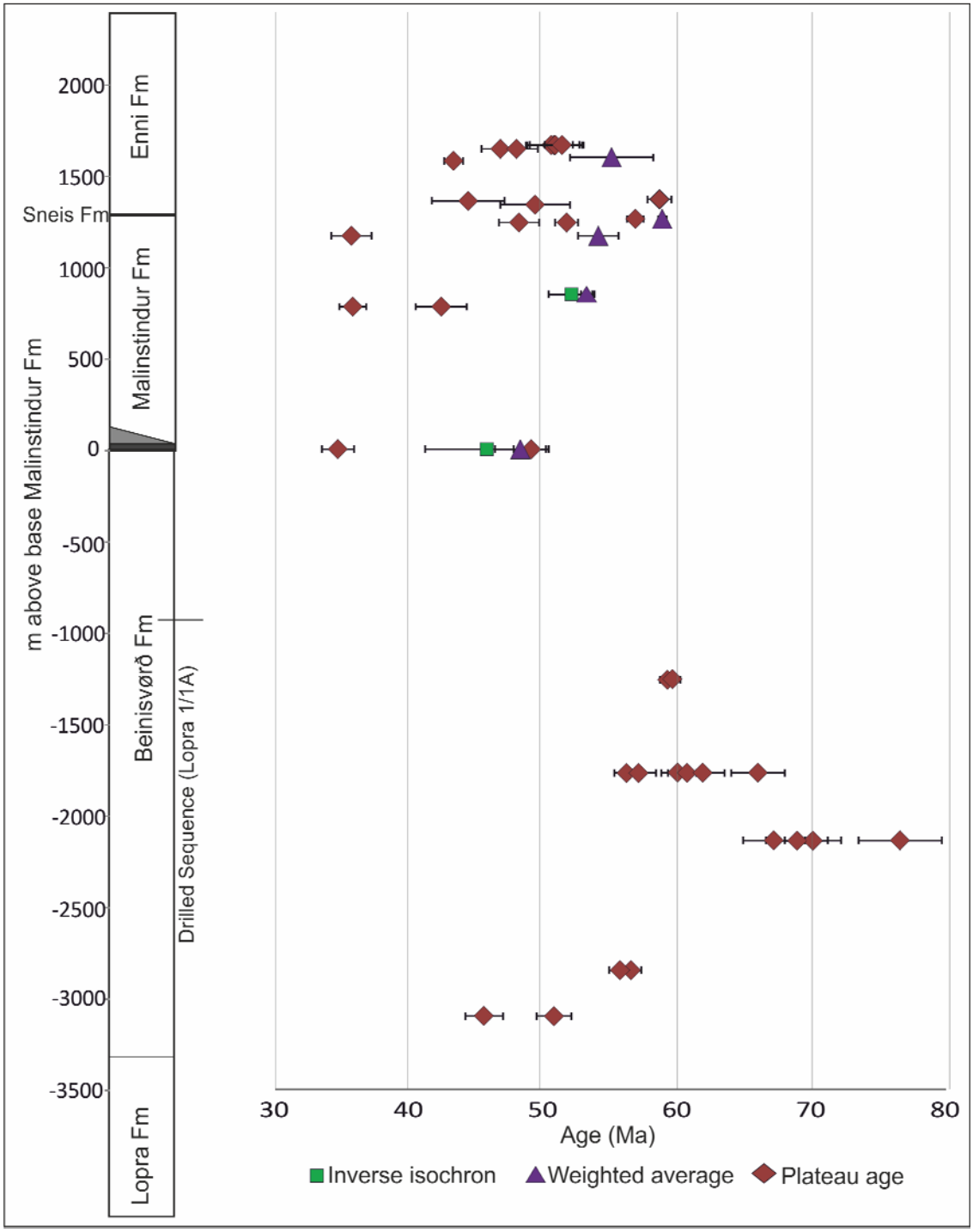

Figure 8: Ar ages plotted against the stratigraphy of the FIBG. Ages are plotted with a 2σ error bar.

Figure 8 shows the plateau ages produced from the samples from the Malinstindur and Enni formations against the stratigraphy and shows that there is no clear pattern of age variations. There is a wide range of apparent ages produced from the samples with many/most of the ages produced for the Malinstindur and Enni Fms were younger than expected, and younger than the published ages for these formations (54.9±0.7 and 55.2±0.7Ma, Storey et al. 2007). Younger than expected plateau ages could be the result of several effects on the Ar system of the basalts. A younger apparent age requires a lowering of the $^{40}Ar^*/^{39}Ar$ ratio of the samples and this could be a result of lowering the $^{40}Ar^*$ (radiogenic

^{40}Ar) content calculated for the sample. This could be a result of Ar loss as discussed in Foland et al. (1993), when the highest K content is found mainly in the matrix of the basalt, the fine-grained and unstable nature of the minerals and glass forming the basalt groundmass make them prone to Ar* loss even from mild disturbances, such as hydration reactions at surface temperatures.

The data also show some other indicators of disturbances to the Ar system, including ^{39}Ar recoil loss and the presence of excess argon ($^{40}Ar_E$). ^{39}Ar recoil loss during irradiation will lead to higher ^{40}Ar*/^{39}Ar ratios and older apparent ages and typically these older ages occur in the initial, low temperature release steps, where the ^{39}Ar is lost from fine grained clays and alteration products within the sample. As most of the plateau ages don't contain this initial portion of gas release, the effects of recoil may only affect the calculated plateau age is as well as ^{39}Ar loss due to recoil, there is relocation of the ^{39}Ar. During irradiation, the ^{39}Ar that is recoiled from the mineral may not be lost from sample completely but relocate into adjacent minerals with lower K contents (containing less ^{39}Ar), when these phases release their argon during step heating it can result in younger apparent ages in the final steps of release and produce a release spectra that is meaningless with regard to the age of the sample.

The inverse isochron correlation plots for some of the samples give ^{40}Ar/^{36}Ar ratios above the atmospheric ratio of 295.5, suggesting the presence of excess argon within the sample and this will lead to older apparent ages. In many cases this is likely to be associated with alteration products and is released in the initial, lower temperature steps of the release as suggested by the shape of many of the release spectra. This pattern of older apparent ages in the initial steps is the same as can be produced by recoil and in the fine grained basalt samples which have experienced alteration it is possible that both effects have occurred.

The combination of disturbances to the argon system in the Faroe Islands basalts (recoil loss, $^{40}Ar_E$ and some Ar loss) may be producing a variety of effects on the samples and depending on the samples exact mineralogy/chemistry and the degree of alteration one may be more dominant and in the step heating release the differing effects on the different mineral phases in the basalt sample leads to release patterns that are complicated and not always reproducible.

13.3. Timing of Intrusive activity

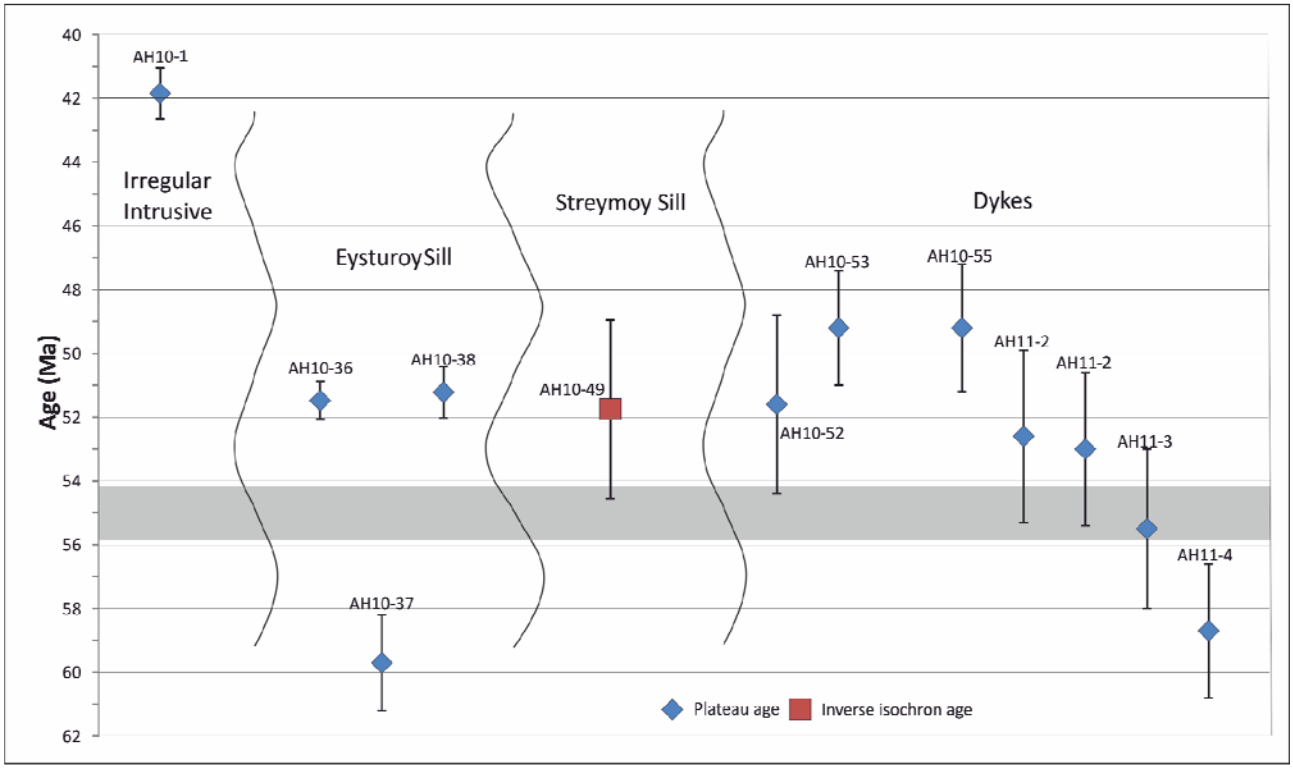

Figure 9: Step heating (+1 inverse isochron age) for the intrusive rocks sampled from the Faroe Islands (2σ errors). Grey box represents the published ages from the Malinstindur and Enni Fms (ages of Storey et al. 2007).

The ages for the sills determined here are younger than those for the lavas, in agreement with published descriptions of field and cross cutting relationships, suggesting that the sills represent the final stages of activity on the Faroe Islands. The ages for the dykes are much closer to the ages determined from the lavas and suggests that these were intruded at the same time/just after the eruption of the lava flows of the Malinstindur and Enni Fms (as suggested by Rasmussen & Noe-Nygaard 1969; 1970, Hald & Waagstein 1991 etc..).

The ages from the irregular intrusives found within the Prestfjall Fm are younger than expected and due to the high degree of alteration suffered by these samples and the disturbed spectra; this age is likely to be too young. From the saucer shaped sills, the 2 within error ages from the Eysturoy sill are within error of the inverse isochron age for the Streymoy Sill and the older apparent age from sample AH10-37 should be disregarded as too old.

A range of ages are seen from the dykes cutting the Malinstindur Fm, the oldest age, from sample AH11-4 (58.7 ± 2.1Ma) is elevated by the presence of excess argon and is older than the age of the Malinstindur Fm and so can be disregarded. The ages from the multiple dyke locality (AH10-52-55) are within error of each other and so likely to be a good representation of the age of this sample. The ages from samples AH11-2 & 3 are older but are still younger or within error of the age of the Malinstindur Fm and so are stratigraphically realistic. It is possible that the dykes were intruded into the Faroe Islands Basalt Group lavas at more than 1 time, with intrusion either over an extended time period or in multiple events with analysis of more samples needed to confirm this.

13.4. Understanding of the Ar system in the FIBG (and in basalts more generally)

The dating of the Malinstindur and Enni formations was particularly difficult and the data produced is much less reliable and much more disturbed than that produced from the basalts of the Beinisvørð Fm (drilled and exposed, with the drilled better than that exposed on Suðuroy). Some of this variation may be due to the differences in the physical characteristics of the lava flows. Within the Malinstindur Fm in particular (and much of the Enni Fm) the lavas are compound lava flows, unlike the much more massive simple inflated lobes of the Beinisvørð Fm and part of the Enni Fm (Passey & Bell 2007). This difference in the eruption style is likely to have affected the style and degree of weathering the lavas have experienced as well as the vesicularity of the samples. Differences in the depth of burial of the lavas (and so the temperatures they may have been subjected to) could also have an effect as could differences in the original chemistry of the lavas (in particular any variations in K_2O content). These possible differences between samples and their possible effects on the argon system are discussed below.

13.4.1. Alteration

One of the major problems with Ar dating these basalt samples from the FIBG appears to be the influence of alteration. All the basalts collected from the Faroe Islands appear to show alteration to some degree and finding 'pristine' samples seems to be very difficult. The samples analysed from the Lopra 1/1A borehole appear to be fresher that those collected from outcrop on the Faroe Islands and of those collected from outcrop, those from the compound lavas of the Malinstindur Fm appear particularly altered. This alteration is evident in almost all samples as clay and zeolite infillings of vesicles and in alteration of the groundmass of the sample (replacement of primary glass and minerals by clays and other alteration products). The poor exposure of the compound lavas of the Malinstindur and Enni fms leaves much of the available, sampling to stream sections and these in general seem more altered than some of the road cuttings. This may be as they have been blasted more recently removing many of the effects of millions of years of surface weathering and alteration, and if samples were to be collected from deeper inside other outcrops (i.e. by drilling instead of hammering from the surface) some of this may be avoided.

13.4.2. Zeolites

As well as the effects of surface weathering of the samples, there are also alteration effects that can result from burial of the samples. The effects of higher temperature alteration, due to the burial of the lavas over millions of years, are likely to be more extreme in the lower parts of the stratigraphy, within the Beinisvorð Fm, from the Lopra 1/1A borehole. The zonation of zeolites identified within the basalts suggests the temperatures experienced by the basalts and the fluids passing through the system and may have reached 100-200°C (Jorgensen 2006). Within the Lopra 1/1A borehole, zeolite zones show increasing temperatures with depth, with a high temperature zeolite assemblages (laumonite, mordenite-prehnite, pumpellyite, chlorite, calcite and quartz) found in the bottom 1320m of the borehole (Jorgensen 2006). This heating of the samples due to burial may be the reason for the younger and more disturbed ages produced from samples from the Lopra 1/1A borehole and the range of ages produced.

In Iceland, Weisenberger & Selbekk (2009) identified 2 main stages of alteration within the basalt, with stage 1 characterised by lining of pore spaces by celadonite, silica minerals and later phyllosilicates (can be subdivided into stages 1a & 1b); the sequence of alteration is likely to be similar in the basalts of the FIBG. The deposition of celadonite is potentially important (if present in the Faroe Islands) as it is K_2O rich, (up to 7.41wt%) and is typically one of the 1st minerals deposited, with infilling of pore spaces by C/S mixed layer phyllosilicates in stage 1b (Weisenberger & Selbekk 2009) occurring in the near surface and then at progressive depth during burial. The second stage is characterised by the deposition of zeolites occurring after the burial of the basalts with the components for the formation of the zeolites derived from the break down of the basalt glass and primary minerals (Weisenberger & Selbekk 2009).

The effects of alteration due to burial may be highly variable and influenced by other characteristics of the basalts, including the thickness of the flow, its chemistry and the vesicularity of the basalt (porosity and permeability) and this can result in varying effects between adjacent flows (and within a flow). The variations in zeolites deposited in lava flows will be affected not just by the temperatures but by the fluid flow conditions, which deposits zeolites and other secondary alteration products within the open spaces of the basalt and there can vary on small scales with changes in fluid flux, chemistry and temperatures.

Distinguishing between the different alteration effects (surface weathering and burial alteration) and there relative importance for the Ar system is difficult and high levels of weathering suffered by some of the samples seems to be masking other effects, as a result the samples from the Lopra 1/1A borehole may appear no more disturbed in relation to the Ar system than the samples from Malinstindur and Enni Formations.

13.4.3. Effects of physical volcanology

As discussed in the previous section, the physical characteristics of the lava flow may have an effect on the Ar system, including differences in the style of emplacement and lava chemistry with these characteristics also having a potential effect on the post depositional processes affecting the samples.

The mode of emplacement of the lavas as well as their chemistry may have an effect on the Ar system within the samples; the degree of degassing of the magma affects the ^{40}Ar and $^{40}Ar/^{36}Ar$ ratio of the magma and the eruption mechanisms may affect how well degassed the magma is. Fully degassed magmas will loose all argon from the magma chamber, resetting the Ar system on eruption and so the age produced in $^{40}Ar/^{39}Ar$ dating will represent the timing of eruption and processes post-eruption. If degassing is incomplete, the samples may retain a non-atmospheric $^{40}Ar/^{36}Ar$ ratio (i.e. different from 295.5) and so one of the assumptions made in Ar dating has been violated.

The distribution of Ar isotopes within the lava will be affected by the degree of degassing of the magma but also by the possibility of later addition (or loss) or Ar from the system after eruption, with these violating the assumption made during dating that the sample has remained as a closed system since eruption. The presence of fluids passing through the system has important implications, leading to the transport in and out of the system of both K and Ar and the replacement of the primary minerals, replacement of secondary minerals and infilling of vesicles with various

secondary minerals. The degree of interconnectivity of the vesicles within the lava flows will be an important control on the ability of fluids to travel through the lavas (both laterally along a lava horizon, and vertically through successive lavas). The different lava types, thick simple sheet lobes (in the Beinisvørð and Enni Fms) and the compound lava flows (of the Malinstindur and Enni Fms) (Passey & Bell 2007) show differing degrees of vesicularity and structures. Many of the compound flows for instance have pipe vesicles at the base as well as vesicle cylinders and sheets of vesicles related to the inflation of the pahoehoe flow lobes (Self et al. 1997; Passey & Bell 2007). These different characteristics may affect the degree of degassing of the lava and as well as the ability of fluids to pass through the lavas at a later stage, affecting the Ar system differently over various scales (different effects between and within individual lavas).

13.4.4. Effect of original chemistry and/or mineralogy on Ar?

Although all the basalts from the FIBG have been classed as tholeiitic in composition, whether are variations in chemistry between (and within) the main lava formations. The basalts can be grouped into high and low TiO_2 basalts, with a small number of lavas with more extreme chemical variations, such as 'high SiO_2' lavas. As well as the variations in TiO_2, there are also differences in the Mg content of the lavas and the percentages of other major elements. The K_2O variations, important for Ar dating, are however small, with the K_2O content of all the basalts being low. The other major difference between basalts in different parts of the stratigraphy is the presence and abundance of phenocrysts within the basalts. In some parts of the stratigraphy the majority of the basalts are aphyric, with no phenocrysts, (e.g. the Beinisvørð Fm) while in parts of the Malinstindur Fm, plagioclase phyric basalts are found. The Within the drilled portion of the Beinisvørð Fm from the Lopra 1/1A borehole, published geochemical data shows a change in the chemistry in the lowermost ~460m of the formation (Passey & Jolley 2009). This lowest portion of the Beinisvørð Fm is formed of flows belonging to Group A of Waagstein (1997; 2006), with relatively high Mg numbers (50-62) and low TiO_2 (1.3 – 2.0%) and high FeO^T (10.3. – 13.9%) (Hald & Waagstein 1984; Waagstein 1988, 1997; Larsen et al 1999, Waagstein 2006). Above this interval, the overlying ~2.57Km of the Beinisvørð Fm flows are higher in TiO_2 (2.1 – 3.8%) and have lower Mg numbers (37-53) (Hald & Waagstein 1984; Waagstein 1988; Larsen et al. 1999).

Looking at the Ar isotope ratios, most importantly the $^{37}Ar/^{39}Ar$ ratio, a proxy for the Ca/K ratio of the data, shows the differences in release patterns through a step-heat as different minerals release there argon, from the groundmass of the basalt, at different temperatures, with samples with very high $^{37}Ar/^{39}Ar$ ratios appear more common in the Malinstindur and Enni formations than in the samples analysed from the Beinisvørð Fm. The Ca/K ratios from some samples are very high in some samples and these samples produce the most disturbed, and generally youngest apparent ages on the release spectra, due to the very low K_2O contents in the samples. As well as the variations in chemistry that may be a result of primary differences in the magmas, other differences are also possibly related to the alteration of the samples. K_2O is a highly mobile element and could be lost from the sample during alteration. The deposition of secondary minerals within the vesicles (and matrix) of the basalts, could also change the bulk chemistry of the basalts, the zeolite minerals are generally Ca rich, and so even without any K_2O loss from the samples, the presence of even a small amount of Ca rich clay or zeolite will further increase, the already high, Ca/K ratio of the sample.
It is possible that the lava chemistry has a direct influence on the Ar system in the samples but it may also be that differences in the chemistry (and other associated characteristics such as emplacement style or vesicularity for example)

have an affect on the susceptibility of samples to weathering and alteration, and it is this that affects the measured Ar ratios.

When dating basaltic rocks, either plagioclase can be separated from the matrix or the groundmass can be dated. Separating a pure enough separate of plagioclase can be very difficult from very fine grained/aphyric basalts and but is much easier from plagioclase-phyric basalts. In the FIBG there are many plagioclase phyric lava flows within the Malinstindur Fm and from some the plagioclase phyric samples, both plagioclase and matrix were analysed in several samples to compare the results but due to the difficulties in producing a pure enough plagioclase separate, they can contain a relatively large volume of adhered matrix. The very low K content of the plagioclase crystals is shown by the very high $^{37}Ar_{Ca}/^{39}Ar_{K}$ ratios from the data of these separates and the errors on the data are much larger than for the groundmass in many cases, due to the low Ar contents and increased errors due to the scale of corrections for isotope production from Ca during irradiation. The plagioclase phenocrysts also appear to be highly susceptible to alteration and in many cases show some replacement by clay minerals, further reducing there suitability for Ar dating.

13.5. Issues with the Ar dating of intrusives

The intrusive samples collected and dated from the Faroe Islands appear to be fresher than many of the outcrop samples and in many cases produced less disturbed results. This may be associated with the non-vesicular nature of the intrusive units, making them less susceptible to alteration caused by the passage of fluids through the rock and the associated loss/gain of Ar and K_2O. Dating of intrusives does have some issues, including the lack of stratigraphic control on the samples (it is only known they should be younger than the surrounding basalt) and this do not allow the same investigation of the plausibility of produced ages as in a sequence of lavas, where out of order ages or a large scatter of apparent ages, aid determining the validity of apparent ages produced from radiometric techniques. Due to the magma not having erupted at the surface, intrusive rocks may not have completely degassed and so the trapped Ar within samples/minerals may not have equilibrated with the atmosphere, leading to different $^{40}Ar/^{36}Ar$ ratios than may be seen in equivalent eruptive products. Contamination of intrusive magmas and the incorporation of excess argon from the surrounding rocks is a common problem in intrusive rocks, especially where the basement and country rock is much older (± high in K) (e.g. Lenoir et al. 2003), in the Faroe islands this is likely to be less of an issue, as almost all the rocks are of basaltic composition and similar in age to that expected for the intrusives.

In the Faroe Islands the cross cutting relationships between the lavas and the different intrusive units shows that the lavas were erupted first and this is followed by dykes, with the sills (which are not seen to be cut by dykes) thought to be the final stages of activity (Rasmussen & Noe-Nygaard 1969;1970, Hald & Waagstein 1991). Recent detailed mapping of the sill complexes by Hansen et al. (2011) also confirmed this with the few exposed accessible dyke-sill contacts suggesting that the sub-vertical dykes predate the sills.

14. Conclusions

1. The FIBG is one of the most complex basaltic provinces displaying a complete array of disturbances to the Ar/Ar system in terms of whole rock, groundmass and plagioclase mineral separates. In spite of this it has been possible to determine new ages for the eruption of the different units.

2. For the Beinisvørð Formation the best calculated age is 56.30±0.99 Ma. This is derived from the weighted mean of L5 plateau and isochron ages, L13 plateau ages, and the 'total fusion' ages of L8, providing good coverage of the drilled portion of the Beinisvørð Formation from the Lopra 1/1A borehole.

3. For the Malinstindur Formation the best calculated age is 56.53±1.1 Ma a weighted mean of the plateau and inverse isochron ages from AH10-28 and including the 'total fusion' age for AH10-25. These are from the top of the Malinstindur Formation.

4. For the Enni Formation the best calculated age is 53.6±3.2 Ma, which is a weighted mean age of the plateau and inverse isochron ages from LCF25 A102 and the 'total fusion' age from AH10-18. The age is derived from sample at the top and base of the Enni Formation.

5. The ages of the intrusives are younger: Eysturoy Sill 52±1 Ma; Streymoy Sill 51±1 Ma; Prestfjall: no discernible age.

6. The FIBG erupted in < 2 Myr with ages of 56.30±0.99 Ma and 53.6±3.2 Ma (within error of one another) bracketing the timing of eruption. This considerably shortens the timescale for eruption and lava emplacement based on previous age estimates.

15. References

Ellis, D., Bell, B. R., Jolley, D. W. & O'Callaghan, M. (2002). The stratigraphy, environment of eruption and age of the Faroes Lava Group, NE Atlantic Ocean. In: Jolley, D. W. (ed.) The North Atlantic Igneous Province: Stratigraphy, Tectonic, Volcanic and Magmatic Processes: Geological Society Special Publication 197, 253-269.

Geoffroy, L., Bergerat, F. & Angelier, J. (1994). Tectonic evolution of the Greenland-Scotland ridge during the Paleogene: New constraints. *Geology* **22**, 653-656.

Gibb, F. G. F. & Kanaris-Sotiriou, R. (1988). The geochemistry and origin of the Faeroe-Shetland sill complex. Geological Society, London, Special Publication 39, 241-252.

Gibb, F. G. F., Kanaris-Sotiriou, R. & Neves, R. (1986). A new Tertiary sill complex of mid-ocean ridge basalt type NNE of the Shetland Isles: a preliminary report. Transactions of the Royal Society of Edinburgh: Earth Sciences. 77 (3), p.223-230

Gradstein, F. M., Ogg, J. G. & Smith, A. G. (2004). A geologic timescale 2004: Cambridge University Press.

Hald, N. & Waagstein, R. (1984). Lithology and Chemistry of a 2-km sequence of Lower Tertiary tholeiitic lavas drilled on Suduroy, Faeroe Islands (Lopra-1). In: Berthelsen, O., Noe-Nygaard, A. & Rasmussen, J. (eds.) The deep drilling project 1980-81 in the Faeroe Islands: Annales Societas Scientiarum Faeroensis, 15-38.

Hald, N. & Waagstein, R. (1991). The dykes and sills of the Early Tertiary Faroe Island basalt plateau. Transactions of the Royal Society of Edinburgh: Earth Sciences 82, 373-388.

Hansen, J., Jerram, D. A., McCaffrey, K. & Passey, S. R. (2011). Early Cenozoic saucer-shaped sills of the Faroe Islands: an example of intrusive styles in basaltic lava piles. Journal of the Geological Society 168, 159-178.

Jolley, D. W. (1997). Palaeosurface palynofloras of the Skye lava field and the age of the British Tertiary volcanic province. In: Widdowson, M. (ed.) *Palaeosurfaces: Recognition, reconstruction and palaeoenvironmental interpretation*: Geological Society of London, Special Publication 120, 67-94.

Jolley, D. W. (2009). Palynofloral evidence for the onset and cessation of eruption of the Faroe Islands lava field. Faroe Islands Exploration Conference: Proceedings of the 2nd Conference: Annales Societatis Scientiarum Faeronsis, Supplementum 48, 149-166.

Jolley, D. W., Clarke, B. & Kelley, S. P. (2002). Paleogene time scale miscalibration: Evidence from the dating of the North Atlantic Igneous province. *Geology* **30**, 7-10.

Larsen, R. B. & Tegner, C. (2006). Pressure conditions for the solidification of the Skaergaard intrusion: Eruption of East Greenland flood basalts in less than 300,000 years. *Lithos* **92**, 181-197.

Larsen, L. M., Waagstein, R., Pedersen, A. K. & Storey, M. (1999). Trans-Atlantic correlation of the Palaeogene volcanic successions in the Faeroe Islands and East Greenland. Journal of the Geological Society, London 156, 1081-1095.

Lenoir, X., Feraud, G. & Geoffroy, L. (2003). High-rate flexure of the East Greenland volcanic margin: constraints from $^{40}Ar/^{39}Ar$ dating of basaltic dykes. *Earth and Planetary Science Letters* **214**, 515-528.

Passey, S. R. & Bell, B. R. (2007). Morphologies and emplacement mechanisms of the lava flows of the Faroe Islands Basalt Group, Faroe Islands, NE Atlantic Ocean. Bulletin of Volcanology 70, 139-156.

Passey, S. R. & Jolley, D. W. (2009). A revised lithostratigraphic nomenclature for the Palaeogene Faroe Islands Basalt Group, NE Atlantic Ocean. Earth and Environmental Science Transactions of the Royal Society of Edinburgh 99, 127-158.

Rasmussen, J. & Noe-Nygaard, A. (1969). Beskrivelse til geologisk kort over Faeroerne. Danmarks Geologiske Undersøgelse 1. Serie 24.

Rasmussen, J. & Noe-Nygaard, A. (1970). Geology of the Faeroe Islands. Danmarks Geologiske Undersøgelse 1. Serie 25.

Ritchie, J. D. & Hitchen, K. (1996). Early Palaeogene offshore igneous activity to the northwest of the UK and it's relationship to the North Atlantic Igneous Province. In: Knox, R. W. O. B., Corfield, R. M. & Dunay, R. E. (eds.) *Correlation of the Early Paleogene in Northwest Europe*: Geological Society of London, Special Publication 101, 63-78.

Self, S., Thordarson, T. & Keszthelyi, L. (1997). Emplacement of continental flood basalt lava flows. In: Mahoney, J. J. & Coffin, M. F. (eds.) Large igneous provinces: continental, oceanic and planetary volcanism: Geophysical Monograph 100, 381-410.

Self, S., Keszthelyi, L. & Thordarson, T. (1998). The importance of pahoehoe. Annual Review, Earth and Planetary Science 26, 81-110.

Smallwood, J. R. & Maresh, J. (2002). The properties, morphology and distribution of igneous sills: modelling, borehole data and 3D seismic from the Faroe-Shetland area. In: Jolley, D. W. (ed.) *The North Atlantic Igneous Province: Stratigraphy, Tectonic, Volcanic and Magmatic Processes*: Geological Society Special Publication 197, 271-306.

Smallwood, J. R. & Harding, A. (2009). New seismic imaging methods, dating, intrusion style and effects of sills: A drilled example from the Faroe-Shetland Basin. Faroe Islands Exploration Conference: Proceedings of the 2nd Conference: Annales Societatis Scientiarum Faeroensis, 104-123.

Storey, M., Duncan, R. A. & Tegner, C. (2007). Timing and duration of volcanism in the North Atlantic Igneous Province: Implications for geodynamics and links to the Iceland hotspot. Chemical Geology 241, 264-281.

Waagstein, R. (1988). Structure, composition and age of the Faeroe basalt plateau. In: Morton, A. & Parson, L. M. (eds.) Early Tertiary volcanism and the opening of the NE Atlantic: Geological Society, London, Special Publication 39, 225-238.

Waagstein, R. (1997). Volcanic Rocks, Lopra-1/1A Faroe Islands 1996. Technical Studies prepared for Dansk Olie og Naturgas A/S 1997. Copenhagen: Geological Survey of Denmark and Greenland.

Waagstein, R., Guise, P. G. & Rex, D. C. (2002). K/Ar and 39Ar/40Ar whole-rock dating of zeolite facies metamorphosed flood basalts: the upper Paleocene basalts of the Faroe Islands, NE Atlantic. In: Jolley, D. W. & Bell, B. R. (eds.) The North Atlantic Igneous Province: Stratigraphy, Tectonic, Volcanic and Magmatic Processes: Geological Society Special Publication 197, 219-252.

Waagstein, R. (2006). Composite log from the Lopra-1/1A well, Faroe Islands. In: Chalmers, J. A. & Waagstein, R. (eds.) *Scientific Results from the Deepened Lopra-1 borehole, Faroe Islands*: Geological Survey of Denmark and Greenland Bulletin.

Waagstein, R., Hald, N., Jørgensen, O., Nielsen, P., H., Noe-Nygaard, A., Rasmussen, J. & Schönharting, G. (1984). Deep drilling on the Faeroe Islands. Bulletin of the Geological Society of Denmark 32, 133-138.

Weisenberger, T. & Selbekk, R. S. (2009). Multi-stage zeolite facies mineralization in the Hvalfjördur area, Iceland. International Journal of Earth Sciences 98, 985-999.

Appendix 1: Sample Location Data

Sample			Elevation (m)	Island	Formation
AH10-1	61°34'748N	006°49'424W	6	Suðuroy	Prestfjall Intrusive
AH10-2	61°34'735N	006°49'339W	12	Suðuroy	Prestfjall Intrusive
AH10-3	61°34'707N	006°49'509W	33	Suðuroy	Malinstindur
AH10-4	61°34'713N	006°49'688W	18	Suðuroy	Malinstindur
AH10-5	61°34'636N	006°49'811W	69	Suðuroy	Malinstindur
AH10-6	61'34'624N	006°49'690W	186	Suðuroy	Malinstindur
AH10-7	61°34'528N	006°49'445W	213	Suðuroy	Malinstindur
AH10-8	61°32'833N	006°44'878W	14	Suðuroy	Hvannhagi
AH10-9	61°35'630N	006°55'566W	81	Suðuroy	Malinstindur
AH10-10	61°35'630N	006°55'566W	81	Suðuroy	Malinstindur
AH10-11	61°35'630N	006°55'566W	81	Suðuroy	Malinstindur
AH10-12	61°36'577N	006°55'638W	60	Suðuroy	Prestfjall Intrusive
AH10-13	61°37'889N	006°55'730W	5	Suðuroy	Malinstindur
AH10-14	61°33'202N	006°53'821W	347	Suðuroy	Malinstindur
AH10-15	61°33'202N	006°53'821W	347	Suðuroy	Malinstindur
AH10-16	61°33'201N	006°53'831W	355	Suðuroy	Malinstindur
AH10-17	61°33'193N	006°53'830W	364	Suðuroy	Malinstindur
AH10-18	61°57'049N	006°47'111W	27	Streymoy	Enni
AH10-19	61°57'010N	006°46'960W	47	Streymoy	Enni
AH10-20	61°56'895N	006°46'778W	71	Streymoy	Enni
AH10-21	61°45'768N	006°46'505W	114	Streymoy	Enni
AH10-22	61°45'768N	006°46'505W	114	Streymoy	Enni
AH10-23	62°18'058N	007°02'642W	223	Eysturoy	Malinstindur
AH10-24	62°18'058N	007°02'642W	223	Eysturoy	Malinstindur
AH10-25	62°17'987N	007°02'136W	399	Eysturoy	Malinstindur
AH10-26	62°17'943N	007°02'037W	742	Eysturoy	Malinstindur
AH10-27	62°17'943N	007°02'037W	742	Eysturoy	Malinstindur
AH10-28	62°17'934N	007°02'020W	492	Eysturoy	Malinstindur
AH10-29	62°17'934N	007°02'020W	492	Eysturoy	Malinstindur
AH10-30					
AH10-31	62°17'903N	007°01'940W	532	Eysturoy	Enni
AH10-32	62°17'888N	007°01'842W	590	Eysturoy	Enni
AH10-33	62°17'888N	007°01'842W	590	Eysturoy	Enni
AH10-34	62°11'523 N	006°58'614W	146	Eysturoy	Eysturoy Sill
AH10-35	62°11'523 N	006°58'614W	146	Eysturoy	Malinstindur
AH10-36	62°11'523 N	006°58'614W	146	Eysturoy	Eysturoy Sill
AH10-37	62°11'521N	006°58'603W	159	Eysturoy	Eysturoy Sill
AH10-38	62°11'512N	006°58'564W	174	Eysturoy	Eysturoy Sill
AH10-39	62°14'043N	007°01'615W	63	Eysturoy	Malinstindur
AH10-40	62°14'044N	007°01'578W	68	Eysturoy	Malinstindur
AH10-41	62°14'044N	007°01'578W	68	Eysturoy	Malinstindur
AH10-42	62°14'063N	007°01'530W	81	Eysturoy	Malinstindur
AH10-43	62°14'075N	007°01'506W	89	Eysturoy	Malinstindur
AH10-44	62°14'075N	007°01'506W	89	Eysturoy	Malinstindur
AH10-45	62°14'075N	007°01'506W	89	Eysturoy	Malinstindur
AH10-46	62°14'133N	007°01'121W	121	Eysturoy	Malinstindur
AH10-47	62°14'009N	007°01'716W	20	Eysturoy	Malinstindur
AH10-48	62°02'833N	006°57'939W	254	Streymoy	Streymoy Sill
AH10-49	62°02'833N	006°57'939W	254	Streymoy	Streymoy Sill

AH10-50	62°02'123N	006°52'343W	313	Streymoy	Enni
AH10-51	62°06'908N	007°03'690W	74	Streymoy	Malinstindur
AH10-52	62°06'908N	007°03'690W	74	Streymoy	Dyke
AH10-53	62°06'908N	007°03'690W	74	Streymoy	Dyke
AH10-54	62°06'908N	007°03'690W	74	Streymoy	Dyke
AH10-55	62°06'908N	007°03'690W	74	Streymoy	Dyke
AH10-56	62°06'908N	007°03'690W	74	Streymoy	Malinstindur
AH11-1	62°4’588N	006°56’215W	308	Streymoy	Malinstindur
AH11-2	62°2’867N	006°55’86W	190	Streymoy	Dyke
AH11-3	62°16’103N	006°56’390W	71	Eysturoy	Dyke
AH11-4	62°15’503N	006°56’924W	41	Eysturoy	Dyke
LCF 25	62°3’423N	006°51’198W	12	Streymoy	Enni

Appendix 2: $^{40}Ar/^{39}Ar$ data tables

		40Ar	+/-	39Ar	+/-	38Ar	+/-	37Ar	+/-	36Ar	+/-	40Ar*/39Ar	+/-	Age	+/- (no J error)
AH10-1	**J = 0.009846991 ± 0.000049252**														
A57	Step 1	0.03209	0.00051	0.00493	0.00011	0.00002	0.00002	0.01190	0.00095	0.00007	0.00003	2.53691	1.76944	44.51386	30.66747
A57	Step 2	0.24721	0.00089	0.04415	0.00019	0.00038	0.00005	0.12017	0.00095	0.00042	0.00004	2.80423	0.27431	49.14094	4.74208
A57	Step 3	0.59905	0.00070	0.11796	0.00025	0.00096	0.00003	0.40116	0.00095	0.00090	0.00003	2.81612	0.08603	49.34654	1.48705
A57	Step 4	0.83835	0.00106	0.17828	0.00044	0.00163	0.00009	1.03029	0.00095	0.00117	0.00004	2.76917	0.06832	48.53476	1.18154
A57	Step 5	0.99221	0.00152	0.21522	0.00061	0.00203	0.00005	1.46594	0.00095	0.00144	0.00004	2.63175	0.05706	46.15678	0.98810
A57	Step 6	1.06791	0.00085	0.23455	0.00065	0.00212	0.00009	1.89077	0.00095	0.00152	0.00004	2.64008	0.05219	46.30109	0.90365
A57	Step 7	1.09605	0.00150	0.24664	0.00070	0.00268	0.00013	2.53463	0.00095	0.00168	0.00004	2.43377	0.04995	42.72537	0.86653
A57	Step 8	1.52959	0.00135	0.35101	0.00110	0.00310	0.00016	4.41177	0.00095	0.00242	0.00004	2.32013	0.03569	40.75265	0.61989
A57	Step 9	1.86011	0.00147	0.43556	0.00105	0.00396	0.00023	5.50047	0.00095	0.00288	0.00008	2.31549	0.05802	40.67211	1.00770
A57	Step 10	2.43998	0.00315	0.58736	0.00434	0.00491	0.00028	7.30073	0.00095	0.00348	0.00006	2.40100	0.03457	42.15672	0.59992
A57	Step 11	2.26324	0.00536	0.55547	0.00130	0.00494	0.00026	7.10953	0.00095	0.00310	0.00007	2.42779	0.03724	42.62153	0.64607
AH10-12	**J = 0.00980040 ± 0.000049000**														
A45	Step 1	0.00099	0.00106	0.00013	0.00028	-0.00001	0.00005	0.00161	0.00324	0.00001	0.00003	-5.11012	-60.53096	-92.68782	1126.60895
A45	Step 2	0.02547	0.00103	0.00478	0.00027	-0.00003	0.00005	0.04473	0.00324	0.00004	0.00002	2.59790	1.20763	45.35592	20.82084
A45	Step 3	0.47539	0.00153	0.07919	0.00038	0.00057	0.00005	0.40941	0.00324	0.00077	0.00003	3.13929	0.09927	54.66608	1.70267
A45	Step 4	1.23711	0.00189	0.22956	0.00093	0.00199	0.00015	1.27141	0.00324	0.00186	0.00004	2.99597	0.05754	52.20606	0.98830
A45	Step 5	2.31600	0.00459	0.48357	0.00107	0.00428	0.00011	3.95642	0.00324	0.00297	0.00006	2.97593	0.03984	51.86197	0.68439
A45	Step 6	1.18316	0.00231	0.25325	0.00102	0.00194	0.00009	2.31863	0.00127	0.00151	0.00003	2.90521	0.04037	50.64663	0.69392
A45	Step 7	2.04852	0.00132	0.45346	0.00123	0.00380	0.00036	4.06180	0.00128	0.00249	0.00003	2.89350	0.02277	50.44530	0.39155
A45	Step 8	2.59022	0.00253	0.62871	0.00117	0.00478	0.00030	7.25741	0.00128	0.00282	0.00003	2.79667	0.01705	48.77971	0.29334
A45	Step 9	1.19240	0.00207	0.30113	0.00072	0.00260	0.00012	3.46073	0.00128	0.00128	0.00004	2.70218	0.04209	47.15304	0.72496
A45	Step 10	2.31060	0.00268	0.58386	0.00071	0.00490	0.00030	8.26626	0.00128	0.00249	0.00005	2.69826	0.02712	47.08546	0.46706
A45	Step 11	1.51113	0.00241	0.40013	0.00075	0.00322	0.00010	5.80177	0.00128	0.00170	0.00004	2.52033	0.03213	44.01805	0.55439
A45	Step 12	1.64254	0.00050	0.42837	0.00171	0.00341	0.00015	6.71094	0.00128	0.00175	0.00004	2.62707	0.03115	45.85883	0.53690
A45	Step 13	2.30867	0.00306	0.62490	0.00095	0.00551	0.00022	9.60114	0.00128	0.00259	0.00004	2.46770	0.02146	43.10977	0.37042
A45	Step 14	2.29709	0.00359	0.62366	0.00113	0.00485	0.00024	9.75607	0.00128	0.00246	0.00005	2.51612	0.02610	43.94553	0.45029
AH10-15	**J = 0.009792086 ± 0.000048960**														
A43	Step 1	0.00166	0.00070	0.00007	0.00003	0.00004	0.00003	-0.00057	0.00108	-0.00002	0.00003	94.92740	116.55534	1185.78411	1067.11029
A43	Step 2	0.01183	0.00071	0.00044	0.00004	0.00000	0.00004	0.00286	0.00108	0.00004	0.00003	-1.13378	-17.70417	-20.14099	316.26728
A43	Step 3	0.02366	0.00075	0.00215	0.00005	0.00002	0.00004	0.00812	0.00108	0.00007	0.00003	1.33340	3.62941	23.40292	63.28969
A43	Step 4	0.25576	0.00071	0.02111	0.00011	0.00021	0.00004	0.08889	0.00109	0.00076	0.00003	1.49219	0.37038	26.16990	6.44881
A43	Step 5	0.76132	0.00150	0.05307	0.00020	0.00079	0.00005	0.42453	0.00109	0.00226	0.00005	1.76167	0.29576	30.85565	5.13625
A43	Step 6	1.07789	0.00194	0.07628	0.00033	0.00105	0.00005	0.84072	0.00109	0.00300	0.00003	2.51014	0.10580	43.80711	1.82423
A43	Step 7	0.80530	0.00137	0.05519	0.00018	0.00072	0.00005	0.62162	0.00109	0.00237	0.00003	1.91369	0.18680	33.49370	3.23918
A43	Step 8	1.83161	0.00244	0.10536	0.00030	0.00143	0.00010	1.59448	0.00109	0.00528	0.00004	2.57568	0.12459	44.93676	2.14677
A43	Step 9	1.43647	0.00140	0.10399	0.00030	0.00160	0.00007	2.48398	0.00109	0.00413	0.00003	2.06563	0.07685	36.12665	1.33074
A43	Step 10	2.02790	0.00183	0.16471	0.00045	0.00221	0.00012	4.28168	0.00109	0.00581	0.00008	1.89230	0.14765	33.12284	2.56080
A43	Step 11	1.29313	0.00191	0.10472	0.00041	0.00139	0.00007	3.57144	0.00109	0.00363	0.00004	2.11635	0.12514	37.00469	2.16580
A43	Step 12	1.21602	0.00154	0.10863	0.00038	0.00136	0.00006	3.58118	0.00109	0.00348	0.00004	1.71821	0.12008	30.10086	2.08616
A43	Step 13	1.26366	0.00105	0.13725	0.00032	0.00168	0.00008	4.33991	0.00143	0.00329	0.00006	2.11947	0.12193	37.05856	2.11013
A43	Step 14	0.98936	0.00140	0.10543	0.00022	0.00139	0.00009	3.88258	0.00143	0.00266	0.00005	1.91982	0.13463	33.60015	2.33438

		40Ar	+/-	39Ar	+/-	38Ar	+/-	37Ar	+/-	36Ar	+/-	40Ar*/39Ar	+/-	Age	+/- (no J error)
AH10-15	**J = 0.009796063 ± 0.000048980**														
A44	Step 1	0.15875	0.00105	0.01141	0.00010	0.00013	0.00004	0.05753	0.00093	0.00048	0.00003	1.58758	0.71928	27.84111	12.51712
A44	Step 2	0.95963	0.00142	0.06217	0.00048	0.00076	0.00006	0.36535	0.00093	0.00284	0.00004	1.91601	0.21208	33.54751	3.67906
A44	Step 3	1.73240	0.00193	0.10791	0.00042	0.00152	0.00008	0.83455	0.00093	0.00482	0.00004	2.85498	0.12302	49.76289	2.11489
A44	Step 4	2.32220	0.00165	0.13298	0.00033	0.00189	0.00009	1.21750	0.00093	0.00665	0.00005	2.68867	0.11968	46.90156	2.06077
A44	Step 5	1.21678	0.00104	0.08032	0.00026	0.00096	0.00006	1.01568	0.00386	0.00341	0.00003	2.59521	0.10432	45.29139	1.79799
A44	Step 6	2.86046	0.00261	0.15618	0.00040	0.00241	0.00007	2.87632	0.00386	0.00839	0.00004	2.44232	0.08646	42.65456	1.49221
A44	Step 7	1.39207	0.00136	0.09345	0.00038	0.00146	0.00007	1.91189	0.00387	0.00389	0.00004	2.58065	0.14223	45.04043	2.45166
A44	Step 8	3.53299	0.00257	0.23104	0.00060	0.00357	0.00016	6.28572	0.00387	0.01030	0.00008	2.12349	0.10661	37.14321	1.84579
A44	Step 9	4.08719	0.00459	0.28678	0.00040	0.00443	0.00013	8.49463	0.00387	0.01213	0.00019	1.75282	0.19782	30.71445	3.43707
A44	Step 10	2.44210	0.00186	0.21240	0.00054	0.00281	0.00010	6.46166	0.00388	0.00689	0.00006	1.91320	0.08919	33.49880	1.54726
A44	Step 11	2.80790	0.00227	0.24579	0.00095	0.00316	0.00015	7.47080	0.00388	0.00790	0.00010	1.92421	0.12366	33.68968	2.14504
AH10-16	**J = 0.009784132 ± 0.000048921**														
A41	Step 1	0.06575	0.00106	0.00157	0.00009	-0.00002	0.00004	0.01526	0.00111	0.00020	0.00002	3.64170	4.73205	63.16207	80.65329
A41	Step 2	0.22632	0.00104	0.00758	0.00012	0.00011	0.00003	0.03391	0.00111	0.00063	0.00002	5.37066	0.71649	92.39252	12.01556
A41	Step 3	1.26485	0.00139	0.03513	0.00017	0.00078	0.00008	0.40570	0.00111	0.00393	0.00004	2.95079	0.36144	51.34764	6.20083
A41	Step 4	2.35011	0.00305	0.06360	0.00019	0.00142	0.00005	0.84804	0.00111	0.00722	0.00003	3.39448	0.16313	58.94360	2.78684
A41	Step 5	4.19265	0.00356	0.12286	0.00039	0.00268	0.00012	2.11374	0.00111	0.01331	0.00013	2.11971	0.31617	37.03298	5.46751
A41	Step 6	3.30214	0.00333	0.10110	0.00024	0.00214	0.00009	2.48429	0.00111	0.01037	0.00011	2.35570	0.32629	41.10925	5.62978
A41	Step 7	4.84263	0.00436	0.15355	0.00037	0.00308	0.00005	5.73947	0.00111	0.01538	0.00011	1.94706	0.21604	34.04499	3.74210
A41	Step 8	4.92308	0.00706	0.19150	0.00104	0.00361	0.00018	7.65160	0.00111	0.01578	0.00018	1.35903	0.28167	23.83055	4.90653
A41	Step 9	4.43666	0.00500	0.17742	0.00047	0.00392	0.00015	9.73752	0.00111	0.01432	0.00012	1.16147	0.20450	20.38589	3.56920
A41	Step 10	1.12628	0.00157	0.05843	0.00022	0.00091	0.00006	3.08578	0.00088	0.00371	0.00006	0.50996	0.31687	8.97908	5.56538
A41	Step 11	3.13716	0.00258	0.15836	0.00047	0.00274	0.00008	10.51051	0.00088	0.01021	0.00013	0.75273	0.24651	13.23797	4.31942
A41	Step 12	1.18878	0.00146	0.06877	0.00035	0.00110	0.00004	4.82664	0.00088	0.00399	0.00004	0.14466	0.18954	2.55169	3.34090
A41	Step 13	1.58299	0.00236	0.08577	0.00037	0.00135	0.00006	6.41586	0.00088	0.00544	0.00006	-0.27957	-0.21835	-4.94149	3.86470
A41	Step 14	1.50545	0.00158	0.09160	0.00030	0.00134	0.00008	6.31266	0.00088	0.00508	0.00007	0.06166	0.23440	1.08802	4.13500
AH10-18	**J = 0.009807993 ± 0.000049040**														
A47	Step 1	0.04415	0.00055	0.01010	0.00014	0.00007	0.00003	0.04147	0.00160	0.00007	0.00001	2.22645	0.33257	38.97167	5.75887
A47	Step 2	0.31228	0.00079	0.07275	0.00023	0.00063	0.00002	0.31393	0.00160	0.00040	0.00002	2.66340	0.08486	46.52222	1.46337
A47	Step 3	0.86678	0.00093	0.21495	0.00064	0.00151	0.00006	1.08012	0.00160	0.00086	0.00002	2.85280	0.02994	49.78528	0.51543
A47	Step 4	1.84146	0.00218	0.44406	0.00078	0.00353	0.00014	2.86331	0.00160	0.00189	0.00004	2.89217	0.02785	50.46268	0.47926
A47	Step 5	2.16231	0.00271	0.50884	0.00096	0.00402	0.00011	4.58115	0.00160	0.00252	0.00004	2.78590	0.02482	48.63323	0.42753
A47	Step 6	1.56369	0.00193	0.35707	0.00111	0.00349	0.00013	4.35788	0.00160	0.00190	0.00001	2.80733	0.01461	49.00236	0.25167
A47	Step 7	1.55132	0.00195	0.37523	0.00066	0.00370	0.00008	5.31203	0.00161	0.00209	0.00002	2.49107	0.01844	43.54808	0.31857
A47	Step 8	1.21488	0.00230	0.31042	0.00098	0.00296	0.00008	5.14398	0.00314	0.00145	0.00005	2.53794	0.05030	44.35743	0.86849
A47	Step 9	1.16709	0.00166	0.29945	0.00052	0.00276	0.00007	4.15757	0.00314	0.00153	0.00003	2.39099	0.03265	41.81870	0.56444
A47	Step 10	1.89083	0.00326	0.48186	0.00138	0.00410	0.00019	6.46355	0.00314	0.00246	0.00005	2.41822	0.03323	42.28941	0.57442
A47	Step 11	2.43906	0.00389	0.61970	0.00232	0.00499	0.00036	9.10447	0.00315	0.00305	0.00008	2.48357	0.04050	43.41847	0.69966
A47	Step 12	2.04677	0.00266	0.53526	0.00062	0.00427	0.00019	8.42466	0.00315	0.00240	0.00003	2.50125	0.01950	43.72394	0.33681
A47	Step 13	1.56536	0.00199	0.40741	0.00098	0.00374	0.00017	6.37847	0.00315	0.00190	0.00004	2.46558	0.03160	43.10770	0.54600

		40Ar	+/-	39Ar	+/-	38Ar	+/-	37Ar	+/-	36Ar	+/-	40Ar*/39Ar	+/-	Age	+/- (no J error)
AH10-21	**J = 0.007871974 ± 0.000039360**														
A100	Step 1	0.13474	0.00092	0.01359	0.00034	0.00014	0.00005	0.06662	0.00204	0.00027	0.00005	3.99348	1.18537	55.84077	16.32117
A100	Step 2	0.89454	0.00239	0.10756	0.00024	0.00151	0.00010	0.62442	0.00204	0.00166	0.00004	3.74357	0.10334	52.39657	1.42565
A100	Step 3	1.25610	0.00183	0.19135	0.00120	0.00242	0.00010	1.34927	0.00204	0.00184	0.00007	3.71921	0.11568	52.06052	1.59607
A100	Step 4	1.43199	0.00127	0.24801	0.00091	0.00342	0.00018	2.19857	0.00204	0.00168	0.00008	3.77536	0.09971	52.83498	1.37519
A100	Step 5	1.28086	0.00340	0.23456	0.00141	0.00348	0.00019	3.06937	0.00204	0.00144	0.00007	3.65076	0.09587	51.11579	1.32353
A100	Step 6	1.07881	0.00288	0.21109	0.00067	0.00280	0.00015	3.80690	0.00204	0.00106	0.00008	3.62515	0.11735	50.76221	1.62030
A100	Step 7	0.81960	0.00277	0.17835	0.00096	0.00289	0.00015	4.65175	0.00204	0.00068	0.00006	3.47334	0.10858	48.66486	1.50099
A100	Step 8	0.69843	0.00239	0.15771	0.00092	0.00250	0.00009	5.26386	0.00204	0.00053	0.00005	3.44482	0.08927	48.27049	1.23432
A100	Step 9	0.47669	0.00184	0.11049	0.00077	0.00171	0.00012	4.22208	0.00204	0.00034	0.00004	3.40195	0.10319	47.67766	1.42727
A100	Step 10	0.53318	0.00180	0.12374	0.00067	0.00195	0.00013	4.87963	0.00205	0.00043	0.00005	3.28946	0.13241	46.12117	1.83295
A100	Step 11	0.49735	0.00134	0.11642	0.00088	0.00186	0.00009	4.87927	0.00205	0.00040	0.00010	3.26447	0.26131	45.77524	3.61804
AH10-21	**J = 0.007893156 ± 0.000039466**														
AA101	Step 1	0.10996	0.00115	0.00954	0.00025	0.00014	0.00004	0.05059	0.00169	0.00025	0.00006	3.82773	1.95214	53.69912	26.98295
AA101	Step 2	0.41594	0.00188	0.04652	0.00048	0.00087	0.00004	0.29249	0.00169	0.00077	0.00005	4.02121	0.34362	56.37153	4.74259
AA101	Step 3	1.10675	0.00349	0.15258	0.00118	0.00225	0.00009	0.99372	0.00170	0.00170	0.00005	3.96384	0.11016	55.57947	1.52114
AA101	Step 4	1.26014	0.00177	0.20641	0.00124	0.00297	0.00012	1.86467	0.00170	0.00169	0.00009	3.68869	0.13373	51.77628	1.85045
AA101	Step 5	1.04436	0.00406	0.19497	0.00151	0.00280	0.00013	2.44875	0.00170	0.00105	0.00010	3.76038	0.15833	52.76802	2.18955
AA101	Step 6	0.60328	0.00328	0.11841	0.00076	0.00164	0.00013	2.05288	0.00170	0.00054	0.00004	3.75240	0.11617	52.65758	1.60665
AA101	Step 7	0.66197	0.00300	0.13854	0.00206	0.00224	0.00009	3.16235	0.00170	0.00056	0.00007	3.57526	0.16501	50.20608	2.28529
AA101	Step 8	0.50964	0.00167	0.11332	0.00089	0.00184	0.00013	3.54515	0.00170	0.00041	0.00005	3.42157	0.14293	48.07641	1.98178
AA101	Step 9	0.57350	0.00267	0.13342	0.00109	0.00202	0.00010	4.98776	0.00170	0.00037	0.00004	3.47837	0.10466	48.86371	1.45046
AA101	Step 10	0.55247	0.00214	0.13383	0.00074	0.00244	0.00009	5.65685	0.00170	0.00029	0.00008	3.48121	0.18378	48.90315	2.54695
AH10-22	**J = 0.007957983 ± 0.000039790**														
A90	Step 1	0.34251	0.00100	0.01899	0.00026	0.00032	0.00006	0.06879	0.00257	0.00085	0.00004	4.78895	0.66024	67.47635	9.13090
A90	Step 2	0.94786	0.00454	0.06944	0.00087	0.00119	0.00011	0.32729	0.00257	0.00234	0.00006	3.68068	0.27335	52.08367	3.81274
A90	Step 3	1.34008	0.00342	0.13236	0.00121	0.00214	0.00005	0.78676	0.00257	0.00285	0.00008	3.75952	0.18605	53.18312	2.59354
A90	Step 4	1.51658	0.00406	0.20036	0.00079	0.00317	0.00016	1.89495	0.00257	0.00251	0.00012	3.87133	0.17987	54.74102	2.50513
A90	Step 5	0.73197	0.00237	0.11850	0.00073	0.00190	0.00018	1.83198	0.00257	0.00108	0.00008	3.47373	0.20435	49.19484	2.85483
A90	Step 6	0.61801	0.00328	0.10258	0.00084	0.00195	0.00008	2.40468	0.00257	0.00090	0.00006	3.42543	0.18220	48.51989	2.54642
A90	Step 7	0.57000	0.00263	0.10281	0.00059	0.00198	0.00010	3.27990	0.00257	0.00070	0.00009	3.53130	0.26375	49.99892	3.68306
A90	Step 8	0.46635	0.00172	0.08816	0.00099	0.00158	0.00013	3.48791	0.00258	0.00048	0.00006	3.69692	0.21152	52.31029	2.94995
A90	Step 9	0.39410	0.00105	0.08052	0.00084	0.00143	0.00015	3.62666	0.00258	0.00041	0.00009	3.39544	0.33637	48.10066	4.70211
A90	Step 10	0.37694	0.00242	0.07628	0.00057	0.00127	0.00009	3.73743	0.00258	0.00046	0.00007	3.16302	0.27938	44.84875	3.91253
AH10-22	**J = 0.007919598 ± 0.000039598**														
A91	Step 1	0.22037	0.00246	0.01058	0.00022	0.00027	0.00006	0.04618	0.00115	0.00056	0.00005	5.05965	1.38565	70.87928	19.03477
A91	Step 2	1.27576	0.00315	0.08573	0.00098	0.00170	0.00006	0.39351	0.00115	0.00340	0.00007	3.15296	0.23380	44.49490	3.25909
A91	Step 3	1.81768	0.00486	0.17754	0.00075	0.00292	0.00015	1.13921	0.00115	0.00383	0.00009	3.85514	0.16003	54.25651	2.21866
A91	Step 4	1.43771	0.00246	0.17649	0.00085	0.00280	0.00014	1.52663	0.00115	0.00270	0.00015	3.62152	0.25644	51.01461	3.56171
A91	Step 5	1.78785	0.00436	0.25541	0.00156	0.00395	0.00012	3.22167	0.00115	0.00302	0.00012	3.50225	0.14522	49.35719	2.01887
A91	Step 6	1.02788	0.00211	0.15999	0.00068	0.00290	0.00006	2.92160	0.00115	0.00142	0.00008	3.79707	0.15803	53.45122	2.19193
A91	Step 7	0.62271	0.00178	0.10131	0.00107	0.00187	0.00014	2.84173	0.00115	0.00082	0.00008	3.74376	0.22424	52.71153	3.11159
A91	Step 8	0.58169	0.00287	0.10918	0.00094	0.00202	0.00011	3.83650	0.00115	0.00078	0.00008	3.21607	0.20792	45.37442	2.89691
A91	Step 9	0.53629	0.00334	0.10063	0.00118	0.00190	0.00010	3.81746	0.00115	0.00076	0.00009	3.11152	0.28142	43.91714	3.92405
A91	Step 10	0.67831	0.00202	0.13216	0.00078	0.00213	0.00008	6.24802	0.00115	0.00082	0.00009	3.29641	0.19191	46.49332	2.67219

		40Ar	+/-	39Ar	+/-	38Ar	+/-	37Ar	+/-	36Ar	+/-	40Ar*/39Ar	+/-	Age	+/- (no J error)
AH10-25															
plagioclase	**J = 0.009828144 ± 0.000049141**														
A32	Step 1	0.00135	0.00042	0.00022	0.00003	-0.00002	0.00002	0.01327	0.00129	-0.00001	0.00002	17.64066	24.49733	288.44342	370.17627
A32	Step 2	0.04464	0.00067	0.00656	0.00010	0.00003	0.00002	0.13844	0.00129	0.00011	0.00002	1.92626	0.81915	33.83478	14.25429
A32	Step 3	0.11720	0.00054	0.01306	0.00014	0.00018	0.00002	0.38116	0.00130	0.00024	0.00003	3.45215	0.56829	60.19369	9.74550
A32	Step 4	0.32677	0.00073	0.07013	0.00030	0.00075	0.00003	1.19103	0.00130	0.00069	0.00003	1.75468	0.14208	30.84652	2.47639
A32	Step 5	0.44487	0.00058	0.12075	0.00026	0.00113	0.00005	2.92428	0.00130	0.00079	0.00003	1.75077	0.08286	30.77834	1.44429
A32	Step 6	0.26534	0.00053	0.07466	0.00026	0.00071	0.00004	2.36138	0.00130	0.00035	0.00003	2.17166	0.13373	38.10001	2.32163
A32	Step 7	0.29073	0.00065	0.08138	0.00032	0.00078	0.00006	3.10766	0.00185	0.00043	0.00003	1.99497	0.11383	35.02989	1.97946
A32	Step 8	0.29807	0.00062	0.08182	0.00026	0.00087	0.00006	3.23241	0.00185	0.00041	0.00002	2.15701	0.07932	37.84559	1.37724
A32	Step 9	0.25408	0.00038	0.07117	0.00031	0.00067	0.00004	2.75844	0.00186	0.00041	0.00002	1.88010	0.09050	33.03133	1.57554
A32	Step 10	0.44777	0.00063	0.12686	0.00051	0.00113	0.00006	5.44621	0.00186	0.00065	0.00003	2.00454	0.07457	35.19646	1.29671
AH10-25	**J = 0.009821502 ± 0.000049108**														
A29	Step 1	0.00022	0.00047	-0.00007	0.00009	-0.00001	0.00002	0.01174	0.00041	0.00000	0.00003	-17.45003	-138.97150	-339.16689	2971.70846
A29	Step 2	0.00508	0.00047	0.00078	0.00009	0.00000	0.00002	0.00595	0.00041	0.00001	0.00003	3.34377	11.57614	58.29526	198.59276
A29	Step 3	0.12064	0.00064	0.02016	0.00012	0.00022	0.00002	0.08473	0.00041	0.00018	0.00003	3.38131	0.44614	58.93921	7.65089
A29	Step 4	1.04429	0.00241	0.24767	0.00111	0.00236	0.00010	1.29462	0.00041	0.00080	0.00003	3.26564	0.04028	56.95451	0.69160
A29	Step 5	1.49872	0.00150	0.40263	0.00111	0.00364	0.00009	2.97365	0.00041	0.00076	0.00004	3.16305	0.02938	55.19237	0.50486
A29	Step 6	1.28617	0.00095	0.35734	0.00072	0.00335	0.00014	2.89374	0.00185	0.00056	0.00004	3.13223	0.03539	54.66263	0.60835
A29	Step 7	2.30883	0.00325	0.65381	0.00115	0.00612	0.00018	6.66098	0.00185	0.00108	0.00004	3.04480	0.02064	53.15911	0.35514
A29	Step 8	2.57392	0.00341	0.74189	0.00288	0.00513	0.00078	7.88096	0.00185	0.00119	0.00007	2.99415	0.03122	52.28754	0.53732
A29	Step 9	2.27198	0.00228	0.65802	0.00070	0.00611	0.00016	4.35747	0.00185	0.00174	0.00008	2.67275	0.03670	46.74686	0.63371
A29	Step 10	0.94774	0.00092	0.27103	0.00055	0.00251	0.00007	2.74275	0.00186	0.00044	0.00002	3.01187	0.02675	52.59251	0.46030
A29	Step 11	1.03801	0.00113	0.29978	0.00061	0.00303	0.00007	2.24814	0.00186	0.00077	0.00003	2.70759	0.03272	47.34828	0.56479
A29	Step 12	1.25582	0.00089	0.36030	0.00063	0.00330	0.00007	3.66848	0.00186	0.00054	0.00003	3.04300	0.02747	53.12819	0.47259
AH10-27	**J = 0.009336725 ± 0.000046684**														
A79	Step 1	0.00827	0.00032	0.00110	0.00009	-0.00004	0.00002	0.00487	0.00077	0.00001	0.00002	5.18646	6.16112	85.31224	98.98555
A79	Step 2	0.08593	0.00053	0.01336	0.00011	0.00007	0.00004	0.07290	0.00077	0.00014	0.00002	3.32001	0.50657	55.07355	8.27623
A79	Step 3	0.25854	0.00092	0.04943	0.00029	0.00041	0.00003	0.38351	0.00077	0.00033	0.00002	3.26720	0.13893	54.21056	2.27095
A79	Step 4	0.71240	0.00131	0.15417	0.00055	0.00144	0.00005	1.68977	0.00077	0.00092	0.00003	2.85317	0.06279	47.43026	1.03020
A79	Step 5	0.63485	0.00153	0.14336	0.00138	0.00135	0.00006	2.03783	0.00032	0.00076	0.00003	2.86387	0.06201	47.60587	1.01729
A79	Step 6	0.70664	0.00092	0.17583	0.00050	0.00147	0.00007	2.56344	0.00032	0.00079	0.00003	2.69175	0.04556	44.77984	0.74857
A79	Step 7	0.42934	0.00078	0.10920	0.00047	0.00098	0.00010	1.87544	0.00032	0.00047	0.00003	2.65432	0.07280	44.16474	1.19652
A79	Step 8	0.14252	0.00029	0.03580	0.00020	0.00023	0.00002	0.50904	0.00008	0.00015	0.00002	2.71133	0.17473	45.10154	2.87057
AH10-27	**J = 0.009325171 ± 0.000046626**														
A80	Step 1	0.10957	0.00200	0.01320	0.00030	0.00018	0.00006	0.08775	0.00294	0.00026	0.00003	2.49733	0.74135	41.53171	12.18820
A80	Step 2	0.34733	0.00222	0.05602	0.00041	0.00076	0.00004	0.42552	0.00295	0.00055	0.00003	3.30008	0.17667	54.68114	2.88338
A80	Step 3	0.91214	0.00343	0.17935	0.00038	0.00234	0.00005	1.64718	0.00295	0.00103	0.00003	3.39535	0.05715	56.23537	0.93190
A80	Step 4	1.06341	0.00270	0.24200	0.00058	0.00334	0.00006	3.42560	0.00296	0.00091	0.00003	3.27726	0.04212	54.30877	0.68758
A80	Step 5	1.47381	0.00254	0.35873	0.00081	0.00509	0.00006	7.56958	0.00296	0.00103	0.00003	3.26274	0.02329	54.07171	0.38022
A80	Step 6	1.12469	0.00613	0.28660	0.00159	0.00417	0.00012	7.03334	0.00296	0.00072	0.00004	3.18323	0.05211	52.77312	0.85145
A80	Step 7	1.15496	0.00488	0.29583	0.00131	0.00424	0.00009	8.06921	0.00296	0.00079	0.00003	3.11084	0.03343	51.58991	0.54658
A80	Step 8	1.33911	0.00401	0.34148	0.00149	0.00489	0.00005	9.21437	0.00296	0.00094	0.00004	3.10744	0.04171	51.53429	0.68189
A80	Step 9	0.81059	0.00089	0.20905	0.00066	0.00285	0.00006	5.89971	0.00349	0.00055	0.00003	3.10208	0.04636	51.44675	0.75796

		40Ar	+/-	39Ar	+/-	38Ar	+/-	37Ar	+/-	36Ar	+/-	40Ar*/39Ar	+/-	Age	+/- (no J error)
AH10-33	**J = 0.009406046 ± 0.000047030**														
A73	Step 1	0.06417	0.00024	0.00097	0.00006	0.00001	0.00004	0.02831	0.00036	0.00018	0.00002	10.73412	4.87147	173.52994	75.08418
A73	Step 2	0.50760	0.00057	0.00999	0.00009	0.00031	0.00005	0.29244	0.00036	0.00156	0.00003	4.60845	0.96105	76.55436	15.63065
A73	Step 3	1.01723	0.00075	0.03585	0.00016	0.00058	0.00005	1.34476	0.00036	0.00297	0.00004	3.86888	0.34625	64.48561	5.66924
A73	Step 4	0.75761	0.00091	0.04400	0.00023	0.00068	0.00006	2.47738	0.00036	0.00224	0.00003	2.15531	0.22008	36.20811	3.66030
A73	Step 5	0.35962	0.00204	0.02979	0.00024	0.00039	0.00005	1.73884	0.00036	0.00115	0.00006	0.67814	0.61180	11.47099	10.31589
A73	Step 6	0.49847	0.00122	0.05189	0.00046	0.00054	0.00005	3.21339	0.00036	0.00162	0.00005	0.39290	0.29517	6.65492	4.99043
A73	Step 7	0.33834	0.00046	0.03910	0.00013	0.00054	0.00005	3.14045	0.00036	0.00109	0.00002	0.43660	0.18049	7.39363	3.05030
A73	Step 8	0.17567	0.00038	0.02205	0.00021	0.00024	0.00006	1.85243	0.00036	0.00058	0.00002	0.21395	0.31661	3.62692	5.36185
A73	Step 9	0.12324	0.00077	0.01624	0.00016	0.00012	0.00004	1.26962	0.00036	0.00048	0.00003	-1.20002	-0.59273	-20.47926	10.17302
AH10-33	**J = 0.009394493 ± 0.000046972**														
A74	Step 1	0.42579	0.00170	0.00914	0.00018	0.00039	0.00003	0.33209	0.00751	0.00135	0.00002	2.79338	0.76412	46.73267	12.61945
A74	Step 2	1.65535	0.00082	0.05205	0.00018	0.00161	0.00005	2.05118	0.00752	0.00508	0.00005	2.96862	0.29176	49.62444	4.81074
A74	Step 3	2.13062	0.00185	0.08746	0.00037	0.00245	0.00005	3.82526	0.00752	0.00640	0.00004	2.74143	0.14332	45.87466	2.36804
A74	Step 4	2.72490	0.00609	0.13192	0.00028	0.00345	0.00005	7.67762	0.00753	0.00798	0.00007	2.78509	0.16700	46.59588	2.75822
A74	Step 5	2.16548	0.00697	0.15841	0.00064	0.00363	0.00006	13.51177	0.00754	0.00588	0.00008	2.69801	0.16083	45.15703	2.65850
A74	Step 6	1.49969	0.00180	0.15103	0.00066	0.00319	0.00007	17.44365	0.00754	0.00387	0.00008	2.35802	0.16512	39.52835	2.73781
A74	Step 7	1.16080	0.00184	0.13009	0.00070	0.00275	0.00007	16.65304	0.00755	0.00292	0.00006	2.29147	0.12805	38.42467	2.12444
A74	Step 8	1.26330	0.00149	0.14359	0.00029	0.00303	0.00006	19.83091	0.00755	0.00323	0.00004	2.15636	0.08592	36.18163	1.42733
AH10-36	**J = 0.009345913 ± 0.000046730**														
A65	Step 1	0.19863	0.00064	0.02316	0.00026	0.00020	0.00003	0.01979	0.00097	0.00039	0.00002	3.64129	0.27676	60.37325	4.51285
A65	Step 2	0.67353	0.00225	0.10904	0.00045	0.00098	0.00005	0.09183	0.00097	0.00098	0.00003	3.52732	0.08752	58.51403	1.42854
A65	Step 3	0.94887	0.00188	0.19685	0.00095	0.00154	0.00007	0.17230	0.00080	0.00089	0.00003	3.47738	0.05223	57.69868	0.85284
A65	Step 4	1.48725	0.00158	0.34183	0.00185	0.00278	0.00008	0.41601	0.00080	0.00101	0.00003	3.47771	0.03399	57.70411	0.55498
A65	Step 5	1.83255	0.00211	0.47398	0.00140	0.00408	0.00013	0.85258	0.00080	0.00087	0.00002	3.32121	0.01810	55.14656	0.29602
A65	Step 6	2.11691	0.00405	0.59269	0.00260	0.00490	0.00019	1.25751	0.00080	0.00068	0.00003	3.23413	0.02254	53.72191	0.36883
A65	Step 7	2.52013	0.00674	0.73429	0.00113	0.00625	0.00010	2.13635	0.00080	0.00064	0.00004	3.17286	0.01980	52.71890	0.32427
A65	Step 8	2.14415	0.00118	0.63261	0.00188	0.00485	0.00015	1.73211	0.00081	0.00050	0.00002	3.15520	0.01453	52.42967	0.23796
A65	Step 9	2.34894	0.00395	0.70464	0.00124	0.00602	0.00027	1.85130	0.00081	0.00053	0.00003	3.11142	0.01570	51.71254	0.25719
A65	Step 10	3.87201	0.00918	1.17655	0.00309	0.00846	0.00043	2.76385	0.00081	0.00079	0.00003	3.09310	0.01391	51.41237	0.22801
A65	Step 11	3.23842	0.00348	0.97809	0.00380	0.00662	0.00029	1.65439	0.00081	0.00063	0.00003	3.12007	0.01599	51.85427	0.26194
A65	Step 12	2.96172	0.00226	0.90332	0.00320	0.00726	0.00020	1.81207	0.00081	0.00057	0.00002	3.09220	0.01362	51.39772	0.22319
AH10-36	**J = 0.009354874 ± 0.000046774**														
A66	Step 1	0.45681	0.00076	0.05955	0.00013	0.00051	0.00005	0.02314	0.00121	0.00077	0.00003	3.82908	0.15832	63.55225	2.58186
A66	Step 2	1.49393	0.00642	0.26359	0.00067	0.00149	0.00012	0.09407	0.00121	0.00177	0.00005	3.68851	0.05880	61.25843	0.96018
A66	Step 3	1.99494	0.01459	0.43513	0.00269	0.00275	0.00030	0.34007	0.00121	0.00171	0.00005	3.42326	0.05090	56.92185	0.83311
A66	Step 4	1.38944	0.00185	0.32813	0.00120	0.00221	0.00013	0.24716	0.00078	0.00094	0.00006	3.39107	0.05703	56.39499	0.93369
A66	Step 5	1.87668	0.00837	0.46629	0.00317	0.00326	0.00016	0.60857	0.00078	0.00118	0.00003	3.27646	0.03539	54.51743	0.58012
A66	Step 6	2.42947	0.02995	0.63309	0.00914	0.00483	0.00030	1.14700	0.00078	0.00126	0.00006	3.25027	0.07254	54.08808	1.18925
A66	Step 7	1.83500	0.00330	0.52616	0.00097	0.00376	0.00013	0.97053	0.00078	0.00069	0.00003	3.09729	0.02034	51.57833	0.33391
A66	Step 8	1.43860	0.01492	0.41957	0.00432	0.00236	0.00017	0.49413	0.00113	0.00047	0.00002	3.09911	0.05088	51.60833	0.83520

		40Ar	+/-	39Ar	+/-	38Ar	+/-	37Ar	+/-	36Ar	+/-	40Ar*/39Ar	+/-	Age	+/- (no J error)
AH10-37	**J = 0.007881214 ± 0.000039406**														
A92	Step 1	0.15706	0.00202	0.02973	0.00022	0.00036	0.00005	0.02323	0.00359	0.00006	0.00003	4.66605	0.29252	65.15256	4.01160
A92	Step 2	0.66544	0.00307	0.12592	0.00066	0.00123	0.00005	0.17307	0.00359	0.00033	0.00004	4.50456	0.09134	62.93658	1.25421
A92	Step 3	1.48152	0.00355	0.28205	0.00047	0.00355	0.00017	0.54312	0.00359	0.00065	0.00004	4.56721	0.04919	63.79656	0.67516
A92	Step 4	2.17056	0.00955	0.42329	0.00140	0.00519	0.00011	2.10222	0.00359	0.00106	0.00006	4.38699	0.05173	61.32153	0.71093
A92	Step 5	0.72243	0.00404	0.15179	0.00101	0.00171	0.00011	1.73841	0.00360	0.00025	0.00006	4.27739	0.12930	59.81465	1.77853
A92	Step 6	0.83814	0.00283	0.17237	0.00103	0.00202	0.00012	3.29647	0.00360	0.00031	0.00006	4.32290	0.11298	60.44057	1.55351
A92	Step 7	0.64109	0.00175	0.13348	0.00119	0.00188	0.00015	5.26877	0.00360	0.00037	0.00005	3.97936	0.12618	55.71068	1.73949
A92	Step 8	0.42174	0.00201	0.09094	0.00110	0.00110	0.00008	5.48297	0.00306	0.00022	0.00005	3.93717	0.17623	55.12904	2.43029
A92	Step 9	0.39555	0.00177	0.09010	0.00061	0.00128	0.00007	6.67383	0.00306	0.00024	0.00007	3.60297	0.23641	50.51427	3.26855
A92	Step 10	0.47258	0.00174	0.11216	0.00130	0.00126	0.00006	8.39021	0.00306	0.00014	0.00008	3.85732	0.21998	54.02745	3.03550
A92	Step 11	0.29106	0.00108	0.06831	0.00061	0.00100	0.00006	5.57959	0.00306	0.00009	0.00005	3.87164	0.22721	54.22503	3.13489
AH10-37	**J = 0.007842829 ± 0.000039214**														
A93	Step 1	0.02652	0.00074	0.00430	0.00013	0.00002	0.00005	0.00524	0.00193	0.00010	0.00003	-0.53072	-1.75281	-7.56183	25.02667
A93	Step 2	0.32860	0.00189	0.06106	0.00025	0.00078	0.00005	0.12526	0.00193	0.00017	0.00003	4.57985	0.16759	63.97003	2.29982
A93	Step 3	0.83192	0.00217	0.15100	0.00105	0.00176	0.00009	0.35216	0.00193	0.00056	0.00004	4.42235	0.09060	61.80749	1.24480
A93	Step 4	1.31937	0.00655	0.21819	0.00166	0.00273	0.00012	0.82689	0.00193	0.00120	0.00006	4.42202	0.09528	61.80285	1.30915
A93	Step 5	0.85092	0.00327	0.16470	0.00165	0.00191	0.00016	1.12773	0.00237	0.00050	0.00003	4.27611	0.07749	59.79702	1.06584
A93	Step 6	0.82173	0.00317	0.15130	0.00111	0.00193	0.00005	2.49410	0.00237	0.00063	0.00004	4.19243	0.09258	58.64566	1.27425
A93	Step 7	0.70432	0.00205	0.14319	0.00113	0.00185	0.00012	4.39600	0.00237	0.00039	0.00008	4.11361	0.17270	57.56053	2.37837
A93	Step 8	0.33537	0.00151	0.07294	0.00061	0.00094	0.00005	4.44048	0.00237	0.00021	0.00005	3.75337	0.21798	52.59249	3.01020
A93	Step 9	0.33427	0.00116	0.07717	0.00071	0.00105	0.00009	5.23968	0.00237	0.00017	0.00003	3.69352	0.13885	51.76586	1.91838
A93	Step 10	0.39493	0.00338	0.09054	0.00072	0.00133	0.00008	6.52312	0.00237	0.00022	0.00004	3.65534	0.12461	51.23824	1.72217
A93	Step 11	0.40644	0.00160	0.09067	0.00072	0.00127	0.00009	7.34964	0.00238	0.00022	0.00006	3.77368	0.20820	52.87292	2.87469
AH10-38	**J = 0.009359832 ± 0.000046799**														
A77	Step 1	0.00476	0.00037	0.00046	0.00012	-0.00002	0.00002	0.00292	0.00113	0.00000	0.00003	9.70488	18.02422	156.85447	279.01018
A77	Step 2	0.15441	0.00049	0.01756	0.00017	0.00016	0.00004	0.04638	0.00113	0.00027	0.00003	4.25946	0.47275	70.52789	7.67669
A77	Step 3	0.57498	0.00096	0.09087	0.00065	0.00099	0.00006	0.28319	0.00113	0.00084	0.00004	3.60675	0.11966	59.89769	1.95460
A77	Step 4	0.92589	0.00197	0.18572	0.00080	0.00150	0.00004	0.71290	0.00113	0.00101	0.00004	3.37407	0.05975	56.09291	0.97810
A77	Step 5	0.98938	0.00119	0.23390	0.00073	0.00175	0.00007	1.21754	0.00113	0.00081	0.00004	3.20789	0.05738	53.37066	0.94062
A77	Step 6	1.02350	0.00102	0.25966	0.00128	0.00197	0.00010	1.59803	0.00113	0.00069	0.00004	3.15850	0.04383	52.56084	0.71884
A77	Step 7	1.01755	0.00311	0.27426	0.00085	0.00186	0.00007	1.74488	0.00113	0.00060	0.00003	3.06444	0.03365	51.01751	0.55235
A77	Step 8	1.07775	0.00090	0.29864	0.00104	0.00237	0.00007	2.47593	0.00113	0.00055	0.00003	3.06904	0.02997	51.09305	0.49189
A77	Step 9	0.55024	0.00055	0.15440	0.00029	0.00120	0.00004	1.23583	0.00016	0.00028	0.00004	3.03738	0.06858	50.57319	1.12594
A77	Step 10	0.19997	0.00053	0.05667	0.00030	0.00046	0.00005	0.56077	0.00016	0.00012	0.00003	2.88288	0.14575	48.03473	2.39647
AH10-38	**J = 0.009348278 ± 0.000046741**														
A78	Step 1	0.15141	0.00144	0.01321	0.00022	0.00028	0.00005	0.02758	0.00458	0.00038	0.00002	3.05646	0.53966	50.82450	8.84852
A78	Step 2	0.95333	0.00101	0.11957	0.00033	0.00183	0.00005	0.31038	0.00458	0.00193	0.00004	3.21386	0.09172	53.40353	1.50172
A78	Step 3	2.33027	0.00177	0.38704	0.00059	0.00531	0.00006	1.32985	0.00459	0.00373	0.00005	3.17619	0.03523	52.78668	0.57707
A78	Step 4	3.26153	0.00734	0.66614	0.00218	0.00880	0.00014	3.24506	0.00459	0.00439	0.00006	2.95065	0.03181	49.08873	0.52212
A78	Step 5	3.34152	0.01016	0.75548	0.00190	0.00985	0.00009	4.85106	0.00459	0.00421	0.00006	2.77802	0.02915	46.25329	0.47915
A78	Step 6	3.18411	0.00757	0.77180	0.00124	0.01002	0.00011	6.28732	0.00459	0.00387	0.00005	2.64550	0.02038	44.07357	0.33545
A78	Step 7	2.78968	0.00310	0.74434	0.00070	0.00936	0.00011	7.40096	0.00460	0.00335	0.00003	2.41964	0.01253	40.35251	0.20663
A78	Step 8	3.17136	0.00376	0.86168	0.00255	0.01104	0.00025	10.27105	0.00460	0.00410	0.00005	2.27586	0.01749	37.97989	0.28881
A78	Step 9	3.34211	0.00908	0.94259	0.00319	0.01224	0.00011	11.95002	0.00460	0.00435	0.00005	2.18330	0.01869	36.45070	0.30889
A78	Step 10	3.83676	0.00853	1.10721	0.00221	0.01378	0.00016	15.18965	0.00461	0.00524	0.00005	2.06791	0.01492	34.54256	0.24688

		40Ar	+/-	39Ar	+/-	38Ar	+/-	37Ar	+/-	36Ar	+/-	40Ar*/39Ar	+/-	Age	+/- (no J error)
AH10-39	**J = 0.009381756 ± 0.000046909**														
A69	Step 1	0.08158	0.00061	0.00198	0.00018	0.00003	0.00003	0.00465	0.00140	0.00026	0.00002	2.88238	3.48175	48.13754	57.37846
A69	Step 2	0.56914	0.00087	0.01762	0.00019	0.00036	0.00006	0.06178	0.00140	0.00180	0.00002	2.08595	0.39210	34.96456	6.50902
A69	Step 3	1.04724	0.00104	0.03707	0.00031	0.00068	0.00005	0.32839	0.00140	0.00330	0.00003	1.93718	0.25869	32.49323	4.30022
A69	Step 4	0.84708	0.00136	0.03439	0.00028	0.00070	0.00004	0.69834	0.00140	0.00268	0.00004	1.57799	0.36048	26.51241	6.01228
A69	Step 5	0.93115	0.00181	0.04012	0.00021	0.00085	0.00007	1.45551	0.00140	0.00306	0.00004	0.65412	0.31056	11.03744	5.22431
A69	Step 6	0.88935	0.00159	0.04120	0.00041	0.00088	0.00009	2.12780	0.00082	0.00296	0.00005	0.35504	0.37418	5.99915	6.31219
A69	Step 7	0.96513	0.00079	0.04611	0.00021	0.00098	0.00004	2.84853	0.00082	0.00321	0.00006	0.36496	0.39537	6.16651	6.66893
A69	Step 8	0.59608	0.00067	0.03046	0.00023	0.00062	0.00007	2.16942	0.00083	0.00196	0.00021	0.56351	2.04212	9.51254	34.38188
A69	Step 9	0.39823	0.00066	0.01894	0.00012	0.00039	0.00004	1.83755	0.00083	0.00139	0.00003	-0.61442	-0.51620	-10.42937	8.78750
AH10-41	**J = 0.009399678 ± 0.000046998**														
A71	Step 1	0.01794	0.00048	0.00045	0.00005	0.00007	0.00003	0.01317	0.00077	0.00004	0.00002	12.48706	15.45379	200.21937	234.53316
A71	Step 2	0.16392	0.00058	0.00575	0.00007	0.00008	0.00003	0.19874	0.00077	0.00048	0.00003	3.71840	1.67483	61.97870	27.44224
A71	Step 3	0.59889	0.00102	0.02029	0.00018	0.00043	0.00004	0.87094	0.00077	0.00183	0.00002	2.80335	0.34903	46.92295	5.76687
A71	Step 4	0.82913	0.00116	0.02329	0.00011	0.00054	0.00004	1.13327	0.00077	0.00258	0.00004	2.80690	0.53498	46.98155	8.83880
A71	Step 5	1.02564	0.00098	0.02946	0.00021	0.00075	0.00004	1.74893	0.00077	0.00328	0.00005	1.89899	0.51889	31.91856	8.64495
A71	Step 6	0.63381	0.00132	0.02057	0.00023	0.00065	0.00007	1.57534	0.00077	0.00208	0.00009	0.96748	1.30760	16.33209	21.97416
A71	Step 7	0.80149	0.00122	0.02540	0.00019	0.00062	0.00004	2.50006	0.00131	0.00268	0.00004	0.31788	0.49319	5.38254	8.33853
A71	Step 8	0.99422	0.00416	0.03206	0.00019	0.00070	0.00009	3.97257	0.00131	0.00341	0.00009	-0.46304	-0.84940	-7.86928	14.46694
A71	Step 9	0.71500	0.00142	0.02643	0.00019	0.00057	0.00004	3.19240	0.00131	0.00240	0.00004	0.20236	0.47568	3.42827	8.05109
AH10-45	**J = 0.009363835 ± 0.000046819**														
A67	Step 1	0.14882	0.00070	0.02251	0.00022	0.00014	0.00003	0.04168	0.00072	0.00017	0.00003	4.32514	0.33279	71.62413	5.40296
A67	Step 2	0.94230	0.00100	0.16911	0.00094	0.00142	0.00007	0.25778	0.00072	0.00101	0.00003	3.81272	0.06264	63.28549	1.02172
A67	Step 3	1.17291	0.00131	0.24132	0.00061	0.00198	0.00008	0.55086	0.00072	0.00103	0.00003	3.60012	0.04245	59.81448	0.69374
A67	Step 4	0.77367	0.00093	0.17142	0.00072	0.00144	0.00004	0.58923	0.00072	0.00056	0.00003	3.54970	0.04605	58.99026	0.75295
A67	Step 5	0.95211	0.00120	0.21736	0.00061	0.00181	0.00008	0.84307	0.00072	0.00067	0.00003	3.46718	0.03585	57.64060	0.58657
A67	Step 6	1.11294	0.00093	0.26711	0.00048	0.00236	0.00006	1.63971	0.00072	0.00079	0.00003	3.29193	0.02864	54.77093	0.46941
A67	Step 7	1.02483	0.00108	0.25616	0.00082	0.00168	0.00007	1.79971	0.00072	0.00074	0.00003	3.14916	0.03099	52.42979	0.50855
A67	Step 8	0.78596	0.00216	0.20100	0.00118	0.00183	0.00009	1.77845	0.00072	0.00050	0.00003	3.16954	0.05396	52.76404	0.88526
A67	Step 9	0.59222	0.00056	0.15798	0.00049	0.00150	0.00005	1.69339	0.00073	0.00040	0.00003	3.00720	0.06372	50.09885	1.04697
A67	Step 10	0.84552	0.00133	0.23183	0.00082	0.00199	0.00008	2.42519	0.00102	0.00057	0.00003	2.91528	0.04471	48.58779	0.73516
A67	Step 11	0.78829	0.00259	0.21257	0.00115	0.00186	0.00008	2.41292	0.00102	0.00058	0.00003	2.90563	0.04051	48.42908	0.66619
A67	Step 12	0.48523	0.00098	0.13222	0.00048	0.00119	0.00006	1.77090	0.00102	0.00038	0.00003	2.82598	0.07650	47.11872	1.25906
AH10-45	**J = 0.009372795 ± 0.000046864**														
A68	Step 1	0.81397	0.00237	0.10080	0.00063	0.00145	0.00005	0.19248	0.00139	0.00148	0.00004	3.72487	0.12272	61.91021	2.00504
A68	Step 2	3.37862	0.01621	0.46581	0.00294	0.00665	0.00011	1.13085	0.00330	0.00561	0.00005	3.69283	0.05434	61.38668	0.88805
A68	Step 3	2.64038	0.00315	0.44653	0.00072	0.00606	0.00009	1.51216	0.00331	0.00360	0.00005	3.52991	0.03725	58.72189	0.60965
A68	Step 4	3.37861	0.00330	0.62901	0.00122	0.00862	0.00008	2.69272	0.00331	0.00384	0.00005	3.56808	0.02711	59.34664	0.44362
A68	Step 5	2.53741	0.00562	0.52698	0.00077	0.00747	0.00006	3.36768	0.00331	0.00241	0.00005	3.46388	0.02826	57.64083	0.46290
A68	Step 6	3.05999	0.00234	0.68703	0.00048	0.00955	0.00011	5.97085	0.00332	0.00237	0.00006	3.43468	0.02407	57.16262	0.39435
A68	Step 7	2.61563	0.00172	0.61767	0.00101	0.00878	0.00008	7.10008	0.00332	0.00172	0.00004	3.41158	0.01935	56.78414	0.31700
A68	Step 8	1.70018	0.00253	0.42212	0.00065	0.00589	0.00010	5.97586	0.00662	0.00104	0.00003	3.29956	0.02514	54.94777	0.41238
A68	Step 9	1.73714	0.00282	0.44251	0.00075	0.00632	0.00008	6.74192	0.00663	0.00104	0.00003	3.23303	0.01936	53.85614	0.31774
A68	Step 10	3.02809	0.00202	0.78653	0.00085	0.01129	0.00014	13.66066	0.00664	0.00176	0.00005	3.18732	0.01786	53.10581	0.29321
A68	Step 11	1.67095	0.00185	0.44819	0.00113	0.00622	0.00006	8.34771	0.00664	0.00084	0.00003	3.17337	0.01988	52.87669	0.32644
A68	Step 12	2.06834	0.00177	0.56024	0.00057	0.00773	0.00007	11.31120	0.00665	0.00096	0.00005	3.18751	0.02417	53.10899	0.39680

		40Ar	+/-	39Ar	+/-	38Ar	+/-	37Ar	+/-	36Ar	+/-	40Ar*/39Ar	+/-	Age	+/- (no J error)
AH10-48	**J = 0.009833458 ± 0.000049167**														
A53	Step 1	0.14130	0.00087	0.00458	0.00008	0.00004	0.00003	0.03706	0.00107	0.00046	0.00002	1.32261	1.58480	23.31218	27.75386
A53	Step 2	1.22107	0.00216	0.04825	0.00030	0.00078	0.00008	0.40119	0.00107	0.00343	0.00002	4.29369	0.15808	74.60727	2.69079
A53	Step 3	2.43118	0.00232	0.13755	0.00015	0.00195	0.00008	1.16165	0.00107	0.00634	0.00006	4.05546	0.13351	70.54764	2.27770
A53	Step 4	1.82215	0.00218	0.15738	0.00094	0.00179	0.00008	1.46882	0.00107	0.00414	0.00004	3.80803	0.08397	66.32151	1.43584
A53	Step 5	3.05155	0.00326	0.32224	0.00076	0.00328	0.00011	3.69605	0.00107	0.00670	0.00006	3.32755	0.05808	58.08661	0.99778
A53	Step 6	2.17292	0.00122	0.33059	0.00068	0.00340	0.00013	4.91291	0.00107	0.00384	0.00004	3.14438	0.03901	54.93721	0.67132
A53	Step 7	1.57417	0.00157	0.28289	0.00083	0.00281	0.00008	4.56692	0.00107	0.00270	0.00005	2.74711	0.05545	48.08798	0.95789
A53	Step 8	1.26870	0.00139	0.27132	0.00044	0.00241	0.00008	5.17156	0.00107	0.00195	0.00004	2.55549	0.04719	44.77486	0.81665
A53	Step 9	1.34514	0.00121	0.29426	0.00118	0.00233	0.00010	6.24139	0.00107	0.00224	0.00003	2.31827	0.03571	40.66513	0.61944
A53	Step 10	1.63539	0.00424	0.38573	0.00146	0.00396	0.00020	9.47194	0.00108	0.00245	0.00006	2.36478	0.05020	41.47163	0.87033
A53	Step 11	1.46689	0.00159	0.38608	0.00112	0.00325	0.00017	10.41495	0.00108	0.00252	0.00004	1.87256	0.03477	32.91773	0.60565
AH10-48	**J = 0.009836841 ± 0.000049184**														
A54	Step 1	0.17715	0.00110	0.00385	0.00014	0.00008	0.00003	0.02345	0.00417	0.00057	0.00003	2.12824	2.04911	37.37879	35.61873
A54	Step 2	1.46997	0.00181	0.05609	0.00021	0.00092	0.00005	0.42198	0.00417	0.00414	0.00006	4.41669	0.33091	76.72544	5.62800
A54	Step 3	3.60924	0.00616	0.20746	0.00098	0.00270	0.00003	1.77965	0.00418	0.00942	0.00010	3.98487	0.14878	69.36631	2.54067
A54	Step 4	2.93133	0.00287	0.25202	0.00098	0.00238	0.00009	2.38296	0.00106	0.00697	0.00011	3.45957	0.13202	60.37342	2.26570
A54	Step 5	4.88502	0.00389	0.56446	0.00153	0.00515	0.00018	5.73188	0.00106	0.01060	0.00011	3.10414	0.05953	54.26307	1.02523
A54	Step 6	2.15326	0.00203	0.35822	0.00144	0.00303	0.00013	4.69389	0.00106	0.00382	0.00004	2.86233	0.03219	50.09419	0.55560
A54	Step 7	1.87892	0.00157	0.34556	0.00085	0.00283	0.00011	5.01394	0.00106	0.00325	0.00006	2.65627	0.05457	46.53389	0.94384
A54	Step 8	1.46976	0.00270	0.29804	0.00087	0.00231	0.00013	5.63068	0.00106	0.00259	0.00004	2.36479	0.04575	41.48590	0.79339
A54	Step 9	2.45352	0.00164	0.52839	0.00141	0.00429	0.00016	12.24681	0.00106	0.00429	0.00006	2.24678	0.03189	39.43812	0.55362
A54	Step 10	1.55271	0.00261	0.38902	0.00081	0.00337	0.00010	9.72953	0.00107	0.00278	0.00008	1.87772	0.06361	33.01877	1.10838
AH10-49	**J = 0.009382939 ± 0.000046915**														
A75	Step 1	0.04160	0.00026	0.00149	0.00006	-0.00001	0.00005	0.00455	0.00086	0.00012	0.00002	3.64305	4.55148	60.63740	74.49887
A75	Step 2	1.36487	0.00746	0.08241	0.00039	0.00104	0.00012	0.38190	0.00086	0.00326	0.00009	4.86373	0.33830	80.50757	5.47668
A75	Step 3	0.83253	0.00192	0.07041	0.00036	0.00073	0.00006	0.47715	0.00086	0.00181	0.00004	4.23931	0.17764	70.37066	2.89191
A75	Step 4	0.75383	0.00199	0.07281	0.00041	0.00071	0.00005	0.58833	0.00086	0.00151	0.00003	4.23409	0.13480	70.28560	2.19463
A75	Step 5	0.92253	0.00266	0.10125	0.00065	0.00094	0.00006	1.23795	0.00086	0.00192	0.00004	3.52087	0.12607	58.63640	2.06588
A75	Step 6	0.86074	0.00104	0.12486	0.00061	0.00113	0.00005	2.26668	0.00086	0.00149	0.00003	3.36023	0.07819	56.00212	1.28310
A75	Step 7	0.54940	0.00057	0.10404	0.00062	0.00077	0.00007	2.01363	0.00086	0.00097	0.00002	2.52548	0.06727	42.25157	1.11236
A75	Step 8	0.45625	0.00139	0.09955	0.00050	0.00076	0.00005	2.33608	0.00086	0.00072	0.00002	2.43223	0.07089	40.70898	1.17326
A75	Step 9	0.30225	0.00063	0.07149	0.00023	0.00057	0.00004	1.97540	0.00086	0.00051	0.00003	2.11921	0.13305	35.52107	2.20836
A75	Step 10	0.05604	0.00034	0.01320	0.00012	0.00014	0.00006	0.36818	0.00086	0.00014	0.00002	1.19835	0.51213	20.17191	8.57279
AH10-49	**J = 0.009371385 ± 0.000046857**														
A76	Step 1	0.29808	0.00177	0.01467	0.00029	0.00033	0.00003	0.05033	0.00497	0.00081	0.00003	3.93536	0.69018	65.33638	11.25366
A76	Step 2	1.98295	0.00095	0.12425	0.00041	0.00252	0.00006	0.51446	0.00497	0.00485	0.00007	4.42398	0.15726	73.28599	2.55291
A76	Step 3	3.02791	0.00822	0.22097	0.00057	0.00385	0.00012	1.28489	0.00498	0.00721	0.00004	4.06616	0.06638	67.46791	1.08110
A76	Step 4	5.19573	0.01119	0.46488	0.00054	0.00741	0.00009	3.86650	0.00572	0.01122	0.00009	4.04747	0.06414	67.16351	1.04482
A76	Step 5	4.67981	0.00820	0.51192	0.00065	0.00797	0.00014	6.10543	0.00572	0.00904	0.00005	3.92226	0.03202	65.12283	0.52223
A76	Step 6	3.20922	0.00366	0.46201	0.00085	0.00671	0.00005	7.75771	0.00573	0.00515	0.00006	3.64961	0.03751	60.67115	0.61312
A76	Step 7	2.18123	0.00192	0.42040	0.00082	0.00584	0.00011	10.32836	0.00573	0.00254	0.00004	3.40100	0.02972	56.60235	0.48688
A76	Step 8	1.28601	0.00266	0.27771	0.00082	0.00366	0.00008	8.56963	0.00574	0.00124	0.00003	3.31232	0.03782	55.14885	0.62015
A76	Step 9	1.45029	0.00276	0.33741	0.00053	0.00452	0.00006	13.12882	0.00574	0.00127	0.00006	3.18531	0.05175	53.06488	0.84953
A76	Step 10	1.24337	0.00258	0.30833	0.00117	0.00419	0.00006	14.23634	0.00574	0.00104	0.00005	3.03840	0.05021	50.65158	0.82546
A76	Step 11	0.77977	0.00147	0.19738	0.00041	0.00267	0.00005	11.05789	0.01314	0.00065	0.00003	2.98297	0.05308	49.74021	0.87300

		40Ar	+/-	39Ar	+/-	38Ar	+/-	37Ar	+/-	36Ar	+/-	40Ar*/39Ar	+/-	Age	+/- (no J error)
AH10-50	**J = 0.007829608 ± 0.000039148**														
A98	Step 1	0.01221	0.00046	0.00211	0.00016	-0.00002	0.00004	0.02128	0.00146	0.00001	0.00003	4.54082	3.70207	63.02621	50.49719
A98	Step 2	0.20658	0.00070	0.04843	0.00060	0.00052	0.00007	0.44221	0.00146	0.00018	0.00004	3.18379	0.26877	44.42040	3.70414
A98	Step 3	0.47684	0.00119	0.12448	0.00083	0.00157	0.00008	1.35867	0.00146	0.00034	0.00004	3.01291	0.10571	42.06378	1.45874
A98	Step 4	0.78470	0.00259	0.20440	0.00143	0.00267	0.00009	2.87942	0.00146	0.00044	0.00005	3.20087	0.08079	44.65572	1.11326
A98	Step 5	0.55568	0.00196	0.14290	0.00098	0.00200	0.00011	2.68841	0.00147	0.00022	0.00003	3.42937	0.07673	47.80163	1.05549
A98	Step 6	0.59477	0.00136	0.14954	0.00079	0.00215	0.00013	3.64204	0.00147	0.00035	0.00008	3.28689	0.16311	45.84063	2.24614
A98	Step 7	0.34240	0.00215	0.08339	0.00073	0.00114	0.00009	2.82655	0.00147	0.00017	0.00005	3.51953	0.19194	49.04145	2.63842
A98	Step 8	0.29081	0.00120	0.07087	0.00074	0.00107	0.00009	2.90042	0.00159	0.00009	0.00004	3.73087	0.18525	51.94434	2.54246
A98	Step 9	0.32188	0.00074	0.07924	0.00068	0.00123	0.00010	3.79859	0.00159	0.00016	0.00006	3.46026	0.23443	48.22656	3.22398
A98	Step 10	0.31863	0.00169	0.07673	0.00061	0.00146	0.00008	4.01275	0.00159	0.00012	0.00007	3.67256	0.27970	51.14391	3.84037
A98	Step 11	0.43913	0.00290	0.10410	0.00112	0.00180	0.00010	6.04028	0.00159	0.00035	0.00006	3.23240	0.18323	45.09015	2.52423
AH10-50	**J = 0.007850791 ± 0.000039254**														
A99	Step 1	0.02908	0.00074	0.00530	0.00025	0.00111	0.00010	0.04057	0.00255	0.00002	0.00002	4.44114	1.41293	61.83005	19.33769
A99	Step 2	0.16602	0.00083	0.02921	0.00049	0.00034	0.00007	0.26426	0.00255	0.00024	0.00004	3.26079	0.43618	45.60273	6.02358
A99	Step 3	0.47394	0.00179	0.10063	0.00064	0.00120	0.00006	0.93468	0.00255	0.00055	0.00004	3.08952	0.12820	43.23595	1.77269
A99	Step 4	0.62639	0.00153	0.15385	0.00093	0.00211	0.00008	1.88937	0.00255	0.00043	0.00006	3.24775	0.12087	45.42258	1.66935
A99	Step 5	0.68175	0.00294	0.16783	0.00079	0.00197	0.00011	2.72477	0.00255	0.00031	0.00004	3.52075	0.07918	49.18917	1.09133
A99	Step 6	0.41164	0.00188	0.10102	0.00094	0.00139	0.00012	2.04430	0.00255	0.00026	0.00004	3.32080	0.13024	46.43120	1.79776
A99	Step 7	0.68227	0.00250	0.16667	0.00080	0.00267	0.00012	4.09439	0.00181	0.00042	0.00007	3.34370	0.13003	46.74738	1.79458
A99	Step 8	0.36892	0.00161	0.08565	0.00076	0.00126	0.00006	2.98170	0.00181	0.00033	0.00004	3.17614	0.15458	44.43335	2.13611
A99	Step 9	0.49094	0.00217	0.11252	0.00107	0.00190	0.00009	5.05351	0.00181	0.00041	0.00007	3.28934	0.19362	45.99702	2.67324
A99	Step 10	0.36054	0.00237	0.08379	0.00086	0.00134	0.00009	4.42115	0.00181	0.00041	0.00005	2.86978	0.19202	40.19478	2.65972
A99	Step 11	0.47276	0.00235	0.10832	0.00062	0.00185	0.00007	6.10966	0.00181	0.00035	0.00006	3.41250	0.17417	47.69654	2.40251
AH10-52	**J = 0.009840224 ± 0.000049201**														
A55	Step 1	0.35715	0.00121	0.01129	0.00012	0.00028	0.00003	0.03352	0.00089	0.00111	0.00003	2.60428	0.72509	45.65007	12.55052
A55	Step 2	1.92485	0.00245	0.06768	0.00037	0.00130	0.00007	0.25430	0.00089	0.00575	0.00005	3.33237	0.23657	58.20871	4.06634
A55	Step 3	1.77303	0.00229	0.12701	0.00059	0.00147	0.00006	0.58560	0.00089	0.00459	0.00007	3.27420	0.17023	57.20854	2.92761
A55	Step 4	2.21898	0.00229	0.17405	0.00068	0.00227	0.00011	1.20275	0.00089	0.00582	0.00007	2.86917	0.12425	50.22916	2.14522
A55	Step 5	2.05934	0.00230	0.22673	0.00048	0.00251	0.00010	2.62771	0.00088	0.00499	0.00006	2.57518	0.08202	45.14632	1.42008
A55	Step 6	1.73360	0.00155	0.22541	0.00099	0.00250	0.00013	3.40181	0.00088	0.00414	0.00004	2.26623	0.05828	39.78936	1.01207
A55	Step 7	1.74241	0.00160	0.22509	0.00047	0.00277	0.00009	3.94213	0.00088	0.00433	0.00007	2.05019	0.09501	36.03371	1.65334
A55	Step 8	1.82388	0.00282	0.27838	0.00077	0.00288	0.00012	5.52992	0.00088	0.00415	0.00006	2.14228	0.06752	37.63563	1.17391
A55	Step 9	1.86386	0.00328	0.33063	0.00084	0.00326	0.00018	7.12257	0.00088	0.00412	0.00009	1.95329	0.08295	34.34675	1.44477
A55	Step 10	2.08191	0.00244	0.36709	0.00062	0.00388	0.00019	7.93212	0.00088	0.00452	0.00008	2.03498	0.06671	35.76909	1.16102
A55	Step 11	1.12513	0.00340	0.22802	0.00055	0.00220	0.00008	5.30210	0.00088	0.00224	0.00004	2.02584	0.05892	35.60997	1.02547
AH10-52	**J = 0.009853757 ± 0.000049269**														
A59	Step 1	-0.00006	0.00115	-0.00009	0.00013	-0.00007	0.00006	-0.00192	0.00313	-0.00007	0.00006	-218.43292	-359.64414	NaN	5547.94744
A59	Step 2	0.00007	0.00102	-0.00021	0.00012	-0.00015	0.00006	-0.00356	0.00313	-0.00011	0.00006	-148.36109	-119.24268	NaN	4589.09877
A59	Step 3	0.01206	0.00117	-0.00016	0.00011	-0.00013	0.00007	-0.00466	0.00313	-0.00001	0.00006	-87.57852	-120.23067	-3585.80110	15598.40286
A59	Step 4	0.40521	0.00220	0.00311	0.00019	0.00023	0.00007	0.17685	0.00126	0.00130	0.00007	6.62968	7.01408	114.16562	117.04272
A59	Step 5	0.49318	0.00231	0.02198	0.00038	0.00065	0.00006	1.25036	0.00126	0.00157	0.00007	1.37125	0.99233	24.21333	17.40543
A59	Step 6	0.41117	0.00248	0.06684	0.00070	0.00103	0.00010	4.06613	0.00126	0.00072	0.00008	2.96501	0.37070	51.95356	6.40283
A59	Step 7	0.45882	0.00159	0.10590	0.00097	0.00160	0.00008	6.53689	0.00126	0.00055	0.00007	2.80879	0.20825	49.25312	3.60239
A59	Step 8	0.41336	0.00307	0.11547	0.00050	0.00156	0.00011	6.91668	0.00126	0.00020	0.00004	3.07969	0.10235	53.93319	1.76583
A59	Step 9	0.35214	0.00245	0.09150	0.00078	0.00136	0.00008	5.49312	0.00126	0.00036	0.00006	2.67718	0.18130	46.97517	3.14008
A59	Step 10	0.12203	0.00200	0.03180	0.00052	0.00044	0.00007	1.99747	0.00126	0.00019	0.00005	2.08088	0.43050	36.61760	7.49923

		40Ar	+/-	39Ar	+/-	38Ar	+/-	37Ar	+/-	36Ar	+/-	40Ar*/39Ar	+/-	Age	+/- (no J error)
AH10-53	**J = 0.007804445 ± 0.000039022**														
A94	Step 1	0.13343	0.00148	0.00341	0.00016	0.00009	0.00003	0.01432	0.00290	0.00040	0.00004	4.70420	3.67350	65.04734	49.89060
A94	Step 2	1.15306	0.00357	0.03353	0.00059	0.00112	0.00005	0.18760	0.00290	0.00344	0.00010	4.06079	0.89790	56.28788	12.25393
A94	Step 3	0.95907	0.00239	0.05847	0.00032	0.00117	0.00010	0.44168	0.00290	0.00252	0.00007	3.64671	0.36269	50.62790	4.96535
A94	Step 4	1.11702	0.00367	0.08819	0.00067	0.00159	0.00013	1.13123	0.00290	0.00264	0.00012	3.81597	0.40763	52.94360	5.57332
A94	Step 5	0.85850	0.00424	0.10243	0.00055	0.00174	0.00011	2.09714	0.00291	0.00168	0.00007	3.54848	0.21058	49.28272	2.88504
A94	Step 6	0.81970	0.00327	0.10268	0.00079	0.00188	0.00009	2.60357	0.00291	0.00154	0.00007	3.54823	0.20940	49.27926	2.86892
A94	Step 7	0.62723	0.00322	0.09637	0.00083	0.00160	0.00007	2.95358	0.00291	0.00092	0.00005	3.69283	0.16546	51.25927	2.26439
A94	Step 8	0.61921	0.00235	0.09312	0.00081	0.00147	0.00010	2.92691	0.00291	0.00102	0.00004	3.42756	0.13964	47.62519	1.91493
A94	Step 9	0.98040	0.00281	0.14565	0.00089	0.00229	0.00008	4.82576	0.00291	0.00173	0.00008	3.21689	0.16725	44.73405	2.29713
A94	Step 10	0.73644	0.00217	0.12803	0.00123	0.00201	0.00012	4.37381	0.00291	0.00090	0.00006	3.67034	0.14764	50.95142	2.02081
A94	Step 11	0.76237	0.00449	0.13012	0.00106	0.00217	0.00013	4.55161	0.00291	0.00096	0.00009	3.66793	0.21194	50.91843	2.90104
AH10-55	**J = 0.007808425 ± 0.000039042**														
A97	Step 1	0.01163	0.00054	0.00047	0.00009	-0.00001	0.00003	0.00376	0.00273	0.00002	0.00003	12.75409	16.02460	171.27326	205.29356
A97	Step 2	0.37570	0.00208	0.02310	0.00030	0.00042	0.00004	0.27051	0.00286	0.00100	0.00005	3.45994	0.67116	48.09345	9.20597
A97	Step 3	0.55722	0.00276	0.05155	0.00073	0.00097	0.00007	0.72754	0.00286	0.00127	0.00007	3.53002	0.41545	49.05437	5.69546
A97	Step 4	0.57842	0.00194	0.07583	0.00054	0.00128	0.00008	1.35551	0.00286	0.00101	0.00005	3.67871	0.20551	51.09162	2.81412
A97	Step 5	0.32101	0.00158	0.05727	0.00057	0.00080	0.00007	1.38560	0.00286	0.00032	0.00005	3.97764	0.27209	55.18050	3.71751
A97	Step 6	0.44053	0.00192	0.08579	0.00084	0.00131	0.00011	2.94987	0.00286	0.00055	0.00005	3.23708	0.18327	45.03394	2.51809
A97	Step 7	0.34810	0.00135	0.07508	0.00054	0.00128	0.00007	3.38746	0.00287	0.00028	0.00003	3.51488	0.13473	48.84675	1.84731
A97	Step 8	0.39163	0.00207	0.08403	0.00102	0.00138	0.00008	4.23140	0.00287	0.00032	0.00008	3.53051	0.29041	49.06104	3.98126
A97	Step 9	0.42410	0.00170	0.10163	0.00090	0.00152	0.00007	4.93067	0.00287	0.00020	0.00007	3.60282	0.21139	50.05213	2.89637
A97	Step 10	0.55869	0.00207	0.13682	0.00122	0.00174	0.00006	6.78301	0.00287	0.00026	0.00007	3.53226	0.15919	49.08504	2.18227
AH10-56	**J = 0.009815947 ± 0.000049080**														
A49	Step 1	0.08807	0.00045	0.01108	0.00011	0.00008	0.00002	0.11170	0.00187	0.00020	0.00003	2.67077	0.71685	46.68668	12.37021
A49	Step 2	0.33106	0.00134	0.03804	0.00018	0.00043	0.00003	0.21867	0.00113	0.00074	0.00002	2.98263	0.19342	52.06016	3.32777
A49	Step 3	0.77958	0.00229	0.11090	0.00028	0.00108	0.00005	0.91696	0.00113	0.00159	0.00003	2.78945	0.09093	48.73334	1.56741
A49	Step 4	1.15076	0.00151	0.18790	0.00064	0.00169	0.00006	1.44246	0.00114	0.00217	0.00003	2.70851	0.05358	47.33767	0.92419
A49	Step 5	1.21973	0.00213	0.21740	0.00062	0.00236	0.00008	3.12739	0.00114	0.00222	0.00003	2.59912	0.04699	45.44978	0.81136
A49	Step 6	1.01626	0.00178	0.18616	0.00037	0.00185	0.00014	2.84352	0.00114	0.00185	0.00003	2.52131	0.05397	44.10568	0.93272
A49	Step 7	1.11510	0.00165	0.21334	0.00078	0.00209	0.00008	3.31076	0.00114	0.00210	0.00004	2.32238	0.06012	40.66458	1.04084
A49	Step 8	1.38266	0.00200	0.26649	0.00022	0.00288	0.00016	4.79015	0.00114	0.00278	0.00004	2.10035	0.04814	36.81626	0.83524
A49	Step 9	1.22945	0.00171	0.24372	0.00095	0.00237	0.00011	4.91771	0.00114	0.00252	0.00003	1.98781	0.04222	34.86251	0.73343
A49	Step 10	1.71305	0.00265	0.34169	0.00112	0.00328	0.00020	8.88196	0.00114	0.00343	0.00006	2.04662	0.05521	35.88382	0.95838
A49	Step 11	1.32840	0.00155	0.25976	0.00048	0.00250	0.00016	6.53321	0.00114	0.00292	0.00005	1.78877	0.06027	31.40194	1.04885
AH10-56	**J = 0.009887600 ± 0.000049438**														
A40	Step 1	0.00071	0.00027	-0.00006	0.00003	-0.00004	0.00002	-0.00029	0.00112	-0.00001	0.00002	-57.42619	-109.30064	-1513.41049	4511.19056
A40	Step 2	0.00305	0.00028	0.00004	0.00003	-0.00001	0.00003	-0.00150	0.00112	0.00004	0.00001	-217.30662	-191.55708	NaN	2974.81442
A40	Step 3	0.02228	0.00040	0.00057	0.00004	0.00000	0.00003	0.00699	0.00112	0.00010	0.00001	-11.72021	-7.61890	-222.20418	153.71959
A40	Step 4	0.16464	0.00114	0.00924	0.00012	0.00014	0.00002	0.12270	0.00112	0.00045	0.00002	3.50802	0.73702	61.51532	12.70614
A40	Step 5	0.21649	0.00109	0.01986	0.00007	0.00024	0.00002	0.30525	0.00112	0.00051	0.00002	3.32588	0.34218	58.37242	5.90943
A40	Step 6	0.27837	0.00059	0.03331	0.00017	0.00038	0.00002	0.64407	0.00112	0.00062	0.00003	2.86232	0.28352	50.34882	4.91823
A40	Step 7	0.52100	0.00045	0.08892	0.00049	0.00091	0.00003	2.08090	0.00112	0.00099	0.00004	2.57412	0.13872	45.34260	2.41308
A40	Step 8	0.30467	0.00067	0.06818	0.00025	0.00057	0.00003	1.85476	0.00112	0.00051	0.00002	2.26487	0.09970	39.95505	1.73956
A40	Step 9	0.25590	0.00058	0.06342	0.00020	0.00061	0.00003	1.82009	0.00112	0.00035	0.00002	2.41514	0.10693	42.57488	1.86293
A40	Step 10	0.24708	0.00050	0.06357	0.00022	0.00058	0.00004	2.03105	0.00112	0.00032	0.00002	2.39093	0.10677	42.15303	1.86050
A40	Step 11	0.16426	0.00063	0.04434	0.00016	0.00039	0.00003	1.47239	0.00112	0.00019	0.00003	2.43933	0.21329	42.99631	3.71506
A40	Step 12	0.34238	0.00073	0.09021	0.00019	0.00091	0.00003	3.00700	0.00112	0.00048	0.00002	2.21280	0.05058	39.04626	0.88290

		40Ar	+/-	39Ar	+/-	38Ar	+/-	37Ar	+/-	36Ar	+/-	40Ar*/39Ar	+/-	Age	+/- (no J error)
AH11-1	**J = 0.008073136 ± 0.000040366**														
A87	Step 1	0.04865	0.00102	0.00384	0.00023	0.00001	0.00007	0.00490	0.00279	0.00011	0.00003	4.37653	2.23095	62.64206	31.38388
A87	Step 2	0.28284	0.00237	0.02472	0.00037	0.00022	0.00007	0.03700	0.00279	0.00060	0.00004	4.27932	0.54924	61.27392	7.73227
A87	Step 3	1.72892	0.00440	0.19234	0.00087	0.00246	0.00008	0.37294	0.00279	0.00312	0.00007	4.19534	0.11591	60.09133	1.63284
A87	Step 4	1.69488	0.00435	0.21889	0.00128	0.00286	0.00016	0.58196	0.00279	0.00266	0.00006	4.14569	0.09117	59.39165	1.28479
A87	Step 5	2.97934	0.00481	0.41762	0.00129	0.00606	0.00019	1.71648	0.00279	0.00412	0.00007	4.21597	0.05449	60.38192	0.76746
A87	Step 6	2.33789	0.00605	0.35764	0.00156	0.00471	0.00015	2.07493	0.00279	0.00291	0.00011	4.13334	0.09572	59.21761	1.34915
A87	Step 7	2.30077	0.00445	0.38924	0.00172	0.00497	0.00020	2.89308	0.00279	0.00254	0.00005	3.98081	0.04614	57.06665	0.65111
A87	Step 8	1.78488	0.00694	0.33083	0.00162	0.00456	0.00015	3.25009	0.00279	0.00156	0.00010	4.00379	0.09567	57.39086	1.34973
A87	Step 9	1.83986	0.00665	0.35686	0.00142	0.00477	0.00016	4.07064	0.00280	0.00132	0.00006	4.06244	0.05816	58.21814	0.82018
A87	Step 10	2.07964	0.00667	0.41043	0.00201	0.00562	0.00018	5.11737	0.00280	0.00129	0.00007	4.13612	0.05879	59.25683	0.82863
A87	Step 11	1.82146	0.00444	0.37321	0.00221	0.00511	0.00009	4.63245	0.00280	0.00112	0.00005	3.99265	0.05054	57.23363	0.71305
AH11-2	**J = 0.008034752 ± 0.000040174**														
A88	Step 1	0.03268	0.00075	0.00266	0.00016	0.00005	0.00002	0.06774	0.00163	0.00009	0.00002	2.69044	2.45615	38.58323	34.84937
A88	Step 2	0.19144	0.00098	0.02214	0.00033	0.00025	0.00007	0.56345	0.00163	0.00040	0.00005	3.24251	0.68156	46.39940	9.62859
A88	Step 3	0.39348	0.00165	0.05952	0.00065	0.00088	0.00005	1.63836	0.00398	0.00052	0.00006	4.03973	0.31753	57.62685	4.45794
A88	Step 4	0.47357	0.00220	0.08771	0.00100	0.00133	0.00011	2.69870	0.00398	0.00049	0.00004	3.75916	0.15824	53.68347	2.22643
A88	Step 5	0.42125	0.00171	0.08747	0.00070	0.00131	0.00008	2.92183	0.00398	0.00036	0.00005	3.60745	0.18497	51.54768	2.60574
A88	Step 6	0.32870	0.00153	0.07242	0.00055	0.00134	0.00009	3.33049	0.00398	0.00021	0.00005	3.68456	0.22243	52.63348	3.13148
A88	Step 7	0.32054	0.00136	0.07190	0.00071	0.00130	0.00009	4.04165	0.00399	0.00024	0.00006	3.46770	0.26303	49.57794	3.70930
A88	Step 8	0.30102	0.00227	0.06826	0.00078	0.00130	0.00007	5.64552	0.00399	0.00031	0.00005	3.08539	0.23940	44.17838	3.38623
A88	Step 9	0.22425	0.00227	0.05246	0.00026	0.00098	0.00008	4.93972	0.00399	-0.00004	0.00004	4.48280	0.25778	63.83672	3.60671
A88	Step 10	0.30647	0.00141	0.07289	0.00083	0.00112	0.00006	7.94927	0.00399	0.00028	0.00005	3.08803	0.22523	44.21568	3.18574
AH11-2	**J = 0.007996367 ± 0.000039982**														
A89	Step 1	0.01130	0.00062	0.00075	0.00009	-0.00002	0.00003	0.02374	0.00194	0.00001	0.00002	11.19754	9.87405	154.70902	130.73748
A89	Step 2	0.08303	0.00079	0.00767	0.00015	0.00014	0.00005	0.19262	0.00194	0.00023	0.00003	2.14979	1.28641	30.74942	18.24415
A89	Step 3	0.36643	0.00232	0.04163	0.00053	0.00062	0.00007	1.05863	0.00194	0.00071	0.00006	3.79350	0.44429	53.91165	6.22065
A89	Step 4	0.40010	0.00147	0.06557	0.00082	0.00103	0.00011	1.85491	0.00194	0.00052	0.00004	3.73732	0.19876	53.12489	2.78415
A89	Step 5	0.38625	0.00140	0.07609	0.00069	0.00104	0.00010	2.33771	0.00194	0.00033	0.00005	3.80757	0.20612	54.10866	2.88566
A89	Step 6	0.41961	0.00182	0.08797	0.00073	0.00110	0.00003	3.63654	0.00194	0.00024	0.00004	3.95543	0.14883	56.17748	2.08116
A89	Step 7	0.31761	0.00154	0.07118	0.00069	0.00128	0.00009	4.00677	0.00195	0.00017	0.00005	3.73825	0.22116	53.13795	3.09782
A89	Step 8	0.27735	0.00140	0.06400	0.00062	0.00090	0.00008	4.51904	0.00195	0.00026	0.00006	3.13963	0.28870	44.73324	4.06278
A89	Step 9	0.20892	0.00128	0.04907	0.00062	0.00080	0.00007	4.33804	0.00195	0.00017	0.00006	3.25404	0.37634	46.34265	5.29136
A89	Step 10	0.19694	0.00104	0.04687	0.00063	0.00066	0.00007	4.45686	0.00195	0.00015	0.00006	3.28723	0.39397	46.80922	5.53791
A89	Step 11	0.14905	0.00081	0.03592	0.00041	0.00063	0.00008	3.92474	0.00195	0.00017	0.00006	2.78300	0.51093	39.70759	7.21020
AH11-3	**J = 0.007956705 ± 0.000039784**														
A104	Step 1	0.18162	0.00105	0.00332	0.00018	0.00012	0.00004	0.02301	0.00382	0.00056	0.00003	5.04329	3.01625	70.97923	41.62644
A104	Step 2	1.38033	0.00481	0.02729	0.00064	0.00135	0.00007	0.32379	0.00382	0.00454	0.00011	1.44016	1.21579	20.55519	17.25430
A104	Step 3	2.44704	0.00382	0.06162	0.00052	0.00218	0.00011	1.00596	0.00382	0.00800	0.00015	1.35999	0.72572	19.41712	10.30581
A104	Step 4	3.50794	0.00660	0.10551	0.00088	0.00338	0.00013	2.31092	0.00383	0.01056	0.00019	3.66761	0.53839	51.89316	7.50918
A104	Step 5	2.12164	0.00628	0.10368	0.00098	0.00245	0.00009	2.68369	0.00383	0.00579	0.00012	3.95317	0.35214	55.87162	4.90059
A104	Step 6	2.30984	0.00681	0.17582	0.00067	0.00319	0.00010	5.35427	0.00383	0.00536	0.00014	4.13707	0.24062	58.42915	3.34397
A104	Step 7	1.03345	0.00373	0.11592	0.00077	0.00199	0.00011	3.79449	0.00383	0.00205	0.00010	3.69349	0.26131	52.25415	3.64385
A104	Step 8	1.48449	0.00505	0.18623	0.00147	0.00295	0.00013	6.85767	0.00383	0.00250	0.00008	4.00954	0.13652	56.65594	1.89905
A104	Step 9	1.33580	0.00551	0.19309	0.00102	0.00297	0.00010	7.03974	0.00383	0.00204	0.00011	3.79845	0.17405	53.71716	2.42515
A104	Step 10	1.54524	0.00539	0.21215	0.00080	0.00296	0.00009	8.41762	0.00240	0.00269	0.00009	3.53771	0.13054	50.08050	1.82251

		40Ar	+/-	39Ar	+/-	38Ar	+/-	37Ar	+/-	36Ar	+/-	40Ar*/39Ar	+/-	Age	+/- (no J error)
AH11-4	**J = 0.008043215 ± 0.000040216**														
A107	Step 1	0.09062	0.00095	0.00549	0.00014	0.00009	0.00004	0.02764	0.00210	0.00020	0.00003	6.00625	1.73559	85.11437	24.02379
A107	Step 2	0.59741	0.00250	0.04080	0.00066	0.00077	0.00006	0.30192	0.00210	0.00137	0.00005	4.70188	0.38338	66.96850	5.36028
A107	Step 3	1.24389	0.00374	0.11266	0.00075	0.00165	0.00012	1.02794	0.00211	0.00253	0.00012	4.40481	0.31917	62.81020	4.47294
A107	Step 4	1.46590	0.00529	0.17358	0.00103	0.00263	0.00012	2.10875	0.00211	0.00246	0.00011	4.25084	0.19235	60.65113	2.69885
A107	Step 5	1.09789	0.00293	0.15946	0.00058	0.00232	0.00010	2.79271	0.00211	0.00135	0.00009	4.37890	0.16990	62.44696	2.38143
A107	Step 6	0.83233	0.00368	0.14419	0.00059	0.00174	0.00016	3.11825	0.00211	0.00091	0.00008	3.91543	0.16841	55.93894	2.36905
A107	Step 7	0.85231	0.00332	0.15356	0.00099	0.00198	0.00011	4.48098	0.00211	0.00086	0.00009	3.90494	0.17795	55.79125	2.50351
A107	Step 8	0.71120	0.00412	0.13151	0.00090	0.00225	0.00022	4.82729	0.00211	0.00059	0.00005	4.07474	0.12322	58.17863	1.73127
A107	Step 9	0.99075	0.00511	0.18860	0.00106	0.00251	0.00017	8.40654	0.00211	0.00095	0.00009	3.75720	0.14718	53.71165	2.07309
A107	Step 10	0.59160	0.00237	0.11608	0.00084	0.00185	0.00009	5.84633	0.00211	0.00062	0.00007	3.50985	0.18430	50.22432	2.60093
A107	Step 11	0.58036	0.00342	0.11483	0.00102	0.00177	0.00007	6.40770	0.00211	0.00062	0.00008	3.44713	0.21325	49.33904	3.01084
LCF25	**J = 0.007914339 ± 0.000039572**														
A102	Step 1	0.08732	0.00095	0.00239	0.00008	0.00008	0.00004	0.02135	0.00223	0.00027	0.00004	3.23698	4.48373	45.63582	62.41994
A102	Step 2	0.61012	0.00275	0.02140	0.00040	0.00069	0.00008	0.28117	0.00223	0.00182	0.00006	3.37260	0.88517	47.52275	12.30995
A102	Step 3	1.28272	0.00347	0.04487	0.00061	0.00140	0.00010	0.68281	0.00443	0.00407	0.00007	1.79589	0.44415	25.46137	6.25268
A102	Step 4	1.82060	0.00528	0.11216	0.00064	0.00251	0.00020	1.95538	0.00444	0.00500	0.00006	3.05674	0.15949	43.12475	2.22339
A102	Step 5	1.37991	0.00136	0.10003	0.00116	0.00190	0.00008	2.41077	0.00444	0.00346	0.00008	3.57313	0.25455	50.30939	3.53446
A102	Step 6	1.22160	0.00140	0.11799	0.00094	0.00184	0.00014	3.57215	0.00445	0.00241	0.00008	4.31132	0.19286	60.53050	2.66277
A102	Step 7	0.89538	0.00239	0.11775	0.00099	0.00172	0.00012	4.11315	0.00445	0.00150	0.00011	3.84209	0.28784	54.04011	3.98857
A102	Step 8	0.89651	0.00300	0.12946	0.00082	0.00207	0.00010	4.76418	0.00445	0.00150	0.00009	3.50901	0.19680	49.41881	2.73402
A102	Step 9	0.84335	0.00163	0.13140	0.00123	0.00211	0.00010	4.52330	0.00445	0.00124	0.00007	3.62852	0.15403	51.07836	2.13783
A102	Step 10	1.02737	0.00329	0.17533	0.00126	0.00269	0.00012	5.92510	0.00446	0.00138	0.00009	3.53550	0.16262	49.78684	2.25866
A102	Step 11	0.97602	0.00211	0.16077	0.00070	0.00225	0.00013	6.12900	0.00446	0.00127	0.00006	3.72754	0.10858	52.45210	1.50592
LCF25	**J = 0.007935522 ± 0.000039678**														
A103	Step 1	0.16974	0.00130	0.00395	0.00010	0.00017	0.00003	0.04449	0.00176	0.00057	0.00004	0.19111	3.17890	2.73389	45.44111
A103	Step 2	0.84866	0.00364	0.02522	0.00048	0.00086	0.00007	0.38164	0.00176	0.00249	0.00005	4.44566	0.62997	62.54845	8.71155
A103	Step 3	1.26560	0.00552	0.05938	0.00093	0.00157	0.00009	0.99893	0.00176	0.00379	0.00013	2.45816	0.65827	34.85287	9.24373
A103	Step 4	1.56752	0.00357	0.07093	0.00072	0.00167	0.00012	1.53471	0.00176	0.00437	0.00006	3.90674	0.26438	55.08059	3.67108
A103	Step 5	1.03883	0.00464	0.07976	0.00067	0.00180	0.00011	2.10039	0.00176	0.00259	0.00008	3.43975	0.30777	48.58434	4.28901
A103	Step 6	1.13029	0.00307	0.10579	0.00039	0.00191	0.00009	3.62174	0.00176	0.00254	0.00008	3.57869	0.22933	50.51964	3.19255
A103	Step 7	0.76188	0.00243	0.09546	0.00099	0.00174	0.00007	3.73577	0.00176	0.00157	0.00010	3.10971	0.31547	43.97913	4.40753
A103	Step 8	0.74812	0.00323	0.10446	0.00093	0.00151	0.00010	4.35592	0.00176	0.00133	0.00009	3.40135	0.26165	48.04916	3.64745
A103	Step 9	0.85839	0.00424	0.12862	0.00067	0.00201	0.00013	5.48290	0.00177	0.00133	0.00008	3.61669	0.19101	51.04855	2.65822
A103	Step 10	0.72290	0.00259	0.11776	0.00074	0.00164	0.00009	4.62724	0.00177	0.00110	0.00010	3.38502	0.25557	47.82145	3.56313
A103	Step 11	0.64538	0.00246	0.10370	0.00088	0.00163	0.00005	4.27529	0.00177	0.00102	0.00009	3.31516	0.26252	46.84725	3.66196